POTENTIOMETRIC HEAVY METAL SENSING INTEGRATED WITH PAPER-BASED MICROFLUIDIC SOLUTION SAMPLING

SILVA MAHAMALAGE ROCHELLE UDANI

INTERDISCIPLINARY GRADUATE PROGRAMME

NANYANG ENVIRONMENT AND WATER RESEARCH INSTITUTE

2023

POTENTIOMETRIC HEAVY METAL SENSING INTEGRATED WITH PAPER-BASED MICROFLUIDIC SOLUTION SAMPLING

SILVA MAHAMALAGE ROCHELLE UDANI

INTERDISCIPLINARY GRADUATE PROGRAMME

NANYANG ENVIRONMENT AND WATER RESEARCH INSTITUTE

A thesis submitted to the Nanyang Technological University in partial fulfillment of the requirement for the degree of

Doctor of Philosophy

2023

STATEMENT OF ORIGINALITY

I hereby certify that the work embodied in this thesis is the result of original research, is free of plagiarised materials, and has not been submitted for a higher degree to any other University or Institution.

06/01/2023

. . . . . .

Date

. . . . . .

Silva Mahamalage Rochelle Udani

SUPERVISOR DECLARATION STATEMENT

I have reviewed the content and presentation style of this thesis and declare it is free of plagiarism and of sufficient grammatical clarity to be examined. To the best of my knowledge, the research and writing are those of the candidate except as acknowledged in the Author Attribution Statement. I confirm that the investigations were conducted in accord with the ethics policies and integrity standards of Nanyang Technological University and that the research data are presented honestly and without prejudice.

06/01/2023

. . . . . .

Date

. . . . . .

Assoc. Prof. Grzegorz Lisak

AUTHORSHIP ATTRIBUTION STATEMENT

This thesis contains material from two papers published in the following peer-reviewed journals in which I am listed as the first author.

Chapter 1, Chapter 3, and Chapter 4 contain text from as R. Silva, A. Ahamed, Y.H. Cheong, K. Zhao, R. Ding, G. Lisak, Non-equilibrium potentiometric sensors integrated with metal modified paper-based microfluidic solution sampling substrates for determination of heavy metals in complex environmental samples, Anal. Chim. Acta. 1197 (2022) 339495. https://doi.org/10.1016/j.aca.2022.339495.

The contributions of the co-authors are as follows:

- Rochelle Silva: Methodology, Investigation, Formal analysis, Writing - Original Draft
- Ashiq Ahamed: Methodology, Software, Investigation, Writing - Original Draft (life cycle assessment sections)
- Yi Heng Cheong: Investigation (potentiometric measurements, profilometry)
- Zhao Ke: Investigation (SEM equipment training and data analysis, purchase of supplies)
- Ding Ruiyu: Methodology (paper-based sampling)
- Grzegorz Lisak: Conceptualization, Methodology, Resources, Writing - Review & Editing, Supervision, Funding acquisition, Project administration

Chapter 5 contains text from R. Silva, K. Zhao, R. Ding, W.P. Chan, M. Yang, J.S.Q. Yip, G. Lisak, Ion-selective membrane modified microfluidic paper-based solution sampling substrates for potentiometric heavy metal detection, Analyst. 147 (2022) 4500–4509. https://doi.org/10.1039/D2AN01108E.

The contributions of the co-authors are as follows:

- Rochelle Silva: Methodology, Investigation, Formal analysis, Writing - Original Draft
- Zhao Ke: Investigation (SEM training and data analysis, purchase of supplies)
- Ding Ruiyu: Methodology, Investigation, Writing – Review
- Wei Ping Chan: Investigation (FTIR equipment training and data analysis)
- Mingpeng Yang: Investigation (preparation of electrodes and paper substrates)
- Jane Si Qi Yip: Investigation (selectivity test in solution and with paper substrates)
- Grzegorz Lisak: Conceptualization, Methodology, Resources, Writing - Review & Editing, Supervision, Funding acquisition, Project administration

Chapter 6 is a part of a manuscript in preparation. The contributions of the co-authors are as follows:

- Rochelle Silva: Methodology, Investigation, Formal analysis, Writing - Original Draft
- Jane Si Qi Yip: Methodology, Investigation, Formal analysis, Writing - Original Draft
- Grzegorz Lisak: Conceptualization, Methodology, Resources, Writing - Review & Editing, Supervision, Funding acquisition, Project administration

06/01/2023

. . . . . .

Date

. . . . . .

Silva Mahamalage Rochelle Udani

ACKNOWLEDGMENT

The work presented in this thesis was made possible by the support of many organizations and individuals. First, I thank my main supervisor, Assoc. Prof. Grzegorz Lisak, for taking me under his wing and guiding me closely to make sure I didn't fall behind. Thanks for being there for me during the ups and downs in the past few years and providing many opportunities for professional growth. You made the impossible possible. Dziękuję Ci! I'm grateful to my co-supervisor, Prof. Jason Xu Zhichuan, and my mentor Asst. Prof. She Qianhong for their support and guidance. I thank my previous TAC members: Prof. Liu Yu, Prof. Charles Yang Chun, and Asst. Prof. Abid Hussain for their contributions.

The majority of the research work was performed at Residues and Resource Reclamation Centre (R3C), Nanyang Environment and Water Research Institute (NEWRI). Special thanks to my seniors Dr. Ding Ruiyu and Dr. Yi Heng Cheong who were my first mentors at R3C and taught me the basics. Much gratitude to past and present colleagues at R3C including Mr. Zhao Ke, Dr. Ashiq Ahamed, Dr. Wei Ping Chan, Ms. Jane Yip (FYP student from CEE), Dr. Mingpeng Yang (visiting scholar), Dr. Fu Xiaoxu, Mr. Tu Wei Han, Dr. Ge Liya, Dr. Chen Wenqian, Mr. Ong Hang Meng, and Ms. Liang Lili. I convey my gratitude to past and present R3C staff including Ms. Low Siew Cheng, Ms. Ohnmar, Ms. T. Vicnesvari and Ms. Wong Yuet Mun for their help.

I would like to thank the Interdisciplinary Graduate Programme (IGP) of Graduate College – NTU, Ministry of Education - Singapore, and NEWRI for providing the scholarship to continue my studies. Kudos to past and present admins at IGP including Ms. Harmira, Ms. Valarie, Ms. Victoria, and Ms. Kay Lee for their hard work. Special

appreciation to all the NEWRI staff members, especially Ms. Hera Adam for her timely reminders and encouragement. I appreciate the support and guidance received from Assoc. Prof. Richard Webster (Director, NEWRI Education & Training) and Dr. Babu Narayanswamy (Director, NEWRI Operations) at critical junctures of my PhD journey. Thanks to Mr. Jacky and Ms. Hwee Pin from NEWRI office, and members of the NEWRI Analytics Cluster, including Ms. Janelle Ng, Ms. Lam Mei Shan, Ms. Koh Danyu, Ms. Elvy Riani Wanjaya, Mr. She Ka Keng, Ms. Tan Kuan Yi, and Ms. Yuen Jia Wei. I express my gratitude for the support received from School of Civil and Environmental Engineering (CEE) and School of Materials Science and Engineering (MSE), the schools of my main and co-supervisors, respectively. Thanks to Ms. Ng Soo Ching from CEE office, Mr. Tan Han Khiang, Ms. Lim-Tay Chew Wang, and other staff members at CEE laboratories for your help with purchases and teaching assistant duties.

My heartiest gratitude to my companions from NEWRI student office, Nanyang Scholars Toastmasters Club, Interdisciplinary Graduate School Student Club, the NTU Sri Lankan community and many others with whom I had the pleasure of sharing the ups and downs of PhD life with. I'm thankful to Dr. Peter Yeo, Ms. Angeline Jayanthi, and all my medical care providers. Thanks to my beloved family and friends who supported me all the way from Sri Lanka, especially my parents, my brother, my aunt, and my grandmother. An extra special thanks to my fiancé for your love and patience during these past few years.

I would also like to acknowledge the people of Sri Lanka, many of whom are currently undergoing a crippling economic crisis. Their efforts made free education possible right up to my first degree and paved the way to initiate my higher studies. From Holy Cross College, Gampaha, Sri Lanka, to University of Moratuwa, Sri Lanka, and now Nanyang Technological University, Singapore, it has been a journey to remember...

TABLE OF CONTENTS

LIST OF PUBLICATIONS

Peer-reviewed journal papers related to this study

1. **R. Silva**, A. Ahamed, Y.H. Cheong, K. Zhao, R. Ding, G. Lisak, Non-equilibrium potentiometric sensors integrated with metal modified paper-based microfluidic solution sampling substrates for determination of heavy metals in complex environmental samples, Anal. Chim. Acta. 1197 (2022) 339495. https://doi.org/10.1016/j.aca.2022.339495.
2. **R. Silva**, K. Zhao, R. Ding, W.P. Chan, M. Yang, J.S.Q. Yip, G. Lisak, Ion-selective membrane modified microfluidic paper-based solution sampling substrates for potentiometric heavy metal detection, Analyst. 147 (2022) 4500–4509. https://doi.org/10.1039/D2AN01108E.

LIST OF ABBREVIATIONS

CWE	Carbon working electrode
DL	Detection limit
EMF	Electromotive force
FE-SEM	Field emission scanning electron microscopy
GC	Glassy carbon
ICP-OES	Inductively coupled plasma optical emission spectrometry
IPCC AR5	Intergovernmental Panel on Climate Change- Fifth Assessment Report
ISE	Ion-selective electrode
ISM	Ion-selective membrane
LCA	Life cycle assessment
LDL	Lower detection limit
PEDOT(PSS)	Poly(3,4-ethylenedioxythiophene) polystyrene sulfonate
PVC	Poly(vinyl chloride)
RE	Reference electrode

LIST OF SYMBOLS

a_i	Activity of primary ion
A and B	Debye-Hückel constants
c_i	Concentration of primary ion
d_i	Average effective ion radius
E_i	Electrode potential
E_i^0	Standard potential of the electrode
F	Faraday constant, F = 96485 C mol^{-1}
$k_{i,j}$	Selectivity coefficient (i refers to primary ion and j refers to interfering ion)
R	Universal gas constant, R = 8.314 J K^{-1} mol^{-1}
T	Absolute temperature in Kelvin
τ_{90}	Time required for achieving 90 % of the full potential change
z_i	Charge of the primary ion
f_i	Activity coefficient

LIST OF FIGURES

LIST OF TABLES

ABSTRACT

Paper-based microfluidic solution sampling is a viable option for potentiometric sensors to be used for determination of analytes in samples with high solid-to-liquid ratios. Unfortunately, potentiometric heavy metal sensitive electrodes cannot be easily integrated with paper-based solution sampling as heavy metals have strong affinity towards the paper matrix. This work addresses development of paper modifications to diminish, control or eliminate the heavy metals-paper matrix interactions in order to reliably measure ion activities in microvolumes of analytes when ion sensors are coupled with paper-based solution sampling.

In the first study, metal modified paper-based substrates were utilized for microfluidic paper-based solution sampling coupled with Pb^{2+}-ion selective electrodes (ISEs) with the aim of controlling the super-Nernstian response which usually occurs when using unmodified paper substrates. Potentiometric responses of Pb^{2+}-ISEs coupled with gold, platinum and palladium coated paper substrates were investigated. Paper-based substrates coated on both sides with 38 nm gold layers were found to be the most advantageous in controlling the super-Nernstian response of ISEs at non-equilibrium conditions. Characterization of paper substrates showed that the favourable quality of paper substrates being able to absorb the analyte was preserved while the thin metallic layers blocked much of the negatively charged sites on the paper substrates. Durability studies indicated that the lifetime of Pb^{2+}-ISEs could be doubled when ISEs are used with paper-based substrates in complex environmental samples with high solid-to-liquid content compared to when ISEs are used without a paper-based substrate. Determination of lead in real samples using metal modified paper substrates coupled with Pb^{2+}-ISEs was validated by inductively coupled plasma optical emission spectrometry (ICP-OES).

Detailed life cycle assessments were performed for model screen-printed potentiometric sensors with and without metal modified paper-based solution sampling substrates. The results confirmed that the use of modified paper substrates demonstrated lower environmental impact per potentiometric measurement of Pb^{2+}-ISE as compared to sensors without the use of paper substrates.

In the second study, paper substrates were modified with ion-selective membrane (ISM) cocktail (used for Pb^{2+}-ion-selective electrodes (ISEs) preparation) and coupled with model heavy metal Pb^{2+}-ISEs. Upon investigations with various compositions of ISM cocktail, it was found that the super Nernstian response of Pb^{2+}-ISEs was eliminated when 10 to 50 mg ml^{-1} ISM cocktail was used for modification. The modification of the paper substrates by Pb^{2+}-ISM allowed elimination of adsorption sites. Also, it resulted in improvement of sensor performance in terms of their detection limits to be similar of those for conditioned electrodes in standard beaker-based measurements. It is believed that the elimination of super-Nernstian response of the electrodes, improving the potentiometric responses and detection limits of ISEs was attributed to compatibility improvement of the paper substrates and Pb^{2+}-ISEs.

In the third study, the selectivity of Pb^{2+}-ISEs coupled with newly introduced paper-based sampling strategies was studied using the separate solutions method (SSM).The results confirmed that the modifications of paper-based substrates to improve the potentiometric performance with heavy metals influence selectivity of the Pb^{2+}-ISEs, however does not adversely impact overall selectivity pattern and ability of the Pb^{2+}-ISEs to discriminate interfering ions in wide concentration range. The selectivity coefficients were also compared with those obtained with solution-based sampling, unmodified paper-based sampling and a previously introduced paper-based substrate modification in the literature.

CHAPTER 1 INTRODUCTION

1.1. Overview

Heavy metal ions are introduced to the environment through naturally occurring phenomena, e.g. natural weathering of rocks [1] and microbial activity [2], or through ever-increasing anthropogenic activities, such as mining [3], industrial practices [4–7], agriculture [8], solid waste management and wastewater treatment [9–13]. Since heavy metals are toxic, non-biodegradable and are easily mobile in the environment [14–20], they can relatively easily enter human body causing extensive damage to various organs [21,22]. The monitoring of heavy metal ions in environmental samples and management of resources, waste and pollutants is thus essential for human well-being [23–28].

Several analytical techniques to quantify heavy metal concentrations have been established over the years, including but not limited to atomic absorption spectrometry, inductively coupled plasma with either optical or mass discrimination, and cold vapour atomic fluorescence [29–31]. These techniques, however, require relatively standard sample volumes (at least few milliliters), which may not always be available or practical if the sample has low volumes of liquid or high solid-to-liquid ratios. They also implement timely measurement protocols and require trained personnel to handle the measurements, including sample pre-treatment, e.g. filtration, dilution, or buffering [32,33]. The use of potentiometry coupled with microfluidic paper-based solution sampling can mitigate some of these limitations. Potentiometry is a fast, low-cost, and simple electrochemical technique which does not require complicated sample pre-treatment prior to the measurement [34–39]. The use of paper as a sampling substrate allows potentiometry to be used in cases where the sample volume available is limited or samples contain solid matter which can damage the ion-selective membrane (ISM)

[40,41]. This is in addition to the desirable chemical and physical properties of paper as a sampling substrate which makes it low-cost, lightweight, wettable, and easy to be modified [42,43].

Using paper-based microfluidic solution sampling coupled with ISEs for analysis of ions such as K^+, Na^+ and Cl^-, has been shown to be effective and readily available without any paper substrate modifications if the measurements are done within clinical sample concentration ranges [44,45]. However, the use of microfluidic paper-based solution sampling coupled with ISEs for the determination of heavy metal ions poses some challenges [46]. Chemical binding and/or physical adsorption of heavy metal ions to the negatively charged cellulose material [47], gives rise to a super-Nernstian response of most heavy metal-sensitive ISEs [40]. For example, the ideal (thermodynamic) Nernstian response for Pb^{2+}-ISEs should be characterized with a slope of 29.6 mV dec^{-1}. Naturally, due to non-ideal conditions the slope may vary, with the acceptable variations of approximately ± 2 mV. A super-Nernstian response is characterized by slopes greater than the acceptable slope. For ISEs coupled with microfluidic paper-based solution sampling, such super-Nernstian response is usually observed between $10^{-3.1}$ and $10^{-4.0}$ mol dm^{-3} $Pb(NO_3)_2$ [40]. For that reason, modifications of paper substrates to avoid or to control the super-Nernstian response of ISEs were explored and included conditioning of the paper with inorganic salts [48], adjusting the pH of the paper [49] to limit the adsorption of heavy metals onto the paper substrates or replacing paper with sponge [50] or textile [51] as solution sampling substrates. Despite the fact that various modified and unmodified microfluidic solution sampling substrates coupled with heavy metal sensitive electrodes are characterized with close-to-Nernstian potentiometric responses at relatively high analyte concentrations, ISEs suffer from relatively high detection limit as compared to conventional beaker-based measurements

limiting their usability to submicromolar analyte concentrations [52–54]. The possible reason for this is uncontrolled metal adsorption/desorption at the solution sampling substrates when in contact with the analyte [55]. At present, this effect could not be entirely eliminated, giving rise to unreliable potential readings of ISEs close to their detection limits [46]. It is expected that same effect occurs at higher analyte concentrations, however, its extent is overshadowed by the relatively high concentration of the analyte predominantly driving the potential formation at the ISM | paper substrate | sample solution interfaces. It is expected then that heavy metal sensitive electrodes coupled with paper-based sampling solution substrates operate at non-equilibrium conditions, affected by the concentration and time dependent sample solution equilibration with the paper substrates [56].

1.2. Scope and objective

The aim of this thesis is to develop new strategies to overcome the challenges encountered during the potentiometric analysis of heavy metals with paper-based solution sampling. The focus is on modifying paper substrates so that modified paper substrates may be used for successful determination of heavy metals in environmental samples that have high solid-to-liquid ratio.

The objectives of the thesis are as follows.

- Investigate the effect of modifying paper substrates with deposition of metallic layers on top of paper substrates, which could act as barriers and paper fiber surface blockers to control analyte-paper substrate interactions.
- Investigate the effect of modifying paper substrates with components used to formulate heavy metal ion-selective membranes.

- Determining influence of modified microfluidic paper-based solution sampling on selectivity of ISEs.

1.3. Outline of thesis

This thesis contains seven chapters including this introductory chapter.

Chapter 2 provides a detailed literature review about the presence of heavy metals in the environment, analytical techniques for determination of heavy metals, potentiometry and the use of paper in analytics.

Chapter 3 presents the common chemicals, materials, equipment, and methods used for the experimental work performed.

Chapter 4 presents published work on non-equilibrium potentiometric sensors integrated with metal modified paper-based microfluidic solution sampling substrates for determination of heavy metals in complex environmental samples.

Chapter 5 presents published work on ion-selective membrane modified microfluidic paper-based solution sampling substrates for potentiometric heavy metal detection.

Chapter 6 presents determination of selectivity of Pb^{2+}-ISEs coupled with modified microfluidic paper-based solution sampling substrates.

Chapter 7 concludes the thesis by providing a summary of work performed and recommendations for future experiments.

CHAPTER 2 THEORY AND LITERATURE REVIEW

2.1. Heavy metals in the environment

The term “heavy metal” is used to refer to metals which are at least five times denser than water and possess high atomic weight [57]. Although the exact definition of a heavy metal has been debated over the years [58], examples for heavy metals include lead, arsenic, mercury, cadmium and chromium. Heavy metals occur naturally in the environment, but they are becoming increasingly more concerning due to anthropogenic activities which redistribute them in the atmosphere, soil, water and eventually make them easily accessible to living organisms [21,59,60].

For this thesis, lead (Pb) has been selected as a model heavy metal since it is one of the most commonly occurring and highly toxic heavy metals. The primary ores of lead include galena, cerussite, and anglesite [61]. Lead is used for a variety of applications in lead-acid batteries, paints, ammunition, radiation protection, building materials, and some alloys [62]. It can enter the human body mainly via inhalation or ingestion and be absorbed depending on different factors such as age and physiological status. Children are more susceptible to lead absorption and are prone to impaired neuropsychological functioning, growth retardation and behavioral issues [63,64]. In adults, lead poisoning causes fertility issues, memory problems, anemia, increased blood pressure levels, renal and nervous system issues [65,66]. The current Occupational Safety and Health Administration Permissible Exposure Level (OSHA PEL) for lead is 0.050 mg/m^3 TWA [67].

2.1.1. Analytical techniques for determination of heavy metals

The determination of heavy metals in environmental samples is essential for the maintenance of human health and environmental management. A brief introduction to

some of the commonly used analytical techniques developed by regulatory bodies and laboratories are discussed in this section.

It should be noted that most of these techniques are capable of handling detection of different heavy metals including the model heavy metal, Pb. Principles such as discrimination of optical or mass spectra, atomic absorption spectra, atomic fluorescence spectra and electrochemical properties can be used to distinguish specific elements as discussed below.

2.1.1.1. Inductively coupled plasma - optical emission spectrometry (ICP-OES)

ICP-OES is one of the most used analytical techniques which can determine a variety of elements simultaneously, especially at trace levels. First demonstrated in 1965 [68] for the determination of trace metals, it has advanced to be one of the most reliable analytical techniques for heavy metal analysis [69–71]. For most elements, the detection limits are a part per billion (ng/mL) or below [72]. The ICP-OES uses an argon plasma to excite atoms or ions to a higher energy level. When the atoms or ions return to the ground state or a lower energy state, it measures the intensity of the specific wavelength emitted and compares it with a previously established calibration curve [73]. Samples must be pre-treated prior to being tested in the ICP-OES to reduce the impact to sensitive parts of the equipment such as the nebulizer and the plasma. Pre-treatment steps include filtration, reduction of dissolved solids by dilution, and digestion of solid samples [74].

2.1.1.2. Inductively coupled plasma - mass spectrometry (ICP-MS)

ICP-MS is used for ultra-sensitive detection of metals [75]. It can be used for a variety of samples such as environmental [76,77], food [78], clinical and biological samples

[79], and advanced materials [80]. The detection limit can be as low as parts per trillion (ppt) [81].

The ICP-MS also uses an argon plasma to excite atoms or ions which are then measured by a mass spectrometer which consists typically of a scanning quadrupole mass filter and a detector [82]. Sample pre-treatment can include dilution, solid digestion, and filtration [83] depending on the nature of the sample analyzed.

2.1.1.3. Atomic absorption spectrometer (AAS)

Developed in the mid-19th century [84], AAS is a widely used analytical technique for simultaneous detection of heavy metals. Although more recent techniques such as ICP-OES have surpassed the capabilities of AAS, it is still used for trace metal analysis. The AAS works by atomizing the analyte and then recording the reduction of intensity of optical radiation when a beam of radiation is passed through it. During data analysis, the correct method and wavelength has to be selected to give optimal results while performing background corrections such as deuterium and Zeeman background correction [85].

Sample preparation techniques can involve hot plate, microwave, acid, and high-pressure digestions [86]. The detection limit for flame atomic absorption spectrometry (FAAS) is in the order of 1–100 $\mu g\,L^{-1}$ and for graphite furnace atomic absorption spectrometry (GFAAS) it is about 20-200 times lower [87].

2.1.1.4. Atomic fluorescence spectrometer (AFS)

AFS is another analytical technique which has been in use for several decades. It has similar instrumentation to that found in AAS (light source, atom cell, detector, and readout system, etc.) but provides higher sensitivity [30]. Electromagnetic radiation is used to transfer atoms into a state of excitation and the radiation emitted by atoms when

returning to their ground state is recorded. Different types of fluorescence such as resonance fluorescence, stokes direct line fluorescence, and stepwise fluorescence are used for the analysis of metal ions [88]. The detection limit for AFS is at the order of ng L^{-1} [89]. Sample pre-treatment can include acid digestion and dilution [90]. The pretreatment methods are mostly targeted at reducing the interferences such as spectral interference (overlapping of spectra of two different metals) and chemical interference [88].

2.1.1.5. Electrochemical techniques

Electrochemical techniques to determine heavy metals are gaining attention due to their ability to overcome some of the challenges posed by traditional techniques. These techniques are more cost-effective, less complicated, require less pre-treatment, and provide more opportunities for on-site assessment. Examples include potentiometry, conductometry, amperometry, impedimentary, and voltammetry [91].

2.2. Potentiometry

Among the different types of electrochemical techniques currently available, potentiometry is a commonly used technique. Potentiometry is sensitive, compact, low cost, and requires low energy consumption. The technique began to develop in the late 19^{th} century with the discovery of the Nernst formalism by Walther Nernst [92]. It has been used to detect inorganic components such as heavy metals and clinically relevant ions, and organic moieties [24,93].

The setup for potentiometric measurements consists of a reference electrode (RE) and an indicator electrode maintained in closed electric circuit through the contact with the analyte (Figure 2.1). The reference electrode ought to maintain its potential despite any

changes in the composition of the sample or calibrator while the potential of the indicator electrode changes depending on the activity of the primary ion in the solution.

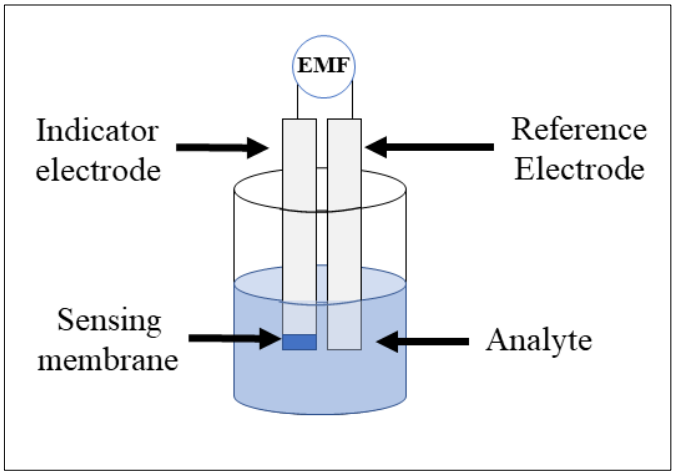

Figure 2. 1 Schematic of a potentiometric measurement setup

To ensure that the chemical composition of the electrodes and analyte remains relatively unchanged, the measurement is taken at a near "zero current condition" which is assured by the use of a high impedance voltmeter when the system is at an equilibrium condition. The electromotive force (EMF) recorded is the difference in potential between the indicator and reference electrodes and can be written as follows (Equation 1):

$$E_{cell} = E_{indicator} - E_{reference} \quad \text{(Equation 1)}$$

The Nernst equation describes how the EMF of the cell is related to the activity of ions in the solution (Equation 2):

$$E = E^0 + \frac{RT}{z_i F} \ln a_i \quad \text{(Equation 2)}$$

where E is the potential of the electrode (mV), E^0 is the standard potential of the electrode (mV), a_i is the activity of the target (primary) ion, z_i is the charge of the primary ion, R is the gas constant (8.314 J mol^{-1} K^{-1}), T is the absolute temperature (K), and F is the Faraday constant (96485 C mol^{-1}).

Activity (a_i) is a quantity which offers the "effective concentration" of a specie in a solution, and it is related to concentration by the following equation (Equation 3):

$$a_i = c_i f_i \quad \text{(Equation 3)}$$

where c_i is the concentration and f_i is the activity coefficient of the ion in the solution.

Activity coefficient can be defined by the Debye-Hückel approximation (Equation 4), where A and B are constants, *z* is the charge number and d_i is the average effective ion radius [94]:

$$\log f_i = -\frac{Az^2\sqrt{I}}{1+Bd_i\sqrt{I}} \quad \text{(Equation 4)}$$

The ionic strength, I, is a measure of the concentration of charges in a solution and can be calculated using Equation 5:

$$I = \frac{1}{2}\sum c_i z_i^2 \quad \text{(Equation 5)}$$

Activity (a_i) is a complex quantity which can be further explained in relation to Gibbs free energy (G) and chemical potential (μ). The Gibbs free energy (G) is a measure of the energy that is available to do useful work in a system, such as a chemical reaction. The chemical potential (μ) is a thermodynamic quantity that is closely related to the Gibbs free energy (G), and it describes the amount of energy required to add one mole of a substance to a system at constant temperature and pressure. In the case of an ion in a solution, the chemical potential is related to the ion's activity through Equation 6:

$$\mu = \mu^{\circ} + RT\ ln\ (a_i) \quad \text{(Equation 6)}$$

where μ° is the standard chemical potential of the ion, R is the gas constant, T is the absolute temperature, and ln (a_i) is the natural logarithm of the ion's activity.

2.2.1. Ion-selective electrodes (ISEs)

Ion-selective electrodes are an important group of potentiometric chemical sensors. As the name suggests, these electrodes have the ability to distinguish between ions. ISEs are usually classified on the basis of the membrane material (glass, crystalline, polymeric) or ISE construction (classical with a liquid internal reference system, solid-contact, screen-printed). ISEs can be characterized by their sensitivity (slope), stability, selectivity to the target ion, response time, reproducibility from electrode-to-electrode or batch-to-batch, etc. [95]. Some of these characteristics are discussed below.

2.2.1.1. Sensitivity of ISEs

The calibration curve (a plot of cell EMF versus logarithm of activity of primary ion) of an ISE is used to determine the working range and slope of the sensor. The upper and lower detection limits (UDL and LDL) give an indication about the working range of the electrode. As shown in Figure 2.2, the linear range is narrower than the working range and is more sensitive to measurement error. Thus, ULRL and LLRL refer to Upper Linear Range Limit and Lower Linear Range Limit, respectively.

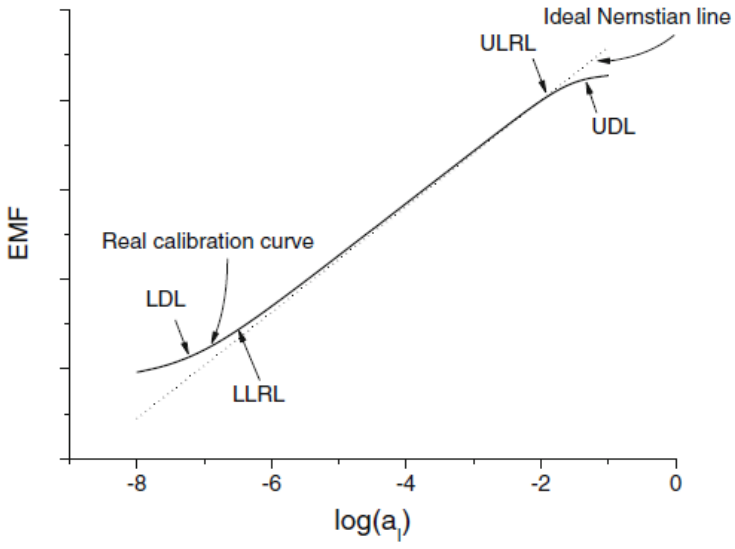

Figure 2. 2 Schematic for working range and slope of an ISE [95]

To understand the slope of ISE, it is important to understand equations governing the linear range of the sensor. The potential of an ISE is described by the Nernst equation (Equation 2) and can be further simplified as given in Equation 7:

$$E = E^0 + \frac{0.059V}{z_i} \log a_i \quad \text{(Equation 7)}$$

Here, the term $\frac{0.059V}{z_i}$ describes the slope, s = d *E*/ d log a_i , of the linear range of the calibration curve. Theoretically, for monovalent ISEs such as Na^+- and K^+-ISEs, the slope should be 59.2 mV dec^{-1} at 25ºC and for divalent ISEs such as Pb^{2+}- and Cd^{2+}-ISEs, the slope should be 29.6 mV dec^{-1} at 25ºC. In practical situations, the slope can be greater or smaller than the theoretical values at certain activity ranges. Typically, the variations are not more than ± 2 mV, if however the variations are larger than ± 2 mV then the slope of the ISEs is referred to as a "super-Nernstian" and "sub-Nernstian", respectively.

2.2.1.2. Potentiometric selectivity

The selectivity of an electrode refers to its ability to distinguish the primary ion in the presence of other ions, further referred to as interfering ions. The Nikolsky–Eisenmann equation (Equation 8) is used to calculate the selectivity coefficient, $k_{i,j}$, where i refers to primary ion and j refers to interfering ion [96]:

$$E = E_0 + \frac{RT}{z_i F} \ln(a_i + \sum_j k_{i,j} a_j^{z_i/z_j}) \quad \text{(Equation 8)}$$

Methods for the experimental estimation of selectivity coefficients include separate solutions method (SSM), fixed interference method (FIM), fixed primary ion method (FPM), two solution method (TSM), and matched potential method (MPM) [97]. The SSM is one of the most commonly used techniques for the determination of selectivity coefficients. If the EMF recorded in pure "IX electrolyte solution" (I^+ being the primary

ion) and pure "JX electrolyte solution" (J^+ being an interfering ion) at equal ion activity, i.e., $a_i = a_j$, the selectivity coefficient can be written as in Equation 9 [97]:

$$\log K_{i,j}^{pot} = \frac{(E_j - E_i) z_i F}{RT \ln 10} + (1 - \frac{z_i}{z_j}) \log a_i \quad \text{(Equation 9)}$$

If $z_i = z_j$ and slope of the calibration curve is denoted by s, the equation further reduces to Equation 10:

$$\log K_{i,j}^{pot} = \frac{(E_j - E_i)}{s} \quad \text{(Equation 10)}$$

Mixed solution methods such as FIM, FPM, TSM and MPM provide more insight into selectivity of ion-selective electrodes in practical situations. However, SSM was selected as the technique for determination of unbiased selectivity in this thesis since it provides a primary understanding of the behaviour of the ISE before moving on to more complex methods.

2.2.1.3. Response time

The response time of an ISE gives an indication about the time needed for establishing a steady value or near steady value EMF. A faster response time allows for more accurate and precise measurements, particularly in dynamic situations where the ion activity is changing rapidly. Additionally, a faster response time can also improve the overall speed and efficiency of the measurement process. Attempts at quantification of the response time included the introduction of terms such as τ_{90}, the time required for achieving 90 % of the full potential change [98]. The response time of an ISE is dependent on electrochemical reactions at the ISM | solution interface and rates of diffusion of the analyte across different phases [99,100].

2.3. Use of paper-based microfluidics in analytics

Microfluidics is the study of manipulation of fluids at the microscopic scale, typically on the order of micrometres. It involves the development of devices and systems that can handle small volumes of fluid, often with precise control over the flow, mixing, and other properties of the fluid [101]. Paper-based microfluidics or microfluidic paper-based analytical devices (μPADs) is a type of microfluidic technology that uses paper as the substrate for the microfluidic devices. Several types of paper such as chromatography paper, filter paper, ITW Technicloth, printing paper, and paper towels could be used depending on the application [102–104].

This approach has several advantages over traditional microfluidic materials, such as silicon or glass, including low cost, flexibility, biocompatibility, and ease of use [105]. One of the major reasons for the growth of μPADs is the fact that capillary forces can be used for the control of flow rather than using additional pumps. Paper-based microfluidics can be used with different analytical methods such as fluorescent, colorimetric, electrochemical, (electro)chemiluminescent, nanoparticles-based, hybrid and other detection[106], and can be used for the detection of various analytes such as clinically relevant ions, pathogens, heavy metal ions, drugs, metabolites, DNA, proteins, pesticides, and antibiotic residues[107–110].

2.3.1. Paper-based microfluidics in potentiometry

Paper-based microfluidic technologies are used for several purposes in combination with potentiometric ion sensing. Paper can be used as a sampling substrate, used to fabricate a reference electrode or an indicator electrode or even be used to produce an all-integrated sensor for potentiometric sensing [41].

2.3.1.1. Paper as a sampling substrate

Traditional potentiometric sensing with ISEs often relies on beaker-based measurements. Paper-based solution sampling is more advantageous in certain sampling situations due to the unique properties of sampling matrix and extends the use of potentiometry for real life applications. Paper-based solution sampling allows potentiometry to be used in samples with high solid-to-liquid ratios, for example in environmental and food samples. In addition to being able to work with a small volume of sample, the paper substrate used for sampling also protects the membrane of the ISE from mechanical damage due to the presence of solid components in the sample by filtering out the large particles which can damage the fragile ISM. Since paper is a cheaper option compared to beaker-based sampling, it is more useful in situations where disposable sampling is preferred and facilitates usage in countries with limited infrastructure. Paper is a versatile material which can be easily modified with physical and chemical techniques to tailor it to the purpose. The wicking action of paper, i.e. material transport by passive capillary forces, allows it to be used in a wide range of microfluidic sensing platforms [111].

The concept of using paper-based sampling for in situ potentiometry was first introduced by Gyurcsányi et al.[112]. They investigated the possibility of using potentiometric detection instead of the typically employed optical detection of proteins adsorbed onto a paper substrate. This was achieved by using Ag^+ ions as an indirect tag for proteins and quantifying the Ag^+ ion content with the use of an Ag^+-ISE and Ca^{2+}-ISE as a reference electrode.

Research conducted by Bobacka et al.[44] demonstrated the feasibility of potentiometric sensing through paper-based microfluidic sampling, using a solid-contact K^+-ISE and

solid-contact RE to measure the concentration (activity) of K^+ ions absorbed into ordinary filter paper placed vertically between the ISE and the RE. The potentiometric response was found to be dependent on the pore size and the shape of the paper substrate.

Usage of the paper substrate in a horizontal configuration as a sampling substrate for the potentiometric analysis of Cd^{2+}, Cl^-, Pb^{2+} and pH was conducted by Lisak et al.[40]. Even though the potentiometric performance of the paper-based sampling for Cl^- was barely affected with comparison to beaker-based sampling, a super-Nernstian effect was observed in the analysis of Pb^{2+} and Cd^{2+} ions. Pb^{2+} analysis was most affected and further studies indicated that formation of complexes with the functional groups in cellulose could be the reason for the super-Nernstian effect and the higher detection limit observed. Attempts to control the super-Nernstian response observed with Pb^{2+}-ISEs coupled with paper-based sampling include modifying the paper-substrate with inorganic salts[48] and acidification[49].

Additionally, the use of paper as a sampling substrate is advantageous in reducing biofouling effects on the ISE surface. Coating of paper substrates with gold nanoparticles was found to be effective in further reducing the biofouling effects observed with clinical samples[113].

2.3.1.2. Paper as a reference electrode or an indicator electrode

Paper-based electrodes offer several advantages compared to conventional electrodes for potentiometry, including cost-effectiveness, ease of fabrication, flexibility, portability, and rapid analysis.

Fabrication of micro-electrodes on a paper-based platform involves different methods for the preparation of components such as the electronic conductor, the ion-to-electron transducer, the ion selective membrane (in ISEs), or a reference membrane (in REs).

These fabrication methods include screen/stencil printing[114], ink painting[115], sputtering[116], inkjet printing[117], drop-casting[118], or casting by micro-capillary[119], etc. for the deposition of the different components.

The concept of a disposable paper-based strip for determination of ionic species (specifically K^+) by potentiometry was first developed by Borchardt et al.[120]. A filter paper was used as the paper platform and an evaporated silver line was used as the conducting path. A hole was made on the heat-sealing layer surrounding the sensor for the placement of the K^+-ISM. This study demonstrated the feasibility of mass-fabrication of low-cost ISEs which behave similar to macro-electrodes.

Miniaturization of the RE has proved to be more challenging due to issues related to maintaining a stable potential, particularly due to difficulties in deposition of durable and firmly attached Ag/AgCl films, integrating an internal reference electrolyte, and ensuring the presence of a liquid junction. Studies have been conducted to develop robust paper-based Ag/AgCl REs [54,117,121].

Recent advances in paper-based electrodes include ready-to-use sensors for multiplex determination of ions. For example, Armas et al.[122] developed a paper-based ISE and RE combined on a single strip for the determination of Na^+, K^+, and I^- ions. Ongoing research and development in the field of paper-based electrodes are addressing challenges such as limited durability and narrower measurement range and expanding the potential applications of these electrodes.

2.3.1.3. Paper as an all-integrated sensor for potentiometric sensing

The development of paper-based electrodes eventually led to the design of platforms which combine all the elements of a potentiometric sensor, i.e., ISE, RE and sampling platform. This enables the sensors to be conveniently used in cases where on-site

determination of ions is important, e.g. clinical[123,124], environmental[125], and food production[126].

Developing portable readout systems for paper-based sensors is another important and interesting area of research that caught the attention of scientists in this field. These systems often utilize smartphones or handheld devices for signal acquisition, data analysis, and wireless communication. Smartphone integration provides a user-friendly interface, real-time monitoring capabilities, and the potential for remote data sharing, making paper-based sensors accessible and practical for on-site and point-of-care applications. For example, Sakata et al.[127] produced a wearable sensor for determination of pH and Na^+ ion in sweat which employed a wireless interfacial potential detector (IPD) for EMF measurements. Liang et al.[128] utilized a flexible printed circuit board (FPCB) for wireless data acquisition in determination of K^+ in sweat using a three-dimensional paper-based microfluidic electrochemical device (3D-PMED). A trimodal (potentiometric, fluorometric and colorimetric) sensor for detection of the date rape drug "ketamine" was developed by Yehia et al.[129].

2.3.1.4. Limitations of using paper-based microfluidics for potentiometric heavy metal analysis

Despite the numerous advantages of using paper as sampling substrates, electrodes, and all-integrating sensor platforms in potentiometry, it is still an emerging technology with room for improvement, particularly for the sensing of heavy metals. It is important to understand the characteristics of paper as material at this juncture.

Paper is a composite material primarily composed of cellulose fibres (90-99 %) [130]. Fillers added for a variety of purposes such as cost reduction, improving aesthetic appeal, and adjusting the paper-to-paper friction coefficient constitute the second most

abundant material in paper [131]. Materials such as starch and rosin improve the bonding between cellulose fibres and fillers [132]. Pigments can be added to make coloured paper.

Even though different types of paper could be used in paper-based potentiometry, filter[44,48,49,133] and chromatography paper[114,123,134,135] are used most commonly since they can be considered as impurities-free due to their production process. Unlike other types of paper (printing paper, parchment, kraft, etc.), additives which help to reinforce the structure are absent in filter or chromatography paper, and further enables unimpeded performance in analytics[136].

However, the use of filter paper or chromatography paper for quantification of heavy metals by potentiometry is greatly limited by the interactions of heavy metal ions with cellulose fibres, more specifically the negatively charged hydroxyl and carboxyl groups [137]. Paper exhibits adsorption capability for heavy metals and has even been utilized as a raw material for production of adsorbents for heavy metal removal [138,139]. The adsorption characteristics of heavy metals onto cellulose was found to be dependent on the pH and the presence of competing electrolytes[140]. It is essential to control or eliminate unfavourable interactions with cellulose for the successful utilization of paper-based substrates coupled with heavy metal selective ISEs.

When comparing the interactions of different heavy metals with cellulose, and how it affects the potentiometric performance when paper-based substrates are coupled with respective heavy metal selective ISEs, Pb^{2+} analysis was more significantly affected than other heavy metals[40]. Thus, it is hypothesized that if the performance of Pb^{2+}-ISEs coupled with paper-based substrates could be improved, response for the other heavy metals could also be improved.

CHAPTER 3 CHEMICALS, EQUIPMENTS AND METHODS

3.1. Chemicals and materials

Chemicals and materials used in the experiments (obtained in analytical grade unless otherwise mentioned) are mentioned in Table 3.1.

Table 3.1 Chemicals and materials used in the experiments

Chemical/material	**Supplier**
Nitrates of Mg^{2+}, Ca^{2+}, Na^{+}, K^{+}, Ba^{2+}, Zn^{2+}, Co^{2+}, Cd^{2+}, Cu^{2+} and Pb^{2+}	Sigma Aldrich (Germany)
Sodium polystyrene sulfonate (NaPSS)	Sigma Aldrich (Germany)
3,4-ethylenedioxythiophene (EDOT)	Sigma Aldrich (Germany)
Lead ionophore IV (tert-Butylcalix[4]arene-tetrakis(N,N-dimethylthioacetamide))	Sigma Aldrich (Germany)
Potassium tetrakis(4-chlorophenyl) borate (KTClPB)	Sigma Aldrich (Germany)
2-nitrophenyl octyl ether (o-NPOE)	Sigma Aldrich (Germany)
High molecular weight poly(vinyl chloride) (PVC)	Sigma Aldrich (Germany)
Tetrahydrofuran (THF)	Sigma Aldrich (Germany)
Grade 388, 390 quantitative cellulose filter paper	Sartorius (Germany)
3mm diameter glassy carbon (GC) disk electrode encased in Teflon body (6 mm outer diameter)	X2Lab (Singapore)

Ag/AgCl (3 M KCl) reference electrode	BAS (Japan)
Gold (99.999%), platinum (99.95%) and palladium (99.95%) sputtering targets	ACI Alloys (USA)
Lead calibration standard (1000 μg/ml dissolved in 2% HNO_3)	PerkinElmer, Inc. (USA)
Instrument calibration standard 2 for inductively coupled plasma-optical emission spectrometry	PerkinElmer, Inc. (USA)

3.2. Equipment utilized

Equipment utilized for the experiments conducted in this thesis are listed in Table 3.2.

Table 3.2 Equipment utilized

Equipment	**Supplier**
Milli-Q Integral 10 Water Purification System	Sigma Aldrich (USA)
Gamry interface 1000 potentiostat	Gamry Instruments Inc.(USA)
Sputter coater (JFC-1600)	JEOL (Japan)
EMF16 Interface potentiometer	Lawson Labs Inc.(USA)
Field emission scanning electron microscope (FESEM) (JSM-7600F)	JEOL (Japan)
OCA 15 goniometer	Dataphysics (Germany)

Optima 8300 Inductively Coupled Plasma Optical Emission Spectroscopy (ICP-OES)	PerkinElmer, Inc. (USA).
Tensor 27 Fourier Transform infrared spectroscope	Bruker
Profilometer (Tencor P-6)	KLA

3.3. Methods

3.3.1. Preparation of ion selective electrodes

For the preparation of solid-contact Pb^{2+}-ISEs, the glassy carbon (GC) electrodes were first polished on a polishing pad using 0.3 μm alumina slurry (Al_2O_3) and then rinsed with ultra-pure water. The electropolymerization of PEDOT(PSS) on electrodes was conducted in a three-electrode cell, where a platinum electrode served as the counter electrode and Ag/AgCl (3 M KCl) served as the reference electrode. Chronopotentiometry mode on Gamry interface 1000 potentiostat (Gamry, USA) was used to apply a constant current of 0.014 mA (0.2 mA cm^{-2}) for 714 s [141]. The electrolyte for the electropolymerization of conducting polymer film contained 0.01 M EDOT and 0.1 M NaPSS. At the conclusion of electropolymerization, the electrodes were rinsed with ultra-pure water and left at room temperature (23 ± 2 ˚C) to dry overnight. For the membrane drop-casting, a Pb^{2+} selective membrane cocktail containing 1% lead ionophore IV, 0.5% KTClPB, 65.2% o-NPOE and 33.3% PVC (i.e., 1 mg of lead ionophore IV, 0.5 mg KTClPB, 62.69 μL o-NPOE and 33.33 mg PVC) in 2ml of THF was used. Three doses of 20 μL of membrane cocktail portions were casted on top of the dry PEDOT (PSS) layer with 1 hour gap between each dose applied. After

overnight drying of the ion-selective membrane, the ISEs were transferred to 10^{-3} M $Pb(NO_3)_2$ for 24 h for electrodes conditioning. The ISEs were stored in the same solution in between measurements. Basic steps in the preparation of an ISE are shown in Figure 3.1.

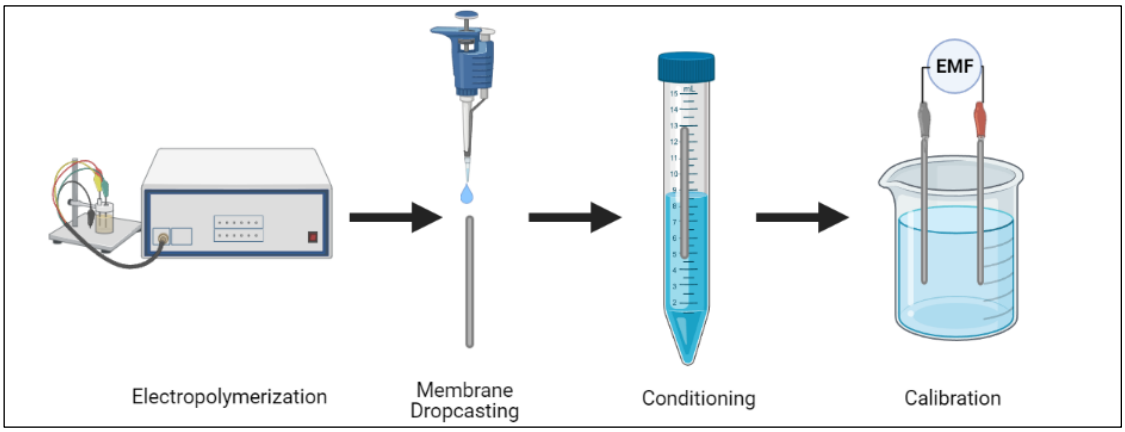

Figure 3. 1 Schematic of steps followed in making a Pb^{2+}-ISE.

3.3.2. Preparation of paper substrates

For the paper substrate preparation, filter paper (Sartorius grade 388 unless otherwise mentioned) was soaked in ultra-pure water for 30 min with gentle stirring to reduce water soluble contaminants and then oven-dried at 70°C before being used as microfluidic paper substrates. Paper substrates were used then in unmodified, and modified arrangements.

3.3.3. Potentiometric measurements with Pb^{2+}-ISEs.

EMF16 Interface potentiometer, Lawson Labs Inc. assisted with EMF16_grf software was used to carry out the potentiometric measurements and the response of Pb^{2+}-ISEs in each solution was logged for 1 minute. The response of Pb^{2+}-ISEs in lead(II) nitrate solutions ranging from $10^{-7.0}$ to $10^{-1.4}$ M in ion activity was analysed in ascending order of primary ion activity. The activity coefficients were calculated according to the Debye-Hückel approximation [94]. Three same measurements from each ion activity

were performed to obtain uncertainty of the measurement in form of the standard deviation (n= 3). Standard deviations in figures and text indicate measurement-to-measurement repeatability for an electrode unless otherwise stated.

Once the conventional beaker-based potentiometric cell response was validated, i.e., electrodes exhibited Nernstian response (slope 29.6 ± 2 mV dec^{-1}), these electrodes were selected to be coupled with the paper-based microfluidic solution sampling. In such measurements, the indicator and the reference electrodes were both placed on top of one piece of filter paper that was previously cut into 2 × 2 cm^2 and which was exposed to the standard or sample solutions (assuring a volume of solution equal to maximum holding capacity of the paper substrate was wicked to the matrix of the paper substrate) as shown in Figure 3.2. The electrodes, supported onto laboratory stand were placed onto the paper substrate, such that no additional force was applied to keep electrodes onto the paper substrate. The EMF of the cell was logged for 1 minute with 1.3 s interval between each potential sampling.

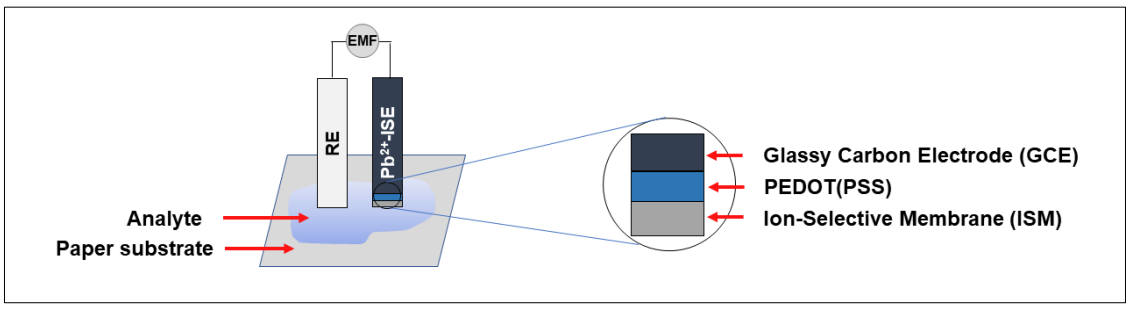

Figure 3. 2 Schematic of set-up used for potentiometric sensing coupled with a paper substrate.

3.3.4. Characterization methods

3.3.4.1. Inductively coupled plasma optical emission spectrometry (ICP-OES)

ICP-OES was used as the established analytical technique to validate the results of paper-based potentiometry. Perkin Elmer Optima 8300 Inductively Coupled Plasma Optical Emission Spectroscopy (ICP-OES) was used for the determination of total lead concentrations. Samples were filtered with 0.45 µm filter and diluted with nitric acid prior to analysis.

3.3.4.2. Field emission scanning electron microscopy (FE-SEM) and energy dispersive X-ray spectroscopy analysis (EDXA)

Electron microscopy was used for the investigation of surface morphology, topography, and composition of paper substrates. Compared to a light microscope, an electron microscope provides images of higher magnification and resolution by scanning the surface of the material with a fine focused beam of electrons. A field emission scanning electron microscope (FESEM) (JSM-7600F, JEOL, Japan) along with energy dispersive X-ray spectroscope (EDX) was used to study the surface and cross section of unmodified and modified paper substrates.

3.3.4.3. Fourier-transform infrared spectroscopy (FTIR)

FTIR spectroscopy uses infrared radiation to analyze a sample and generates spectra that can provide insight into the different chemical structures present in the sample [142]. Tensor 27 Fourier Transform infrared spectroscope (FTIR) operated in attenuated total reflection (ATR) mode was used to investigate the chemical changes in the paper substrate after modification. To do that, the paper substrates were crushed using mortar and pestle before investigation so that the sample could be homogenized instead of

investigating only the surface properties of the paper substrates. The FTIR was also done on unmodified paper substrates.

3.3.4.4. Assessment of hydrophobicity/hydrophilicity

Hydrophobicity/hydrophilicity of a material refers to its nature of affinity to water molecules. It is generally accepted that the static water contact angle being greater than or less than 90º can characterize a material as being hydrophobic (repelling water) or hydrophilic (attracting water). Dataphysics OCA 15 goniometer (Germany) equipped with SCA20 software was used to evaluate the hydrophobicity/hydrophilicity of the paper surface. Hamilton Gastight Syringe (500 µl) was used to deposit an ultrapure water droplet of 5 µL onto the sample. The contact angle was determined using the Sessile Drop method and three measurements were taken on different parts of the paper to investigate the uncertainty of the measurements.

3.3.4.5. Assessment of liquid absorption capacity

Liquid absorption capacity refers to the ability of a material to absorb a liquid. Since aqueous samples are commonly used for potentiometric measurements, liquid absorption capacity of paper substrates was evaluated by immersing a 1×1 cm^2 paper into ultra-pure water for 5 s and determining the mass change.

CHAPTER 4 NON-EQUILIBRIUM POTENTIOMETRIC SENSORS INTEGRATED WITH METAL MODIFIED PAPER-BASED MICROFLUIDIC SOLUTION SAMPLING SUBSTRATES FOR DETERMINATION OF HEAVY METALS IN COMPLEX ENVIRONMENTAL SAMPLES

4.1. Introduction.

Sensing heavy metals in environmental samples is important because it allows for the identification and quantification of heavy metal contamination in various environmental matrices, such as soil, water, and air. Heavy metal pollution is a significant environmental concern as it can lead to a wide range of ecological and human health impacts[22]. Paper-based potentiometry offers several advantages over existing methods for determining heavy metals, making it a promising option for environmental monitoring and other applications[46]. However, their use is limited due to unfavourable interactions between the negatively charged paper substrate and the heavy metal cations which causes a super-Nernstian response[40].

This study investigates the effect of modifying the paper substrates with thin layers of metals that can act as possible spacers between the ISM and the negatively charged paper substrates or as modifiers of cellulose fibers to block active adsorption sites on the paper substrates. The potentiometric response of Pb^{2+}-ISEs coupled with microfluidic solution sampling substrates modified with different metal layer thicknesses of gold, platinum, and palladium were investigated. Since using a modified paper-based substrate is likely to increase the lifetime of an electrode, a durability study was conducted. The data obtained from the study was also used for a detailed life cycle

assessment (LCA). However, screen-printed electrodes were considered for the LCA since they are smaller, portable, reproducible, and more likely to be used in large scale/commercial applications, compared to conventional macro electrodes used in research community. Thus, a comparative LCA of a model screen-printed lead(II)-selective electrode equipped with conventional carbon working electrode (CWE) and poly(3.4-ethylenedioxythiophene) doped with polystyrene sulfonate (PEDOT(PSS)) solid contact coated with Pb^{2+}-ISM coupled with paper substrates modified with a layer of metal were conducted to study their respective environmental footprints as compared to same electrode used without microfluidic paper-based solution sampling.

4.2. Experimental

4.2.1. Preparation of ion-selective electrodes and microfluidic paper substrates.

Ion-selective electrodes and paper substrates were prepared as described in section 3.3. For metal modified paper substrates, a sputter coater (JFC-1600, JEOL, Japan) was used to deposit different thicknesses of a layer of metal (either gold, platinum, or palladium) on top of one or both sides of paper substrates. For each sputtering run, 40 mA current was applied at 3 Pa while varying the time of sputtering to achieve different thicknesses of metal on paper substrates. The paper substrates were named as "X nm Y modified paper substrate (Z side/s modified)", where X refers to thickness of metal layer, Y refers to type of metal, and Z refers to whether the modification was single side or double side (e.g., "38 nm Au modified paper substrate (both sides modified)").

4.2.2. Potentiometric measurements with Pb^{2+}-ISEs.

Initially, potentiometric response on paper sputtered on one side with gold was investigated, followed by the response on paper sputtered with metal on both sides. The

measurements were conducted in comparison to Pb^{2+}-ISEs coupled with unmodified paper substrates.

4.2.3. Durability of Pb^{2+}-ISEs when coupled with and without paper-based microfluidic solution sampling substrates in sample containing high solid-to-liquid ratio.

In order to compare the durability of electrodes at different measurement conditions performed on samples with high solid-to-liquid ratios, complex environmental sample (soil collected and conditioned in 10^{-2} M Pb^{2+}) was used with and without paper substrate. The Pb^{2+}-ISEs were either directly placed in contact with complex environmental sample or were placed in contact with a 38 nm Au modified paper substrate (both sides modified). In details, 10 g of potting soil was placed on a petri dish and 30 ml of 0.01 M $Pb(NO_3)_2$ solution was added. The sample was allowed to equilibrate at room temperature overnight. Electrodes were placed on the petri dish such that three electrodes touched the soil directly while three more electrodes were in contact with a 38 nm gold modified paper substrate (both sides modified) placed on top of soil as shown in Figure 4.1. The reference electrode was placed on paper to avoid possible damage and clogging solution junction of the electrode. The potentiometric response for each electrode was logged as described in section 3.3.3. After each measurement, the electrodes were rinsed and wicked dry before taking another measurement. The steps were repeated until an electrode lost its membrane, or its potential response indicated a flaw in the membrane at which point the particular electrode was removed from the system.

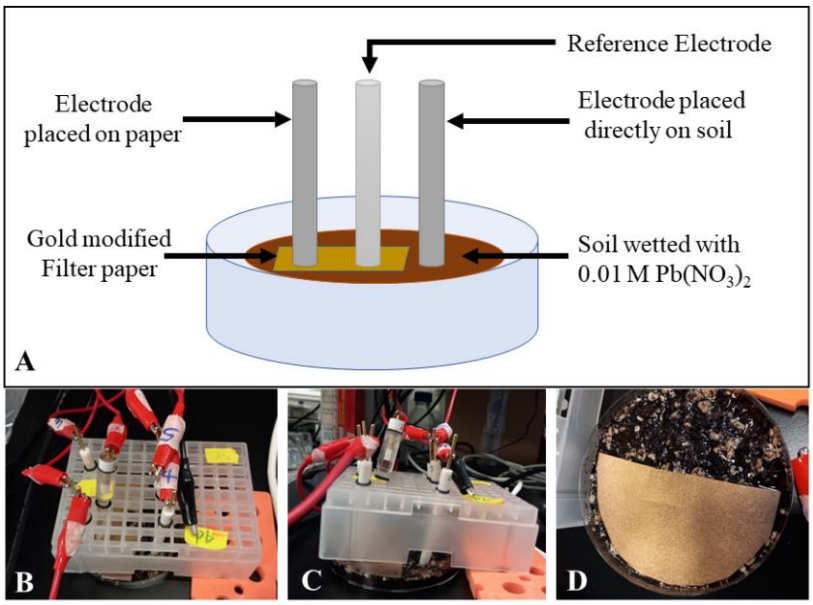

Figure 4. 1 Measuring setup used in durability test of Pb^{2+}-ISEs. (A) Schematic diagram (B) Top view of the actual setup (C) Side view of the actual setup (D) Gold modified paper placed on soil.

4.2.4. Determination of lead(II) in environmental samples.

In order to validate using metal modified paper substrates in environmental samples, four samples were prepared for investigation. All the samples were spiked with random amounts of lead(II) nitrate solutions. The first sample was a leaf soaked in lead solution to mimic the deposition of heavy metals on plants and was named as “plant dew” sample. Graphite powder was added to the solution in another sample to simulate a chemical spill condition. Soil was dispersed in another sample to simulate accumulation of lead in industrial sites and named as “wet soil” sample. The final sample was prepared to simulate street runoff which can contain lead from different sources.

A 38 nm gold modified paper substrate (both sides modified) was used for the paper-based measurements using Pb^{2+}-ISEs. The potentiometric response for each electrode was logged as described in section 3.3.3. Perkin Elmer Optima 8300 Inductively Coupled Plasma Optical Emission Spectroscopy (ICP-OES) was also used to determine

the total lead concentration in the samples so that the two different techniques could be compared.

4.2.5. Life cycle assessment (LCA).

The LCA was conducted using the ISO14040 and ISO14044 standards [143]. The goal of the LCA was to determine the environmental impacts of model screen-printed potentiometric sensor (CWE) (same arrangement for ISM and ion-to-electron transducer as macro Pb^{2+}-ISEs introduced above) and with an additional layer of metal modified paper substrate. The screen-printed electrodes were prepared for potentiometric measurement with methods mentioned in section 3.3.1 for glassy carbon electrodes, with PEDOT(PSS) acting as an ion-to-electron transducer [144]. The individual components were as follows: ceramic substrate as a base layer, graphite as the working electrode, silver as electric contact, plastic layer to encase the components, PEDOT(PSS) and ISM layers. The layout is illustrated in Figure 4.2A. A gold modified paper substrate was placed on the top of the ISM layer when studying the effect of using a modified paper substrate. The scope of the LCA included the production footprints of the studied potentiometric sensors. The functional unit (FU) of the LCA was fixed as one potentiometric measurement of Pb^{2+}-ISE in prepared simulated environmental sample. IPCC AR5 and ReCiPe midpoint methods were applied for the impact assessment. Life cycle inventories (LCI) were built based on a model screen-printed carbon electrode from Metrohm (Dropsens) as shown in Figure 4.2. The mass of the individual components was estimated based on the physical dimensions and the experimental procedure of ISM preparation (Table 4.1). The LCA was conducted on the assumption that the number of ISE reuses are independent of the construction of the ISEs and paper metal modifications. A profilometer (KLA Tencor P-6) was used to determine the thickness of various components of the sensor. Furthermore, a sensitivity analysis with

three different masses of metal coatings were studied to determine its influence on the environmental impacts.

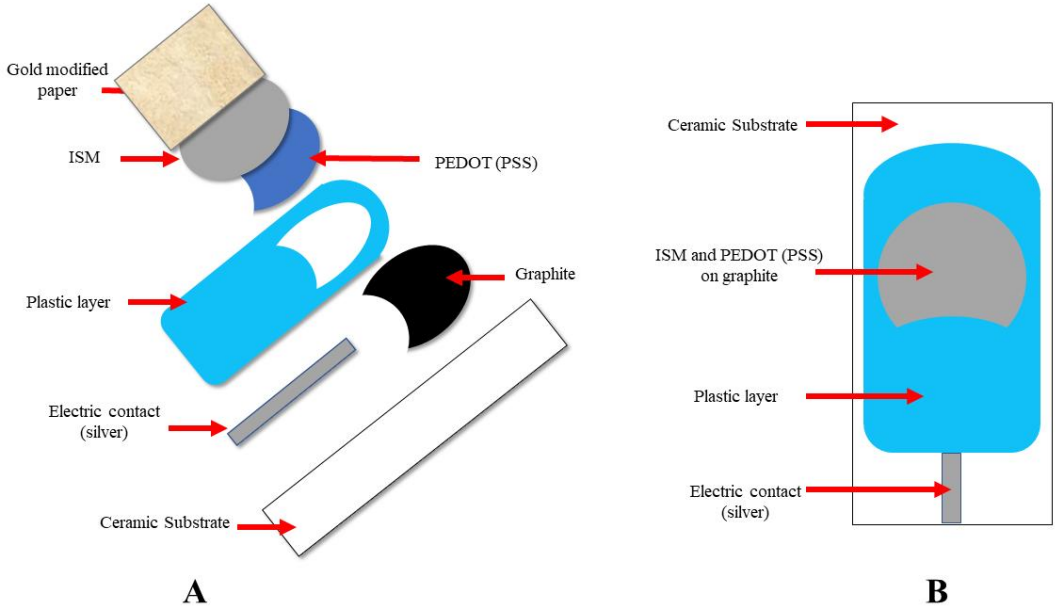

Figure 4.2 Construction of model screen-printed electrode Pb^{2+}-ISE (CWE) used for LCA. (A) CWE detailed components description, including gold modified paper substrate as part of the CWE arrangement (gold modified paper substrate was removed for LCA of electrodes used in conventional manner, i.e., directly contacting sample) and (B) Assembled model screen-printed electrode used as Pb^{2+}-ISE (CWE).

Table 4. 1 Life cycle inventory data for the potentiometric sensor.

Material components	**Unit**	**Quantity per sensor**
Ceramic	g	4.250×10^{-1}
Graphite (Working Electrode)	g	3.974×10^{-4}

Ag (Electric Contacts)	g	1.343×10^{-3}
Plastic layer	g	3.680×10^{-3}
PEDOT(PSS)	g	5.825×10^{-6}
ISM	µl	6.000×10^{1}
Paper as substrate	g	3.360×10^{-2}

Metal coating on paper substrate				
Thickness of metal	nm	25	38	50
Mass of Au	g	1.21204×10^{-5}	1.81806×10^{-5}	2.42408×10^{-5}
Mass of Pt	g	8.06352×10^{-6}	1.20953×10^{-5}	1.61270×10^{-5}
Mass of Pd	g	6.35222×10^{-6}	9.52833×10^{-6}	1.27044×10^{-5}

4.3. Results and discussion.

4.3.1. Paper based potentiometric solution sampling using gold modified paper substrates.

When cellulose-based paper substrates are used as a solution sampling substrate coupled with potentiometric sensors sensitive to heavy metals, usually a super-Nernstian response of the ISEs is observed. This occurs due to the alteration of the primary ion concentration at the ISM | solution interface due to the ion interactions with negatively charged sites on the paper substrate [145,146]. Thus, if the surface of the paper substrate

is modified such that the negatively charged sites on the paper substrate become unavailable to the primary ions while preserving the beneficial qualities of the paper substrates, the super-Nernstian response can be eliminated or controlled. Different approaches to eliminate super-Nernstian response of heavy metal selective electrodes were previously investigated, namely by modifying paper substrates with primary and interfering ions [48] and acidification of the paper substrates [49]. These, however, require chemical modification of the paper substrate before actual implementation that can be time and resource consuming.

Interestingly, except of specific applications in heavy metal sensing, paper based microfluidic solution sampling was also considered for analysis of clinically relevant ions, such as potassium, sodium, and chloride. Recently paper-based substrates modified with gold nanoparticles (AuNPs) and sputtered gold were used in order to improve response of the ISEs in biofouling conditions [113]. In this study, AuNP modified papers were found to be more successful in slowing down/diminishing the protein transport across the paper-based substrate. It was also observed that gold sputtered paper substrates had increased hydrophobicity and facilitated longer response time of ISEs owing to the sputtered layer, which acted as a physical barrier for the solution to easily pass through the paper substrate. This effect can be explored for heavy metal paper-based determination as sputtered gold can be considered as viable physical modification of the paper substrate allowing controlling the functionality of the paper substrate in relation to the presence of heavy metals in the sample solution. With this in mind, the modification of the paper substrate with metallic gold was investigated to identify if layers of metals can act as a spacer between the ISM and the negatively charged paper substrates or if metal layer can act as modifiers of cellulose fibers to block active adsorption sites on the paper substrates. Thus, the paper substrates were modified

such that only one side of the paper substrate was sputtered with metallic gold. Different sputtering times were used to achieve different thicknesses of gold layer on the paper substrates to investigate whether the thickness of the metal layer influenced the potentiometric response of Pb^{2+}-ISEs. In such way, thicker the gold layer at the surface of the paper substrate, greater the distance between the ISM and the negatively charged paper matrix. Since the gold sputtering time is directly proportional to the thickness of the metal layer, provided that other parameters such as distance from target remain constant [147], the gold layer thicknesses were estimated to be 10, 15, 25, 38 and 50 nm at 2, 3, 5, 7.5 and 10 mins of metal sputtering times, respectively. The estimated thickness of gold was further verified experimentally by measuring the mass of a known area of paper substrate before and after metal sputtering. The experimentally determined thickness of gold deposition rate was found to be approximately 5.2 nm per minute, which correlates well with the theoretical estimation.

According to Figure 4.3, potentiometric responses of Pb^{2+}-ISEs coupled with gold-modified substrates (at different gold layer thicknesses) were found to be similar to the lead(II)-selective electrode coupled with unmodified paper substrates, namely exhibiting a super-Nernstian response which was mainly registered between $10^{-3.06}$ and $10^{-4.02}$ M Pb^{2+}. Detailed description of the potentiometric response of studied Pb^{2+}-ISEs, namely their slopes and low detection limits are provided (Table 4.2). In this measurement setup, the gold layers have been facing the ISM, providing different spacer thicknesses between the ISM and the negatively charged paper substrates. Since the potentiometric response of Pb^{2+}-ISEs was not improved as compared to the one obtained with unmodified paper substrate, subsequently the potentiometric response when using the paper substrate such that the gold layers were inverted (gold layers facing the sample) was also investigated (Figure 4.4 and Table 4.2).

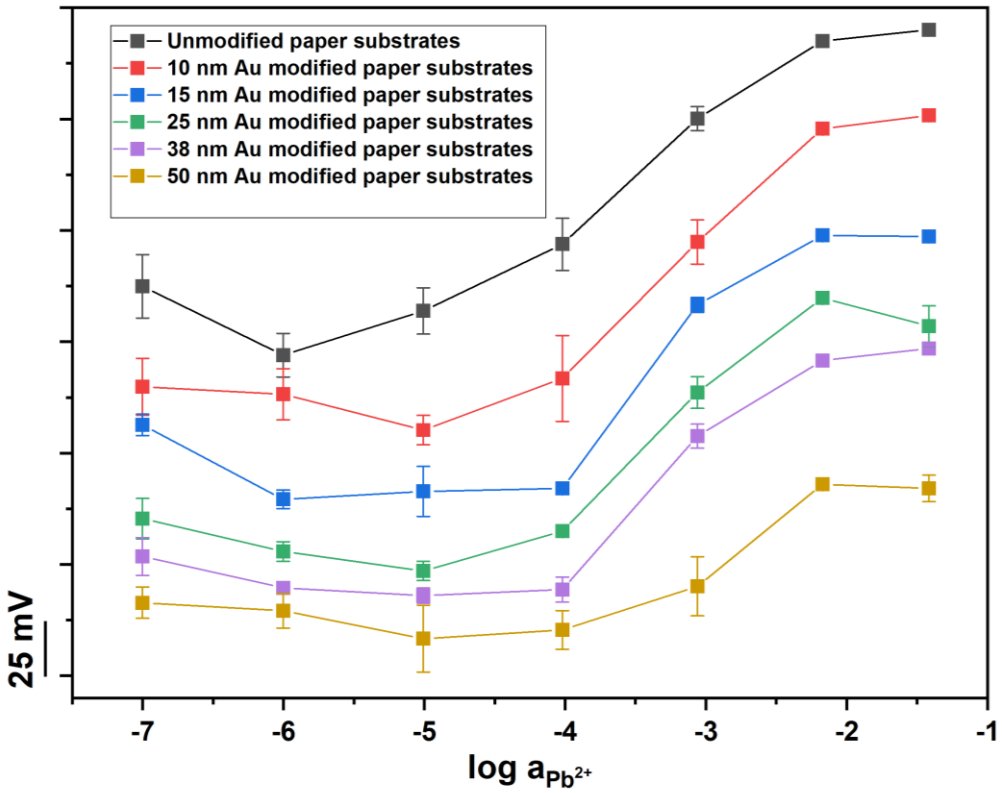

Figure 4.3 Potentiometric response of Pb^{2+}-ISEs coupled with paper substrates without and with metallic gold modifications of various thicknesses on one side of the paper substrates (facing ISM).

Table 4. 2 Detection limits and slopes of Pb^{2+}-ISEs coupled with unmodified and metallic gold modified paper substrates (single side modified).

ISEs/paper substrates	**DL (log a)**	**Slope between $10^{-2.17}$ and $10^{-3.06}$ M Pb^{2+} (mV dec^{-1})**	**Slope between $10^{-2.17}$ and $10^{-4.02}$ M Pb^{2+} (mV dec^{-1})**
In solution	-6	25.0 ± 0.2	30.8 ± 0.3
unmodified	-N.D.*	39.2 ± 6.8	58.8 ± 17.2
10 nm thickness + gold touching ISM	-4.5	57.3 ± 11.9	63.8 ± 28.8

10 nm thickness + sample touching ISM	-5	31.5 ± 1.3	40.5 ± 10.8
15 nm thickness + gold touching ISM	N.D.*	35.1 ± 4.4	85.9 ± 3.6
15 nm thickness + sample touching ISM	N.D.*	29.1 ± 14.9	69.4 ± 5.8
25 nm thickness + gold touching ISM	N.D.*	47.8 ± 8.7	64.9 ± 7.6
25 nm thickness + sample touching ISM	-5	26.3 ± 4.3	62.6 ± 8.8
38 nm thickness + gold touching ISM	N.D.*	38.3 ± 3.3	71.8 ± 4.8
38 nm thickness + sample touching ISM	N.D.*	34.3 ± 6.0	58.8 ± 7.9
50 nm thickness + gold touching ISM	N.D.*	51.5 ± 16.8	20.4 ± 13.3
50 nm thickness + sample touching ISM	-4.5	35.1 ± 2.1	55.1 ± 1.4

*Not determined, owing to non-linear behaviour of the calibration curve

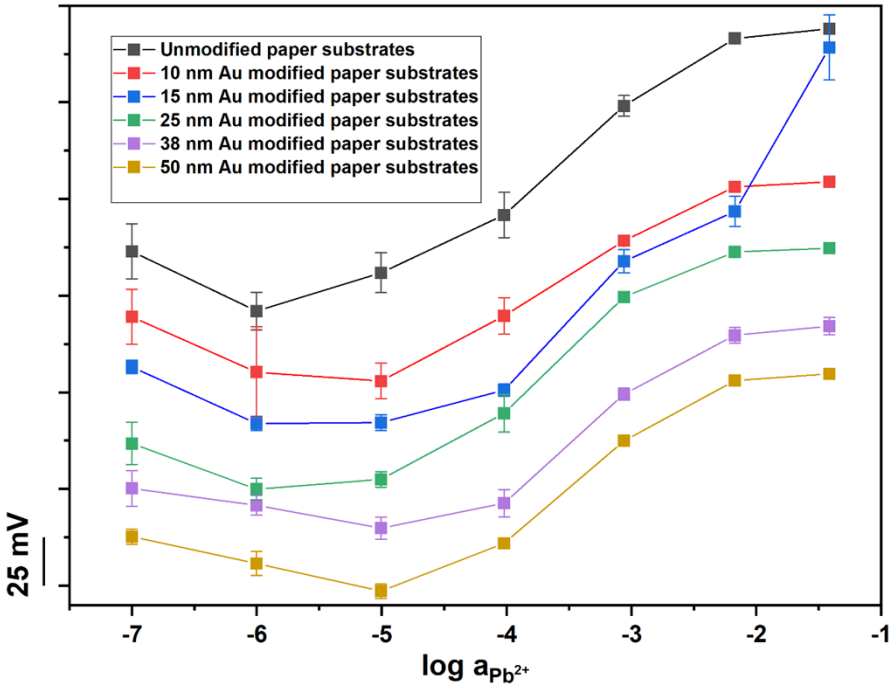

Figure 4. 4 Potentiometric response of Pb^{2+}-ISEs coupled with paper substrates without and with metallic gold modifications (single side modified). The gold modified side was inverted such that the gold surface was facing the sample.

Similarly, to the previous results, they too exhibited a significant super-Nernstian response. The results indicate clearly that purely creating a spacer in form of metal between ISEs and the negatively charged paper substrates does not improve electrodes response to the analyte and thus simplifies the ISM | papers substrate | sample solution interface to be predominantly influenced by the solution-paper substrates interactions, unrelated to the proximity of the ISE to the paper substrate. Simply, since the volume of the analyte is extremely low (µL) the depletion of ion concentration from the solution driven by paper substrate interactions results in its unavailability to the ISEs. Interestingly for both types of paper modifications with gold (modification to either side of the paper substrate), the super-Nernstian response was found to be slightly changing depending on the gold thickness applied. This indicated the possibility of using noble metals for modification of surface of the wood fibres, to eliminate cellulose

functionalities and fibres adsorption sites from participating in sorption of primary ion from the standards and sample solutions. For that reason, further exploration based of paper substrates modifications with metal layers on both sides were investigated.

4.3.2. Potentiometric response of Pb^{2+}-ISEs coupled with paper substrates modified with different thicknesses of metallic gold on both sides of the paper substrates.

Similar to previously investigated one-side gold-paper modifications in the use as microfluidic solution sampling substrates, here, both-side paper substrates modifications with different thicknesses of metallic gold were investigated. The potentiometric responses of Pb^{2+}-ISEs coupled with gold modified paper substrates (both sides modified) are shown in Figure 4.5. The slopes recorded in the $10^{-2.17}$ and $10^{-3.06}$ M Pb^{2+} and $10^{-3.06}$ and $10^{-4.02}$ M Pb^{2+} ranges for metal thicknesses of gold ≥25 nm (Table 4.3) were found to be similar to each other, yet still super-Nernstian as compared to the conventional beaker-based measurements. In comparison, the slopes in the same concentration ranges for unmodified and both sides gold modified with thicknesses of ≤ 20 nm were found inconsistent which translated to nonlinear calibrations curves, with higher super-Nernstian response in the $10^{-3.06}$ and $10^{-4.02}$ M Pb^{2+}. It can be noted that some thicknesses of gold on the paper substrates, particularly 25, 38 and 50 nm, facilitated favourable potentiometric response of Pb^{2+}-ISEs (linear calibration curves in extended lead(II) activity range). For example, 25 nm and 50 nm gold modified paper substrates (both sides modified), coupled with Pb^{2+}-ISE, resulted in linear sensor response in the range of $10^{-4.02}$ to $10^{-2.2}$ M $Pb(NO_3)_2$ with slopes of 43.5 ± 4.6 and 43.9 ± 2.3 mV dec^{-1}, respectively. The use of 38 nm gold modified paper substrate (both sides modified) was found to be particularly advantageous since it resulted in closer to the Nernstian response for Pb^{2+}-ISEs. It showed a linear response of 31.3 ± 1.4 mV dec^{-1} in

the range of $10^{-5.0}$ to $10^{-2.2}$ M $Pb(NO_3)_2$. The lower detection limits for 25, 38 and 50 nm Au modified paper substrates (both sides modified) were $10^{-4.5}$, 10^{-5} and 10^{-4} M Pb^{2+}, respectively. The low detection limits were found comparable to other types of modifications of paper substrates [48,49].

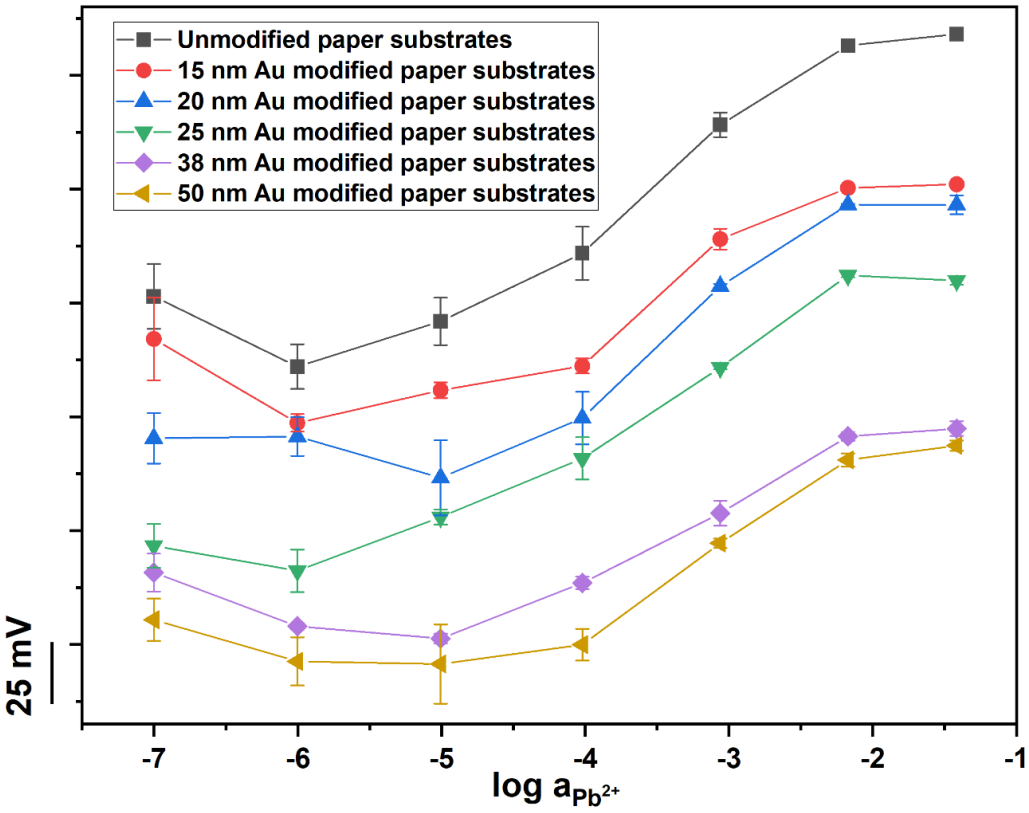

Figure 4. 5 Potentiometric response of Pb^{2+}-ISEs coupled with paper substrates without and with metallic gold modifications of various thicknesses on both sides of the paper substrates.

Table 4. 3 Detection limits and slopes of Pb^{2+}-ISEs coupled with unmodified and with metallic gold modifications of various thicknesses on both sides of the paper substrates.

ISEs/paper substrates	**DL (log a)**	**Slope between $10^{-2.17}$ and $10^{-3.06}$ M Pb^{2+} (mV dec^{-1})**	**Slope between $10^{-3.06}$ and $10^{-4.02}$ M Pb^{2+} (mV dec^{-1})**
In solution	-6	25.0 ± 0.2	30.8 ± 0.3

unmodified	N.D.*	39.2 ± 6.8	58.8 ± 17.2
15 nm gold (both sides)	N.D.*	25.3 ± 5.1	58.1 ± 8.0
20 nm gold (both sides)	-4.5	40.4 ± 0.9	60.3 ± 10.9
25 nm gold (both sides)	-4.5	45.6 ± 1.3	41.6 ± 10.2
38 nm gold (both sides)	-5	38.0 ± 7.8	31.9 ± 8.2
50 nm gold (both sides)	-4	41.1 ± 2.8	46.5 ± 5.8

*Not determined, owing to non-linear behaviour of the calibration curve

The relationship between the gold thickness and super-Nernstian response of Pb^{2+}-ISEs (between $10^{-3.06}$ and $10^{-4.02}$ M Pb^{2+}) when coupled with both side modified paper substrates is visualized in Figure 4.6. It can be deducted that the super-Nernstian response is reduced when using gold modified paper substrates as compared to unmodified paper substrates, and that there is an optimum range of metal thickness at which the super-Nernstian response is the lowest (thickness ≥ 25 nm gold modified paper substrates on both sides). It can be assumed that nearly full coverage of the accessible negative sites on paper surface can be achieved at 25 nm gold layer thickness, and higher thicknesses of metal layers simply deposit on top of the already established metal layers without significantly blocking the negatively charged sites inside the bulk of the paper substrates. To validate that further characterization of the paper substrates was performed.

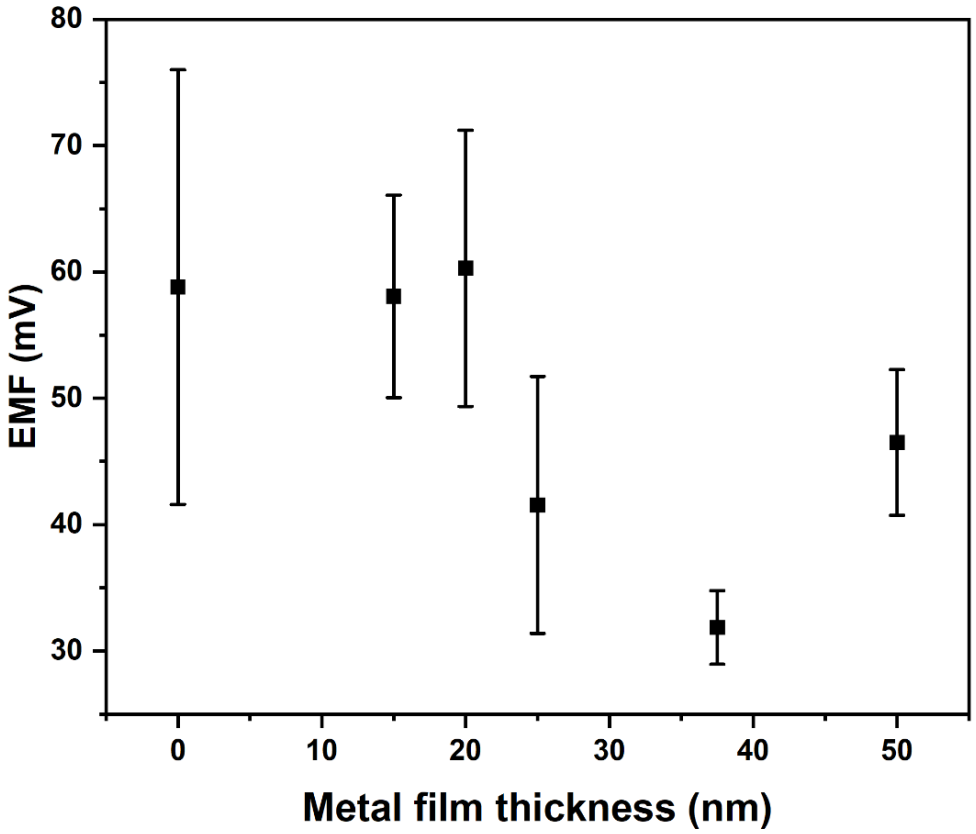

Figure 4. 6 Super-Nernstian response of the Pb^{2+}-ISEs between $10^{-3.06}$ and $10^{-4.02}$ M Pb^{2+} for measurements done with unmodified and gold modified paper substrates (both sides modified)

4.3.3. Characterization of gold modified paper substrates.

The gold modified paper substrates (both sides modified) were subjected to characterization procedures to shed more light on their performance as solution sampling matrices for potentiometric ion determination when coupled with Pb^{2+}-ISEs. As shown in Figure 4.7, the surface images indicate that most of the surface was covered by the metal, while leaving some pores (indicated by the three-dimensional arrangement of wood fibres in the paper substrates) for the transportation of analytes. This suggests that the favourable quality of paper substrates being able to absorb the solution is preserved while blocking much of the negatively charged sites on the paper substrates. When observing the cross-section images, it can be seen that the metal layer (coloured in grey) penetrates to some depth of the paper substrates, leaving some of the middle

region of the paper (coloured in white) unmodified. Thus, a paper substrate modified on both sides will have the metal layers sandwiching a thin layer of unmodified paper.

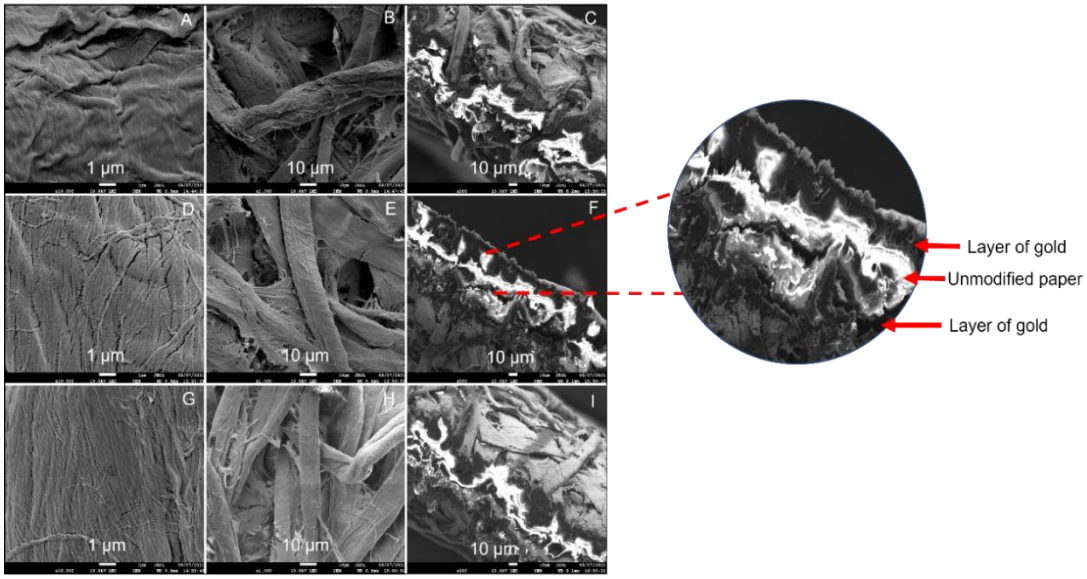

Figure 4. 7 SEM images for gold modified paper substrates (both sides modified) (A, B, C are 25 nm Au modified paper; D, E, F are 38 nm Au modified paper and G, H, I are 50 nm Au modified paper. Images A, B, D, E, G, H are surface images whereas images C, F, I are cross section images).

This may be seen as limitation of using surface modification, as the sputtered metal cannot penetrate throughout the paper substrate. In fact, however, the possibility of having partially unmodified region in the middle of the paper substrates may be beneficial for assuring successful solution sampling. The unmodified part of the paper substrates provides vital analyte sorption capability, as paper was found previously to be able to wick significant sample volumes [136]. Naturally, having unmodified paper substrates means the response of the ISEs sensitive to heavy metals may be uncontrollable and super-Nernstian. Thus, in scope of this work, the thickness of the gold modification was optimized to (i) allow solution sampling via unmodified paper substrate sandwiched between gold modified regions and (ii) control the response of the Pb^{2+}-ISEs to maintain extended linear behaviour (although super-Nernstian) that would

allow determination of ions in specific sample type. Thus, having unmodified paper region in the paper substrate is a calibrated trade-off between controllable Nernstian and super-Nernstian responses of Pb^{2+}-ISEs. It was proven before that ISEs can be found useful, even if their response is super-Nernstian provided that their response is controllable [148]. Further to that, the EDS was conducted and presented in Figure 4.8 to further indicate the presence of channels for solution to pass through the gold modification. This was done by elemental mapping of carbon that is expected to be coming from cellulose amidst the gold modified surface. For comparison unmodified paper substrate was also investigated (Figure 4.9) where only carbon and oxygen were detected, without the presence of the gold. In Figure 4.9, it can be clearly seen that carbon mapping revealed uniformly redistributed sampling solution channels. These were possible to be formed because the paper substrates have 3D structure consisting of the wood fibres that are impossible to be fully covered by one directional surface modification, such as metal sputtering. It is also interesting to note that the availability of channels is evidently getting lower with the increasing thickness of gold layers, as further build-up of the sputtered gold was able to close smaller solution sampling channels. The availability of the sampling channels is expected to influence the response of the Pb^{2+}-ISEs. For that reason, surface properties of paper substrates and potentiometric response of ISEs when coupled with these substrates were investigated.

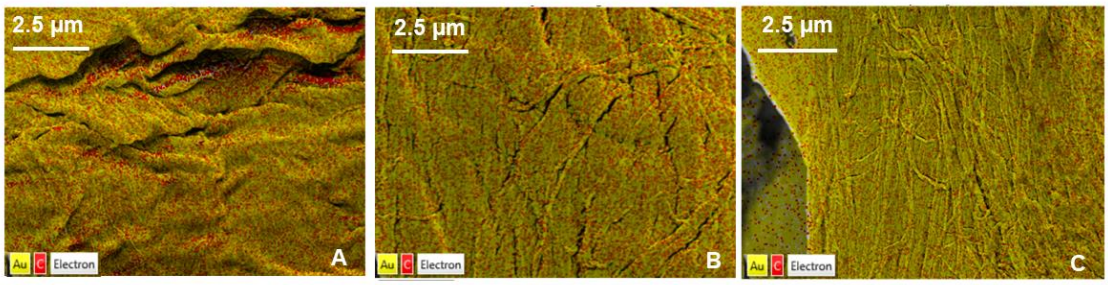

Figure 4. 8 Elemental Analysis for 25 nm (A), 38 nm (B) and 50 nm Au modified paper substrates (both sides modified) (C).

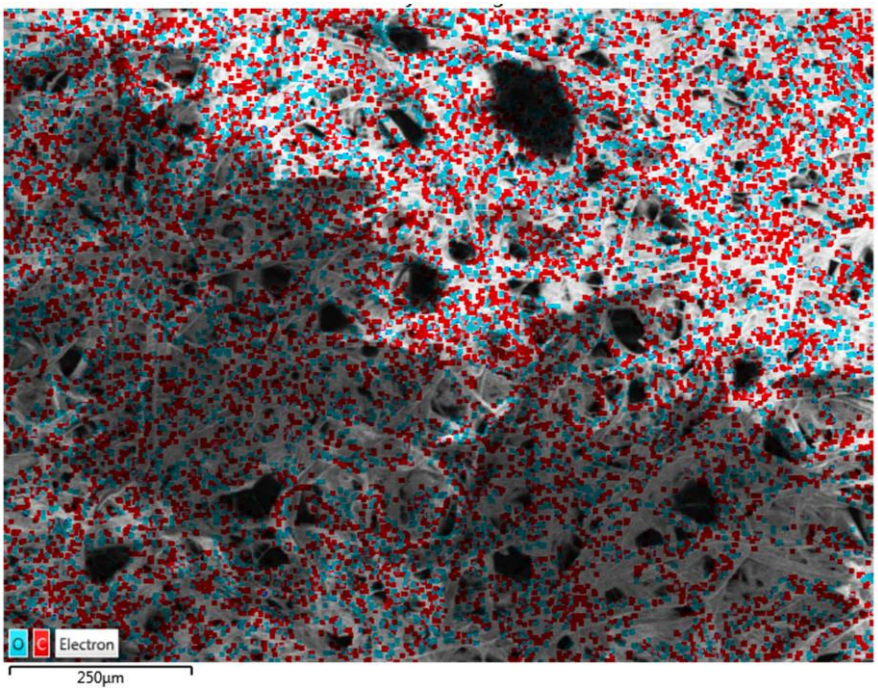

Figure 4. 9 Elemental Analysis for unmodified paper substrate (Grade 388 filter paper).

The contact angle measurements obtained from the goniometer as shown in Figure 4.10 indicated that the hydrophobicity of the paper substrates increased with increasing thickness of the metal layer deposited at the paper substrates. The average contact angles for 25, 38 and 50 nm Au modified paper substrates (both sides modified) were 86.0 ± 8.3°, 89.2 ± 6.7° and 91.7 ± 4.6°, respectively. This correlates well with the buildup of the gold over the cellulose-based channels [113].

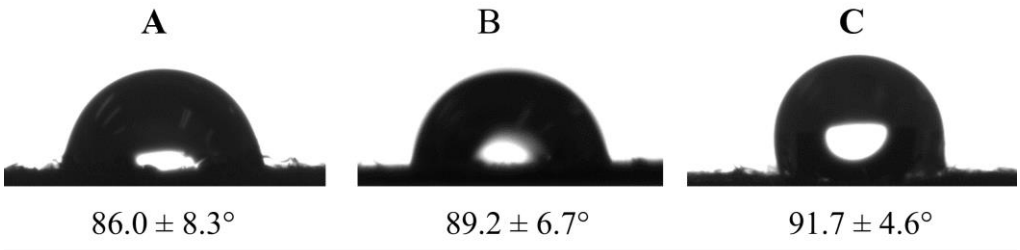

Figure 4. 10 Optical images taken in sessile drop mode for 25 nm (A), 38 nm (B) and 50 nm Au modified paper substrates (both sides modified) (C).

Since higher hydrophobicity of the paper substrates and limited solution uptake capability partially blocked by deposited metal interface might lead to longer solution sampling, response time for electrodes utilizing each type of paper substrate was measured. The average response times for 25, 38 and 50 nm Au modified paper substrates (both sides modified) were 5.0 ± 2.6 s, 8.0 ± 2.0 s, and 21.0 ± 7.5 s, respectively. Even though the response time increases with increasing metal thickness as assumed, it is well within the standard measuring interval of 60 s.

4.3.4. Potentiometric response when utilizing other metal modified paper substrates.

After the response of Pb^{2+}-ISEs coupled with gold sputtered paper substrates was found to be controllable in wider activity of lead(II), the responses of Pb^{2+}-ISEs coupled with other metals, namely platinum (Pt) and palladium (Pd) were also investigated. This was done to validate if the metal modification has an effect on the performance of paper-based substrates when coupled with Pb^{2+}-ISEs. Since previously higher thicknesses, such as 25 nm, 38 nm and 50 nm gold modifications (both sides modified) were found to be effective in assuring controllable super-Nernstian response of the Pb^{2+}-ISEs, the same thicknesses were also used for platinum and palladium. The potentiometric response when utilizing those substrates is shown in Figure 4.11.

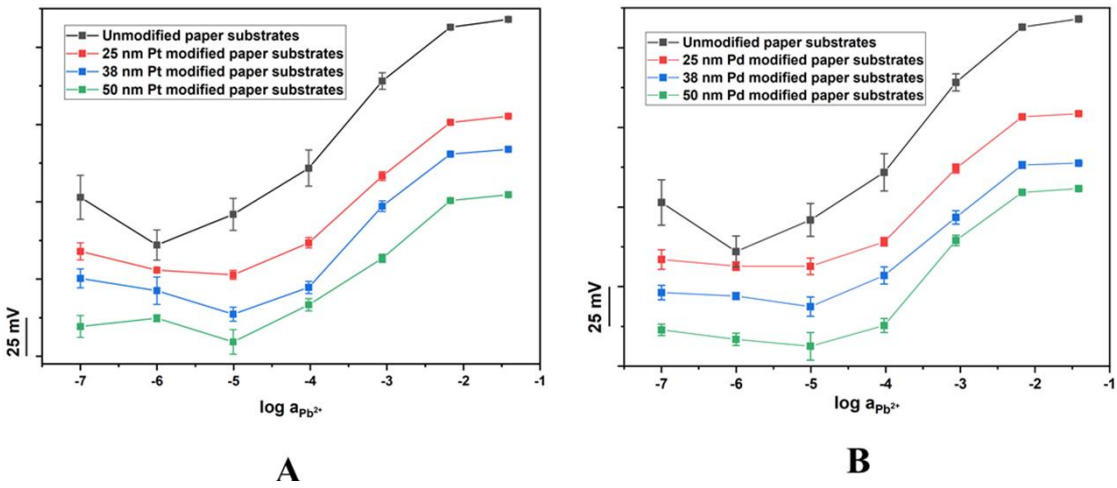

Figure 4. 11 Potentiometric response of Pb^{2+}-ISEs coupled with paper substrates without and with metallic (A) platinum and (B) palladium modifications (both sides modified).

When comparing their performance with gold modified paper substrates, it can be observed that Pt and Pd substrates also have an optimum thickness at which the super-Nernstian response can be best controlled. For Pt modified paper substrates (both sides modified), the 50 nm thickness showed the lowest potential jump between $10^{-3.06}$ and $10^{-4.02}$ M Pb^{2+} (31.4 ± 6.6 mV dec^{-1}) and for Pd, it was at 38 nm thickness (38.0 ± 8.7 mV dec^{-1}). The 38 nm Pd modified paper substrates (both sides modified) showed a linear response in the range of $10^{-4.5}$ to $10^{-2.2}$ M. The lower detection limit for 50 nm Pt modified paper substrates (both sides modified) could not be determined owing to non-linear behavior. However, the observed potential jump between $10^{-3.06}$ and $10^{-4.02}$ M Pb^{2+} as shown in Table 4.4 was considerably higher than that observed in the best performing gold modified paper substrates. As expected, the response time was also higher than unmodified paper substrates. For 25 nm, 38 nm and 50 nm Pt modified paper substrates, the average response times were 9.7 ± 3.2 s, 14.0 ± 4.0 s, and 15.0 ± 6.6 s respectively whereas for Pd modified paper substrates, they were 8.0 ± 4.0 s, 10.7 ± 4.2 s and 21.0 ± 7.9 s respectively. As shown, the use of other metal modifications than gold

is feasible. Since gold was used in this study as model system, the determination of lead(II) in various samples were conducted only with gold modified paper substrates.

Table 4. 4 Detection limits and slopes of Pb^{2+}-ISEs coupled with unmodified and metallic platinum and palladium modified paper substrates (both sides modified).

Type of substrate	**DL (Log a)**	**Slope between $10^{-2.17}$ and $10^{-3.06}$ M Pb^{2+} (mV dec^{-1})**	**Slope between $10^{-3.06}$ and $10^{-4.02}$ M Pb^{2+} (mV dec^{-1})**
In solution	-6	25.0 ± 0.2	30.8 ± 0.3
Unmodified paper	N.D.*	39.2 ± 6.8	58.8 ± 17.2
25 nm Pt modified paper	-4.5	39.1 ± 2.7	45.0 ± 6.5
38 nm Pt modified paper	N.D.*	37.9 ± 3.4	54.8 ± 3.6
50 nm Pt modified paper	N.D.*	42.1 ± 2.6	31.4 ± 6.6
25 nm Pd modified paper	-4.5	36.5 ± 3.5	48.0 ± 4.8
38 nm Pd modified paper	-4.5	37.0 ± 7.1	38.0 ± 8.7
50 nm Pd modified paper	N.D.*	34.0 ± 3.4	55.6 ± 7.9

*Not determined, owing to non-linear behaviour of the calibration curve

4.3.5. Determination of lead using gold modified paper substrates coupled with Pb^{2+}-ISEs.

As shown in Figure 4.12, the results of lead determination obtained from Pb^{2+}-ISEs were mostly comparable to those obtained by ICP-OES. The wet soil sample showed a slight deviation from the acceptable range (± 20%), possibly due to the adsorption of lead ions into the soil matrix. Another possible reason for the minor difference between results using both methods could be the fact the Pb^{2+}-ISE determine ionized component whereas the ICP-OES determines total lead content. However, since the samples are complex involving processes such as adsorption, formation of complexes, speciation of ions, etc, the difference could be expected. In all the cases, the deviation of the ISE from the ICP-OES readings was less than 9%. The plant dew sample and street runoff exhibited deviations less than 5%. Thus, using 38 nm gold modified paper substrates (both sides modified) coupled with Pb^{2+}-ISEs was found to be a feasible technique to determine lead in artificial environmental samples even when the electrode had been characterized with super-Nernstian response.

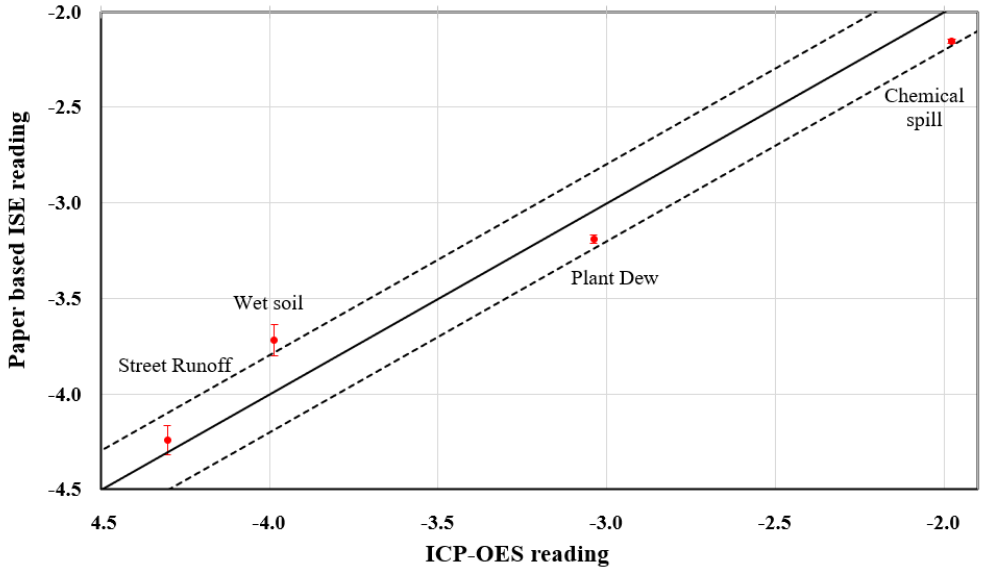

Figure 4. 12 Determination of Pb^{2+}concentrations in environmental samples using ICP-OES and Pb^{2+} - ISEs coupled with Au modified paper substrates (The continuous line is the 1:1 line for ICP-OES and ISE readings. The dotted line shows ± 20% variation from the 1:1 line).

4.3.6. Durability and life cycle assessment of the Pb^{2+}-ISEs coupled with metal modified paper substrates.

The durability assessment of the Pb^{2+}-ISEs coupled with metal modified paper substrates was conducted and compared to the measurements conducted with Pb^{2+}-ISEs when in direct contact with the prepared environmental sample containing high amounts of solid-to-liquid ratio. Three electrodes of each measuring set up were investigated and their response in the environmental samples was measured until (i) the potential readout was random indicating damage to the ISMs or (ii) ISMs got detached from the ISEs. According to Figure 4.13, the use of 38 nm gold modified paper substrates (both sides modified) almost doubles the lifetime of ISEs. The average number of readings for ISEs coupled with gold modified papers was 116 ± 1 and the use of paper substrate was 55 ± 12 measurement potential readings. With regards to the stability of the EMF, the readings from electrodes placed directly on soil show more variation which could be caused by the impact to the ISM from solid particles. The stability of readings from the electrodes protected by gold modified paper substrates was comparatively higher, even though it drifted downwards with usage which is an indication of the re-equilibration of the sensor to the specific measurement conditions. The information about the durability of ISEs (number of ISEs reuses/measurements) with and without paper substrates was used to study the LCA of the two measuring setups to identify which of them is considered to be more environmentally friendly.

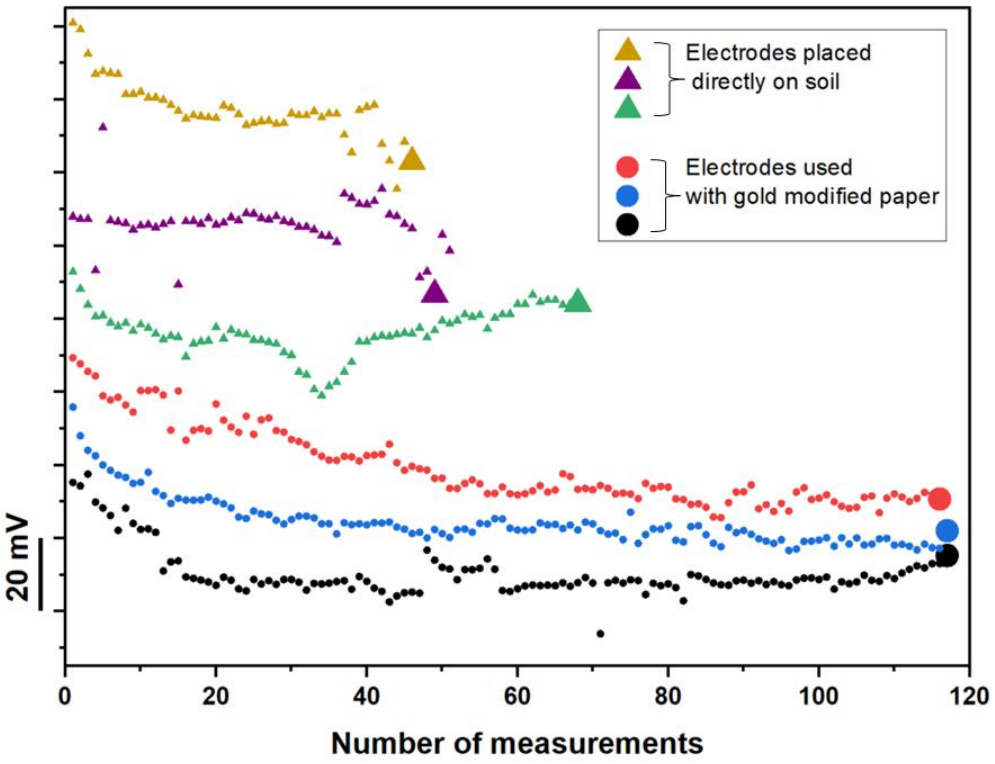

Figure 4. 13 Durability of Pb^{2+}-ISEs with and without paper-based solution sampling applied on complex environmental sample ((●) signs refer to electrodes used with gold modified paper substrates and (▲) signs refer to electrodes placed directly on soil). The end of a series of readings indicates failure of the electrode).

The LCA was conducted on the assumption that the number of ISE reuses are independent of the construction of the ISEs and paper metal modifications. Thus in this LCA, the design of the ISEs was determined based on the environmentally optimal construction of ceramic substrate chip based electrode with screen-printed carbon as previously reported [149] (Figure 4.2). In this study, the ion-to-electron transducer layer and ISM followed previously studied system of macro electrodes (further called CWE). The impact assessment results are presented for the potentiometric sensors with and without paper substrates used for microfluidic solution sampling. The results demonstrate the influence of adding a metal modified paper substrate to the potentiometric sensor from an environmental perspective.

The global warming potential (GWP) based on the IPCC AR5 method for the detection of Pb^{2+} in environmental sample using potentiometric sensor with different substrate materials is presented in Figure 4.14. The GWP reported in terms of the CO_2 emission is one of the most significant impact indicators among the environmental impact categories. The CWE demonstrated up to 1.7, 1.7, and 2 times greater CO_2 emission equivalents than the CWE + Au, Pt, and Pd modified paper substrates, respectively. The membrane, silver, and ceramic components of the CWE contributed to 37, 35, and 27% of the overall environmental impacts. Similarly, impact indicators under the ReCiPe midpoint method, including climate change (including and excluding biogenic carbon), fine particulate matter formation, fossil depletion, freshwater consumption, freshwater ecotoxicity, freshwater eutrophication, human toxicity (cancer and non-cancer), ionizing radiation, land use, marine ecotoxicity, marine eutrophication, metal depletion, photochemical ozone formation (ecosystem and human health), stratospheric ozone depletion, terrestrial acidification, and terrestrial ecotoxicity potentials, are presented in Figure 4.15. The contribution analysis of CWE revealed that membrane, silver, and ceramic components contributed to about 37, 35, and 27% of the overall environmental impacts of climate change potentials. About 77 and 93% of human toxicity - cancer and non-cancer potentials, respectively, was associated with the silver component that was contributed by chromium and zinc emissions. Similarly, silver contributed to about 87 and 87%, and 96 and 58% of freshwater ecotoxicity and eutrophication, and marine ecotoxicity and eutrophication potentials that was attributed to the long-term emissions to freshwater and seawater, respectively. Furthermore, the silver component in CWE accounted for 30 and 88% of fossil and metal depletion; 23% of fine particulate matter formation; 45% of ionizing radiation; 60% of land use; 32 and 39% of photochemical ozone formation (ecosystems and human health); 62% of stratospheric ozone depletion;

51 and 34% of terrestrial acidification and ecotoxicity potentials, respectively. Notably, the membrane component in CWE accounted for 37% in climate change, 44% in fossil depletion, 63% in freshwater consumption, and 41% in terrestrial ecotoxicity potentials. Conversely, the ceramic substrate component contributed 65% to the fine particulate matter formation, 48% to the photochemical ozone formation (ecosystems), and 42% to the photochemical ozone formation (human health) potentials. The CWE demonstrated the greatest environmental impacts in all the impact categories, excluding fine particulate matter formation, freshwater ecotoxicity, freshwater eutrophication, human toxicity (cancer and non-cancer), marine ecotoxicity, marine eutrophication, metal depletion, and terrestrial acidification potentials, when compared to the CWE + metal modified paper substrates, despite the application of additional layer in CWE + metal modified paper substrates. The greater footprint of CWE was attributed to less than twice the number of reuses that was facilitated by the application of metal modified paper substrates.

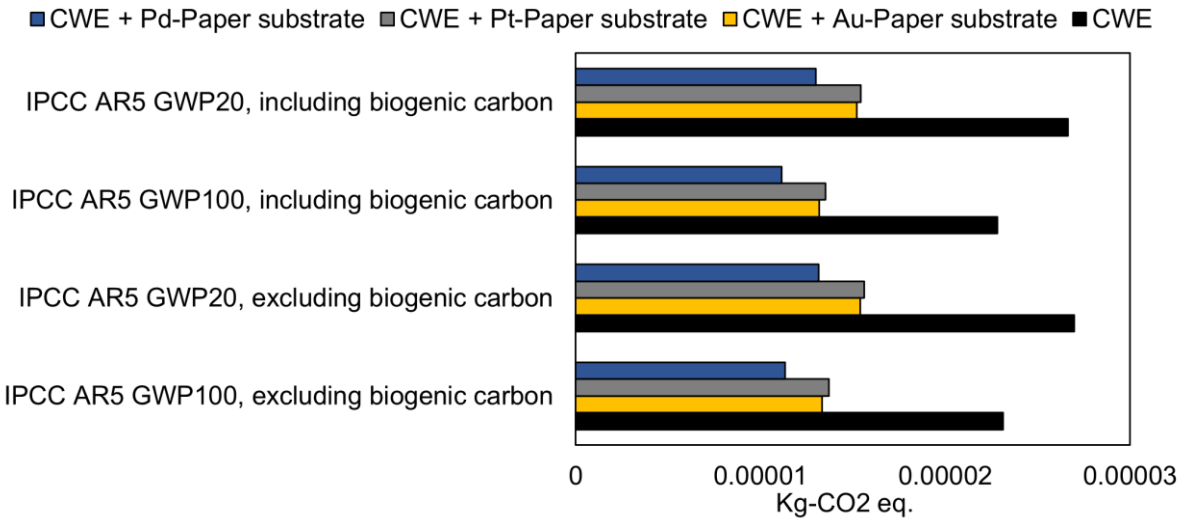

Figure 4. 14 The global warming potentials (GWP) for 100 and 20 years using IPCC AR5 method for one functional unit with different substrates. CWE: Carbon Working Electrode, IPCC AR5: The Intergovernmental Panel on Climate Change - Fifth Assessment Report.

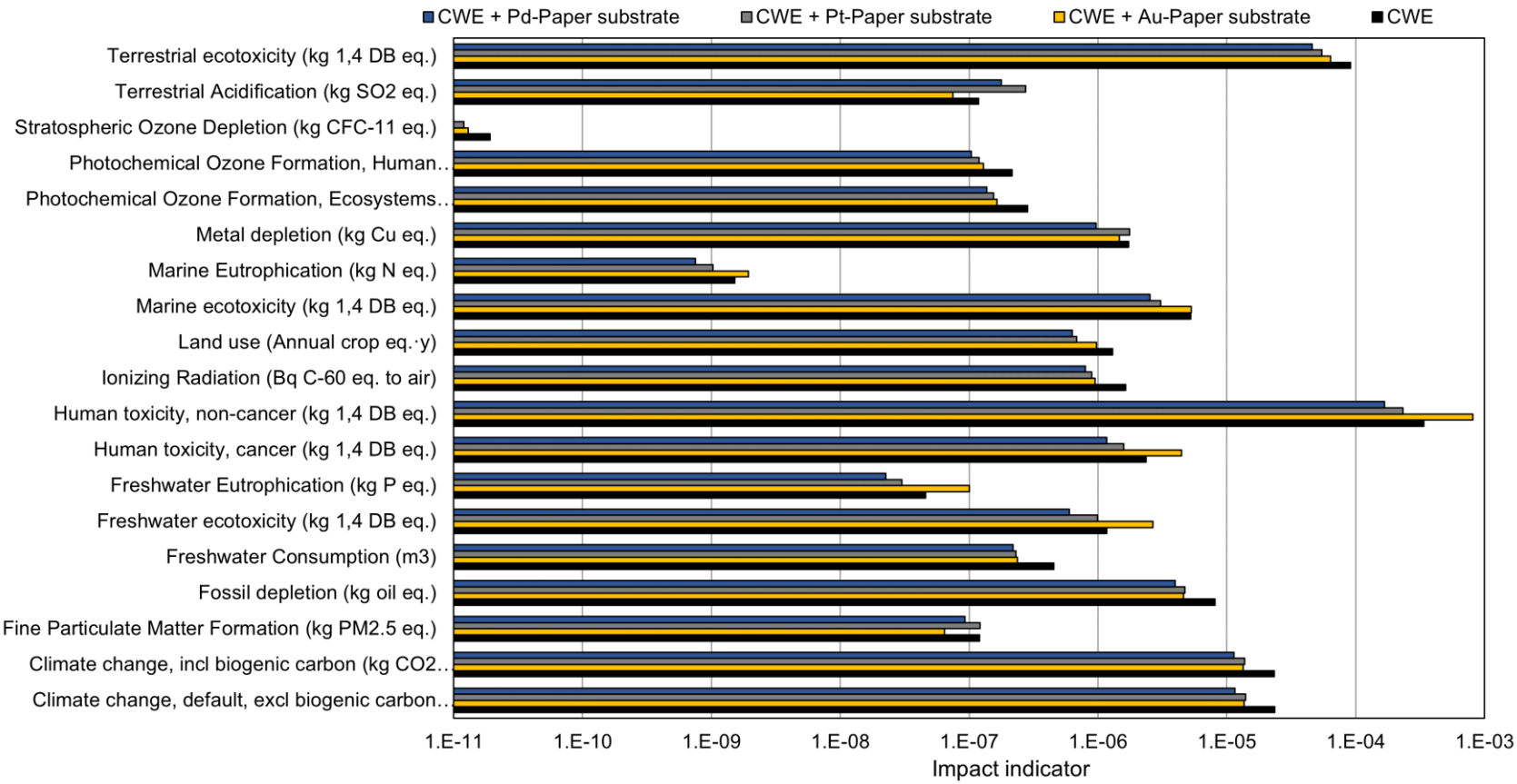

Figure 4. 15 The environmental impact for one functional unit with different substrates using the ReCiPe midpoint method. CWE: Carbon Working Electrode, IPCC AR5: The Intergovernmental Panel on Climate Change- Fifth Assessment Report.

CWE + Pt modified paper substrate demonstrated 133, 2 and 1% greater impact than CWE in terrestrial acidification, metal depletion, and fine particulate matter formation potentials, respectively. Furthermore, CWE + Au modified paper substrate demonstrated the greatest implications in human toxicity (cancer (4.44E-06 kg 1,4-DB eq.) and non-cancer (8.09E-04 kg 1,4-DB eq.)), freshwater ecotoxicity (2.66E-06 kg 1,4-DB eq.), freshwater eutrophication (1.00E-07 kg P eq.), marine ecotoxicity (5.29E-06 kg 1,4-DB eq.), and marine eutrophication (1.94E-09 kg N eq.) potentials. The larger implications in these impact categories were attributed to the significantly greater (>100%) contribution of the respective metal coatings applied in paper substrate. However, CWE + Pd modified paper substrate exhibited the lowest implications in all the impact categories, except fine particulate matter formation and terrestrial acidification. The application of lesser mass of Pd for performing the same potentiometric detection function constituted as an advantage, when compared to Pt and Au. A sensitivity analysis of 25, 38, and 50 nm metal modifications, which correspond to equivalent variations in the masses of metals (Table 4.1), demonstrated ± 33% variation in the environmental impacts from the metal component of the respective CWE + metal modified paper substrate. Overall, the CWE + metal modified paper substrates exhibited lower environmental impacts in all the impact categories when compared to CWE for one FU.

4.4. Conclusions

Pb^{2+}-ISEs coupled with metal modified paper substrates were investigated with the aim of eliminating or controlling the super-Nernstian response commonly observed in heavy metal ion determination using microfluidic paper-based solution sampling. It was found that the magnitude of the super- Nernstian jump observed varied with the thickness of

the metal layer and on whether it was modified on a single side or on both sides. The use of 38 nm gold modified paper substrates (both sides modified) was found to be the most effective in terms of controllable super-Nernstian potential jump and range of linear electrode response. Their effectiveness was validated by measuring lead in simulated environmental samples. The life cycle assessment further confirmed the advantages of using metal modified paper substrates as compared to using sensors directly on complex environmental samples containing high solid-to-liquid ratios.

CHAPTER 5 ION-SELECTIVE MEMBRANE MODIFIED MICROFLUIDIC PAPER-BASED SOLUTION SAMPLING SUBSTRATES FOR POTENTIOMETRIC HEAVY METAL DETECTION

5.1. Introduction

Potentiometric ion-selective electrodes (ISEs) equipped with polymeric membranes are widely used to measure a variety of ions in clinical and environmental samples [93,150–152]. Their low cost, versatility, and low power consumption makes them more desirable in affordable analytical solutions than other standard analytical techniques such as atomic absorption, cold vapour atomic fluorescence, and inductively coupled plasma (mass or optical discrimination) [25,35,153–155]. Recently, the applications of ISEs have been enhanced by the conversion of electric potential in an ISE into other optical [156,157] or electrochemical [158,159] signals to improve sensor sensitivity [160].

The ion-selective membrane (ISM) in an ISE is a vital part which enables the electrode to identify and quantify the target ions in the samples. The ISM typically consists of an ionophore [150], an ionic additive [161], plasticizer [162], and a polymer matrix [163]. Typically, organic lipophilic substances which can selectively bind to the target ion are used as ionophores and these constitute about 0.5 – 2 % of the dry mass of membrane components. The bulk of the dry mass is usually composed of the polymer matrix mixed with the plasticizer. Such a matrix adds elasticity to the membrane, provides more homogeneous redistribution of the membrane components and enhances ion transport

within ISM [164]. The ionic additives further enhance the ISE's Nernstian behaviour [161]. When the ISE is in contact with the sample solution, the target ions will reach an electrochemical equilibrium at the sample | ISM interface. The potential established at this interface theoretically is proportional to the activity of ion in the solution, providing a base for an analytical determination of analyte in the sample with unknown concentration of the primary ion [165].

Modifying paper substrates with the ISM-components could possibly change the sample | ISM interface and alter/improve the potentiometric response of the electrode eliminating super-Nernstian behaviour of ISEs that is observed when heavy metal sensitive ISEs are coupled with unmodified paper substrates. This study investigates the effect of modifying paper substrates with different combinations of ISE's membrane components and using them for solution sampling purpose coupled with Pb^{2+}-ISEs. A favorable combination of membrane components for paper substrate modification was identified.

5.2. Experimental

5.2.1. Preparation of microfluidic paper-based solution sampling substrates.

Unmodified paper substrates were referred to as PS0. Modified paper substrates were obtained by soaking the washed and dried pieces of paper substrates in the respective solutions for 30 min with gentle stirring followed by drying at room temperature overnight (Table 5.1).

Table 5. 1 Composition of modifying solutions used for modification of paper substrates

Paper substrate	**Membrane Components**				
	PVC	o-NPOE	KTClPB	Lead ionophore IV	THF
PS1.0	33.3 mg	-	-	-	2 ml
PS2.0	33.3 mg	65.2 mg	-	-	2 ml
PS3.0	-	65.2 mg	-	-	2 ml
PS4.0	-	-	0.5 mg	-	2 ml
PS5.0	-	-	-	1 mg	2 ml
PS6.0	33.3 mg	65.2 mg	0.5 mg	1 mg	2 ml

Furthermore, different dilutions of PS6.0 were also studied, and the paper substrates were named as PS6.1, PS6.2, PS6.3, PS6.4, PS6.5, and PS6.6, with membrane cocktail concentrations of 35, 25, 10, 5, 1, and 0.1 mg of total dry mass in 1 ml of THF, respectively. For ease of reference, it is to be noted that 50 mg ml^{-1} is the standard concentration of ISM used for preparation of Pb^{2+}-ISEs in this work.

5.2.2. Potentiometric measurements with Pb^{2+}-ISEs.

Initially, the potentiometric responses with paper substrates modified with different combinations of membrane components were studied followed by the response with paper substrates modified with different concentrations of ISM.

For the investigation of effect of different measurement configurations on the potential formation at the paper substrate | ISM interface only PS6.0 was investigated. The following configurations of PS6.0 coupled with Pb^{2+}-ISEs were proposed and tested, namely in solution (standard beaker-based measurement), on PS6.0 in solution (the paper substrate touching ISM directly, while the whole set up was immersed in beaker containing sample solution), on PS6.0 (standard microfluidic paper-based solution sampling coupled with ISEs utilizing unconditioned PS6.0) and on conditioned PS6.0 (standard microfluidic paper-based solution sampling coupled with ISEs utilizing conditioned in respective standard solution for 30 min PS6.0) as shown in Figure 5.1.

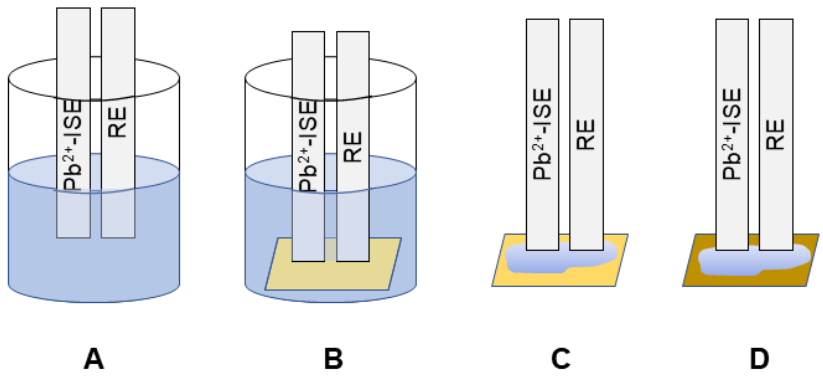

Figure 5. 1 Different measurement configurations used to investigate the potential formation at the paper substrate | ISM interface: in solution (A), on PS6.0 in solution (B), on PS6.0 (C) and on conditioned PS6.0 (D).

For the investigation of effect of conditioning the ISM modified paper substrates with primary ion (Pb^{2+}) on the potential formation at the Pb^{2+}-ISEs coupled with microfluidic

paper-based solutions sampling, PS6.0 paper substrates were soaked first with different activities of lead(II) nitrate solutions ($10^{-1.42}$, $10^{-2.17}$, $10^{-3.06}$, $10^{-4.02}$, $10^{-5.01}$ M Pb^{2+}), washed with ultra-pure water, and dried before measurements. The paper substrates were subsequently used to register the EMF for standard solutions ranging from $10^{-4.02}$ to $10^{-2.2}$ M $Pb(NO_3)_2$. For the investigation of effect of interfering ion (Cd^{2+}) on the potential formation at the Pb^{2+}-ISEs coupled with microfluidic paper-based solutions sampling, PS6.0 paper substrates were soaked in 0.1 M $Cd(NO_3)_2$ for 30 min, washed with ultra-pure water, and dried before measurements. The same Pb^{2+}-ISE was then used for potentiometric measurements coupled with untreated PS6.0. The characterization of modified paper substrates was also done, and the detailed information is provided in section 3.3.4.

5.2.3. Determination of lead(II) in environmental samples.

Different environmental samples, including chemical spill, cultivation soil, wetland, and biowaste samples subjected to Toxicity Characteristic Leaching Procedure (TCLP) metal leaching procedure [33] were used to validate the sensor performance.

Three samples were prepared for the validation of the use of ISM modified paper substrates for solution sampling of high solid-to-liquid ratio complex environmental samples. A simulated chemical spill was prepared by adding a random amount of graphite powder into a lead (II) nitrate solution. The sample was named as “chemical spill”. A wet soil sample was prepared by spiking Pb^{2+} into raw soil collected from productive farmland in Singapore. The sample was named as “cultivation soil” sample. A sample originating from wetland area of a lake containing mostly algal growth and sediment was also collected. The sample was named as “wetland”. A random amount of

lead (II) nitrate solution was used to spike all samples. Aside from samples that had high solid-to-liquid ratios, two more samples with complex solution composition were also studied. Two samples were leachates from different biowaste samples subjected to Toxicity Characteristic Leaching Procedure (TCLP) metal leaching procedure. The leachates were obtained according to the procedure: 100 g of biowaste was soaked in 2 L of acetic acid solution and placed in a rotator rotating at 30 r min^{-1} for 18 h. The leachate was collected and filtered afterwards. The samples were named as "biowaste 1" and "biowaste 2".

PS6.0 was coupled with Pb^{2+}-ISEs for the determination of Pb^{2+} in the complex environmental samples and the measurements were obtained as described in section 3.3.3. Aside of potentiometric determination, the total lead concentrations in all samples were determined using Perkin Elmer Optima 8300 Inductively Coupled Plasma Optical Emission Spectroscopy (ICP-OES).

5.3. Results and discussion

5.3.1. Paper-based microfluidic solution sampling using ISM-components modified paper substrates coupled with Pb^{2+}-ISEs

Several physical and chemical modifications of paper-based substrates have been investigated previously to diminish or control the super-Nernstian responses which occur during detection of heavy metals with cellulose-based paper substrates coupled with potentiometric sensors. For example, pretreatment of the paper substrates with an inorganic salt of the respective primary cation was found to be effective for detection of Pb^{2+} and Cd^{2+} ions [48]. For Pb^{2+}-ISEs, using filter paper treated with 10^{-3} M $Pb(NO_3)_2$ and then dried prior to solution sampling resulted in a Nernstian response in the range

of $10^{-5.0}$ to $10^{-2.17}$ M $Pb(NO_3)_2$. Acidification of paper substrates [49] was also found to be effective for Pb^{2+} ion detection. In the case of paper acidification [49], the optimum potentiometric response was obtained when Pb^{2+}-ISEs were coupled with paper substrates (containing sample solution) at a pH range of 3 to 4. A linear response could be obtained in the range of $10^{-5.0}$ to $10^{-2.17}$ M $Pb(NO_3)_2$ with a lower detection limit of 10^{-5} M Pb^{2+}. One of the disadvantages of these methodologies is that the pretreatment of paper substrates requires additional chemicals apart from the ones used in the preparation of the ISE. Also, the physico-chemical nature of the ISM | modified paper substrate interface is vastly changing depending on the modification of the paper substrate applied. This in turn may introduce additional interferences to the potential formation at the ISM, simply originating from the proximity of the ISM to the modified paper substrates. The use of the ISM-components which are already used in the ISM preparation can simplify the preparation protocol of the modified paper substrates by requiring less chemicals to be used but also simplify the ISM | modified paper substrate interface by being more compatible with the one of ISM. Thus, the modifications of paper substrates with ISM-components were studied with the objective of controlling the super-Nernstian responses which occur when Pb^{2+}-ISEs are coupled with cellulose-based paper substrates.

First, paper substrates were modified with single ISM-components as mentioned in Table 5.1. As shown in Figure 5.2, most paper substrates showed a super-Nernstian response which was observed between $10^{-3.06}$ and $10^{-4.02}$ M Pb^{2+}, similar to the response on unmodified paper substrates (PS0). In the case of PS1.0 (PVC and THF) and PS2.0 (PVC, o-NPOE and THF), even though the super-Nernstian jump was not observed between $10^{-3.06}$ and $10^{-4.02}$ M, the initial slope of the Pb^{2+}-ISEs was sub-Nernstian

between $10^{-3.06}$ to $10^{-2.17}$ M $Pb(NO_3)_2$ (22.8 ± 1.8 mV dec^{-1} for PS1.0 and 20.0 ± 7.0 mV dec^{-1} for PS2.0), limiting the Nernstian response of the Pb^{2+}-ISEs to a very narrow activity range with the lower detection limit of about $10^{-4.0}$ M Pb^{2+}. PS3 (o-NPOE and THF) and PS5.0 (lead ionophore IV and THF) had super-Nernstian jumps of 51.6 ± 4.7 mV dec^{-1} and 80.0 ± 8.0 mV dec^{-1} between $10^{-3.06}$ and $10^{-4.02}$ M Pb^{2+}, respectively. PS4.0 (KTClPB and THF) seemingly showed high uncertainty at each ion activity which was found too high to be considered experimentally useful. However, the increase of the initial Nernstian slope of PS2.0 (PVC, o-NPOE and THF) between $10^{-3.06}$ to $10^{-2.17}$ M $Pb(NO_3)_2$ was obtained by additionally adding to the paper substrate modifying solution other typical membrane components, such as KTClPB and lead ionophore IV. In this case, all ISM-components modified paper substrates PS6.0 (lead ionophore IV, KTClPB, PVC, o-NPOE and THF) coupled with Pb^{2+}-ISEs resulted in a favourable potentiometric response with a close to Nernstian linear slope of 34.9 ± 3.3 mV dec^{-1} in the range of $10^{-5.0}$ to $10^{-2.17}$ M $Pb(NO_3)_2$, and the lower detection limit of $10^{-5.4}$ M Pb^{2+}. This could be obtained since the exact composition to the electrode's ISM was used to modify the paper substrate allowing to chemically simplify the paper substrate │Pb^{2+}-ISE interface, thus increasing the compatibility of the paper substrate to the ISM of the Pb^{2+}-ISEs.

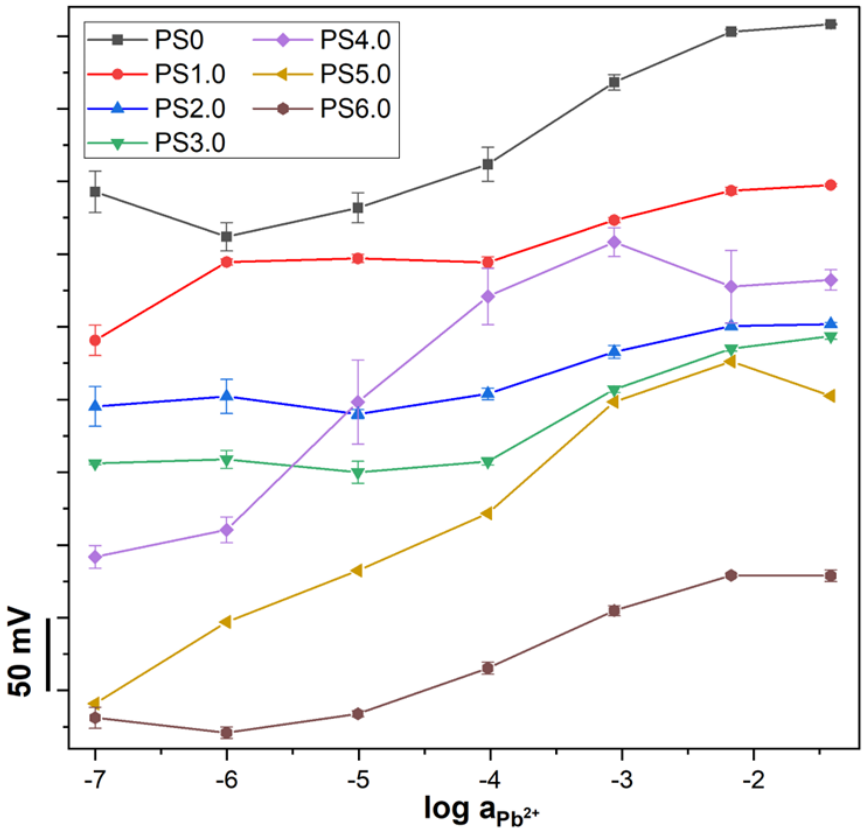

Figure 5. 2 Potentiometric response of Pb^{2+}-ISEs coupled with ISM-components modified paper substrates.

Since PS6.0 performed the best out of investigated paper substrates, variations of PS6.0 were prepared by changing the concentration of the membrane cocktail components in THF that were used for manufacturing of the modified paper substrates. This was performed in order to determine whether the Nernstian response of the Pb^{2+}-ISEs could be obtained when coupled with paper substrates modified with membrane cocktail concentrations lower than the usual concentration used in the ISM preparation (50 mg ml^{-1} dry mass of ISM components in THF). This could be beneficial to reduce the amount of chemicals used for modification of paper substrates. According to Figure 5.3, paper substrates 6.6 to 6.4 (0.1, 1, and 5 mg ml^{-1} dry mass of ISM components in THF) showed either super-Nernstian responses or random potential responses which were not

conducive to potentiometric determination of Pb^{2+} ions. This could be because the concentration of ISM-components on the paper substrates was not sufficient to modify the surface and the bulk of the paper substrates. A favorable potentiometric response could be obtained for paper substrates 6.3 to 6.0 (10, 25, 35, and 50 mg ml^{-1} dry mass of ISM components in THF). PS6.3 had a slope of 30.8 ± 1.7 mV dec^{-1} in the range of $10^{-4.0}$ to $10^{-2.2}$ M $Pb(NO_3)_2$ and PS6.2 had a slope of 25.8± 0.5 mV dec^{-1} in the range of $10^{-6.0}$ to $10^{-2.2}$ M $Pb(NO_3)_2$. The slope for PS6.1 was 29.6 ± 1.3 mV dec^{-1} between $10^{-4.0}$ to $10^{-2.2}$ M $Pb(NO_3)_2$, and for PS6.0 it was 34.9 ± 3.3 mV dec^{-1} in the range of $10^{-5.0}$ to $10^{-2.2}$ M $Pb(NO_3)_2$. Even though the lower detection limit varied between $10^{-6.0}$ to $10^{-4.0}$ M $Pb(NO_3)_2$, Nernstian responses of Pb^{2+}-ISEs could be observed for a sufficient concentration range that would allow target analysis in specific sample types.

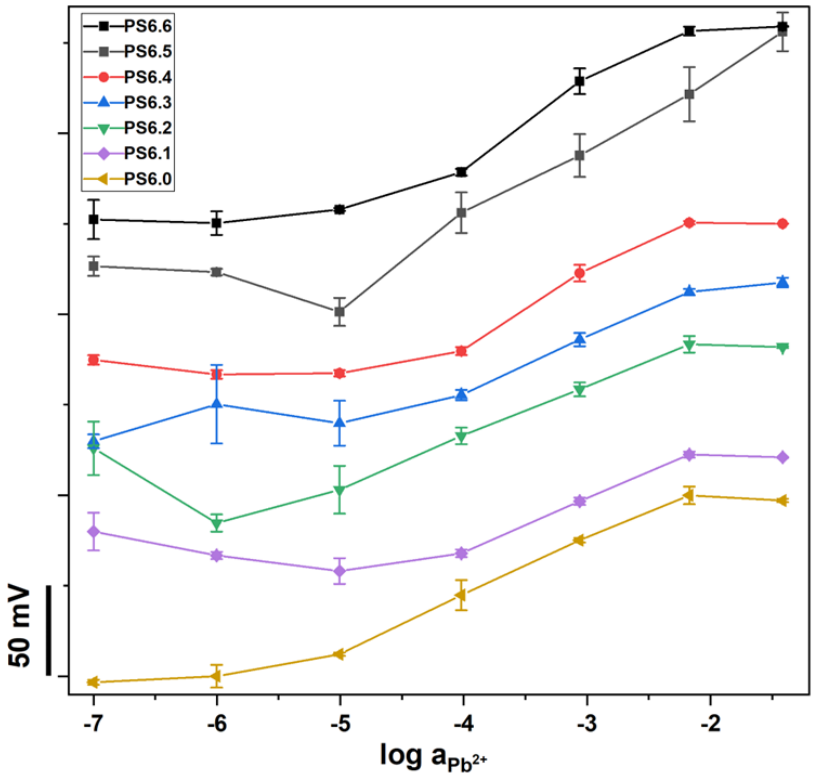

Figure 5. 3 Potentiometric response of Pb^{2+}-ISEs coupled with paper substrates modified with different concentrations of Pb^{2+} membrane cocktail.

5.3.2. Effect of different measurement configurations on the potential formation at the paper substrate │ISM interface

As shown in Figure 5.4, PS6.0 was used in different potentiometric measurement configurations to see the effect of different measurement configurations on the potential formation at the paper substrate │ISM interface. The same electrode was used for all measurements to avoid challenges related to the reproducibility of the measurements done by set of different electrodes. It could be observed that the potentiometric responses of Pb^{2+}-ISE were dependent on the measuring set up investigated. It was reported previously that slopes of ISEs when used with microfluidic paper-based sampling were in general higher than for the same electrodes in beaker-based measurements [40]. Similarly here, the slope of the Pb^{2+}-ISE for microfluidic paper-based solution sampling was 30.7 ± 0.7 mV dec^{-1} in the range of $10^{-5.0}$ and $10^{-2.2}$ M in comparison to the same electrode in beaker measurements with a slope of 27.2 ± 0.9 in the range of $10^{-5.0}$ and $10^{-2.17}$ M Pb^{2+}. Interestingly, when the same electrode was placed on the paper substrate that was immersed in the solution, the potentiometric response of the Pb^{2+}-ISE was characterized with higher than Nernstian response of 35.8 ± 1.7 mV dec^{-1} in the range of $10^{-5.0}$ and $10^{-2.2}$ M Pb^{2+}. This shows that the presence of a larger volume of solution around the electrode that is available for paper substrate does not necessarily improve the potentiometric response of the electrode. The physico-chemical state of the paper substrate that is in direct contact with the ISM during the microfluidic paper-based solution sampling drives the potentiometric response of the Pb^{2+}-ISE. This is valid despite the general availability of the sample solution to the electrode, which was vastly higher than the sorption capacity of the paper substrates. Thus, in this case a local equilibrium between the ISM and paper substrate was established driven by the

paper substrate's physical and chemical interactions with the sample solution and electrode. Finally, the potentiometric measurements done on paper substrates that were conditioned with primary ion resulted in slopes comparable to beaker-based measurements of 25.9 ± 1.3 mV dec^{-1} but with much higher detection limit of $10^{-4.0}$ M Pb^{2+}. In theory, a longer contact time between the sample solution should lead to better absorption of the ions on the paper substrate. However, experimentally, this has resulted in a reduction in the linear range of the calibration curve of Pb^{2+}-ISE. This implies that additional conditioning with the sample solution also does not improve the potentiometric response with PS6.0, as possible over-conditioning of the paper was done which could result in possible desorption of the ion (Pb^{2+}) from the paper substrate to the sample solution when in contact with low concentrations of Pb^{2+}. Similar observations were made for other modifications of the paper substrates [48].

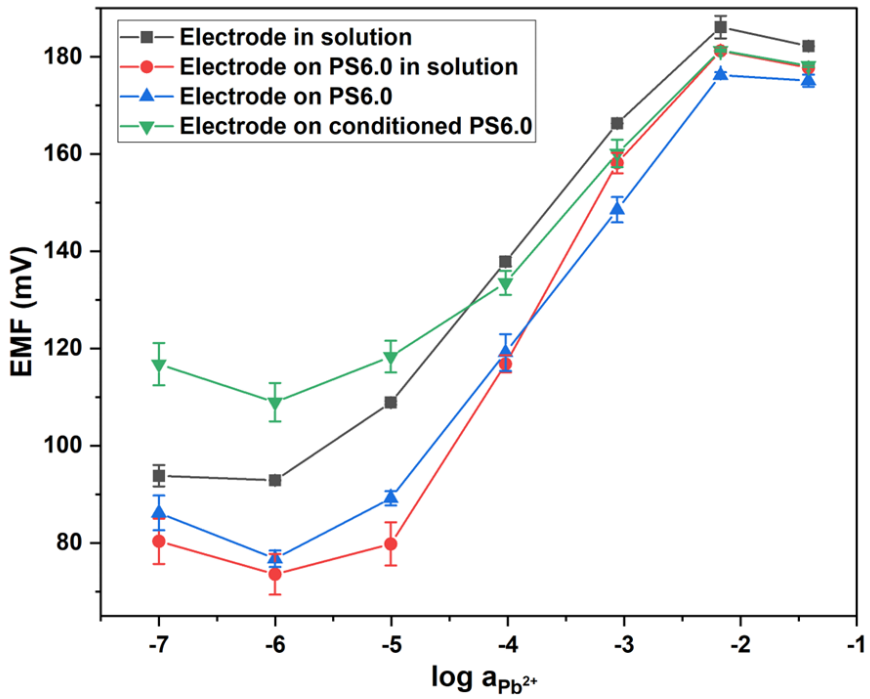

Figure 5. 4 Potentiometric response of Pb^{2+}-ISE in different measurement configurations when coupled with PS6.0.

Since modification of the paper substrate with ISM resembles common practice in preparation of an all-integrated paper-based ISEs [41,115,166,167], the measurement configuration of using PS6.0 with electrodes which only had the PEDOT(PSS) (without Pb^{2+}-ISM) was also explored to see if the ISM on the ISE could be disposed of to simplify the set up to the ones reported for all-integrated paper-based ISEs [41,115,166,167]. PS6.0 was used in both unconditioned and conditioned (conditioned in 10^{-3} M Pb^{2+} solution for 24 hours, washed with water and then dried) states. As shown in Figure 5.5, the electrode coupled with unconditioned PS6.0 displayed a linear response of 27.2 ± 3.8 mV dec^{-1} in the range of 10^{-5} to $10^{-2.17}$ M Pb^{2+}. For the electrode coupled with conditioned PS6.0, a linear response of 14.0 ± 3.8 mV dec^{-1} was observed in the range of 10^{-4} to $10^{-2.17}$ M Pb^{2+}. Thus, it can be concluded that conditioning state of the ISM and PS6.0 plays important role in potential formation and stability at PS6.0 │PEDOT(PSS) based electrode interface. The conditioned PS6.0 may be saturated with salt within available paper matrix and the ISM, affecting sample concentration and solution availability in the subsequent solution sampling. It is believed the ionic and water conditions are different at PS6.0 │PEDOT(PSS) based electrode interface for two cases presented. Moreover, in both cases the EMF values had higher uncertainty in the lower activity of Pb^{2+} (e.g., at 10^{-4} M Pb^{2+}, for unconditioned and conditioned PS6.0 were 7.6 and 12.9 mV, respectively) than the ones reported for Pb^{2+}-ISEs (3.8 mV). Although PEDOT(PSS) based electrode could potentially be used when coupled with unconditioned PS6.0 for specific measurement conditions, the overall sensitivity of the PEDOT(PSS) based electrode to the conditioning state of the paper substate and higher uncertainties of potential response, highlights the importance

of a well-conditioned ISM on the PEDOT(PSS) based electrode for a good potentiometric performance with PS6.0 towards Pb^{2+} detection.

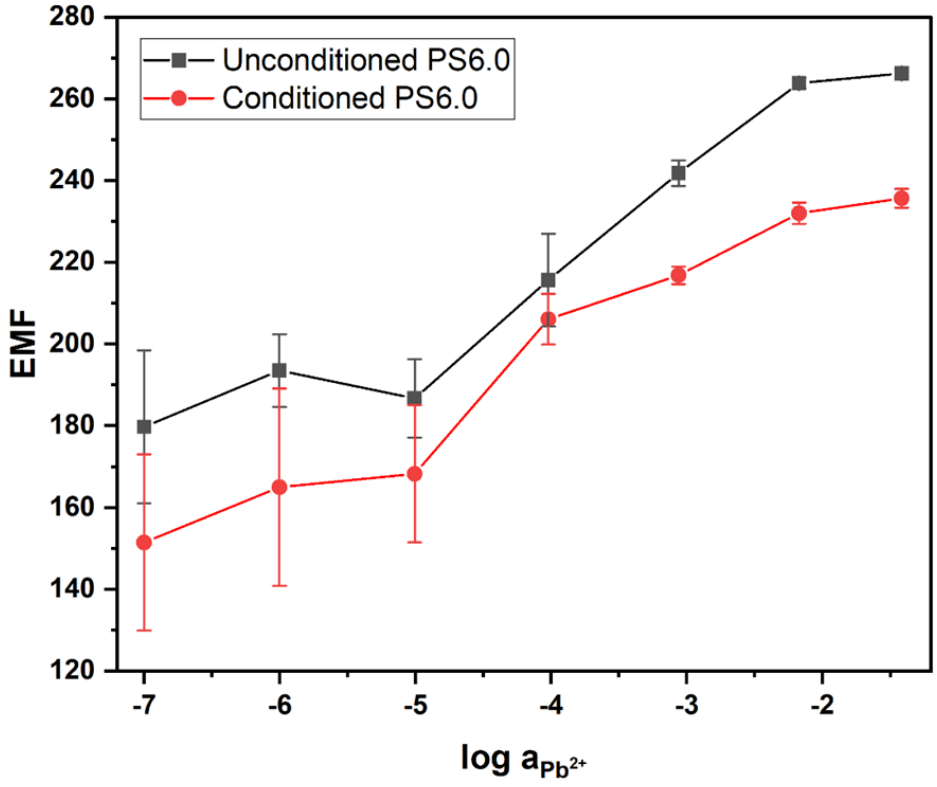

Figure 5. 5 Potentiometric response of Pb^{2+}-ISEs (no ISM) coupled with unconditioned PS6.0 and conditioned PS6.0

5.3.3. Effect of conditioning the ISM modified paper substrates with primary (Pb^{2+}) and interfering ions on the potential formation at the Pb^{2+}-ISEs coupled with microfluidic paper-based solution sampling

Effect of conditioning the ISM modified paper substrates with $Pb(NO_3)_2$ (primary ion) was studied to identify if it can further improve the potentiometric performance of the Pb^{2+}-ISEs coupled with microfluidic paper-based solution sampling (Figure 5.6A). Figure 5.6B further illustrates how the EMF varied at different Pb^{2+} activities for Pb^{2+}-ISEs coupled with ISM-component modified paper substrates conditioned with different

activity of Pb^{2+}. The potentiometric response was logged only for a limited concentration range at which a super-Nernstian response of Pb^{2+}-ISEs could be usually observed. When considering the average slope of potentiometric response between $10^{-2.2}$ M and $10^{-4.0}$ M Pb^{2+}, there was a gradual increase in the slope for PS6.0 conditioned with $10^{-1.42}$ M to $10^{-5.01}$ M Pb^{2+} solutions. The slopes were 19.8 ± 0.7, 22.1 ± 2.2, 25.0 ± 1.5, 25.8 ± 2.3, and 27.1 ± 2.5, mV dec^{-1}, for PS6.0 treated with $10^{-1.42}$, $10^{-2.17}$, $10^{-3.06}$, $10^{-4.02}$, and $10^{-5.01}Pb^{2+}$, respectively. In comparison, the slope of the unconditioned PS 6.0 was 29.4 ± 1.1 mV dec^{-1}. Also, the EMF that was recorded at different Pb^{2+} activities for Pb^{2+}-ISEs coupled with ISM component modified paper substrates conditioned with different activity of Pb^{2+} is shown (Figure 5.6 B). It shows that the ISM-component modified paper substrates are chemically active in terms of their selective interactions with the analyte (Pb^{2+}). Higher the activity of Pb^{2+} used for conditioning of paper substrates, higher the absolute potential of the Pb^{2+}-ISEs. This is especially valid for Pb^{2+}-ISEs responses utilizing $10^{-1.42}$, $10^{-2.17}$, $10^{-3.06}$ M Pb^{2+} solutions, where the slopes of the potential increases were obtained from all sensor responses at specific activity of standard solutions, e.g. 2.4 ± 2.5 mV dec^{-1} (at $10^{-2.17}$ M Pb^{2+}), 3.5 ± 3.0 mV dec^{-1} (at $10^{-3.06}$ M Pb^{2+}), and 8.2 ± 1.7 mV dec^{-1} (at $10^{-4.02}$ M Pb^{2+}). This shows that ISM is selective towards Pb^{2+} and its conditioning state influences the Pb^{2+}-ISEs responses as different conditioned membrane phases are in direct contact with each other (phase 1: ISM on paper substrate, and phase 2: ISM of ISE). However, considering the performance of the PS6.0 conditioned with different primary ion concentrations in comparison to the unconditioned PS6.0, the unconditioned PS6.0 was the best performing paper substrate in terms of controlled potentiometric response, having the best linearity (R^2= 0.9994),

and having lower uncertainty (standard deviation in EMFs measured at each Pb^{2+} activity).

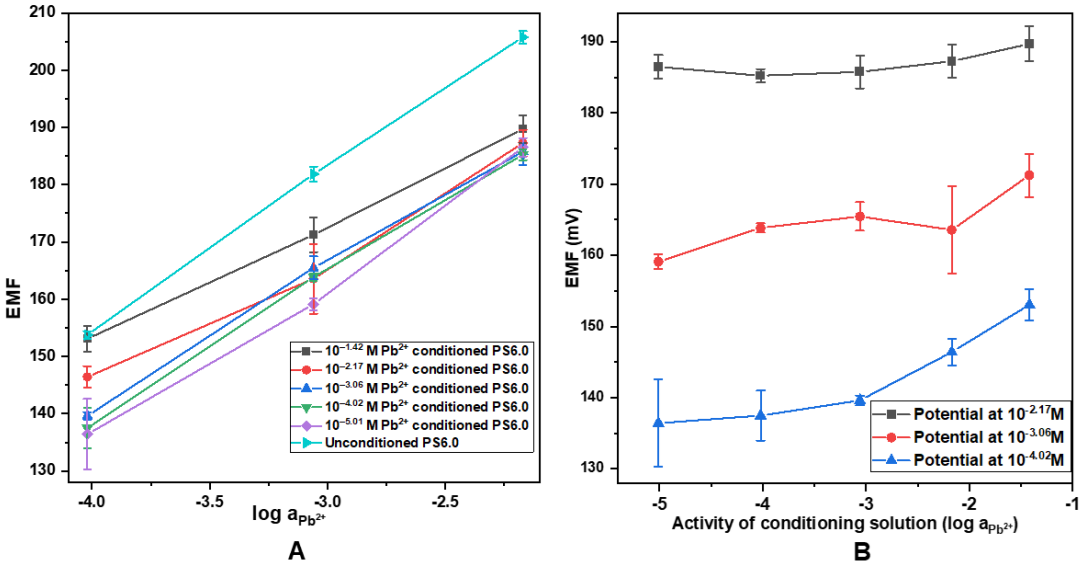

Figure 5. 6 Potentiometric response of Pb^{2+}-ISEs coupled with PS6.0 treated with different concentrations of Pb^{2+} (A) and variation of EMF with activity of conditioning solution used (B)

The effect of conditioning the ISM modified paper substrates with $Cd(NO_3)_2$ (interfering ion) was also studied and the results are shown in Figure 5.7. The Cd^{2+} ion was considered as a model interfering ion in this study as cadmium is one of the major interfering ions for Pb^{2+}-ISEs based on lead ionophore IV with $logK_{Pb^{2+},Cd^{2+}} = -3.8$ [168]. It was found that conditioning of PS6.0 with interfering ion (Cd^{2+}) did not influence (positively or negatively) the response of the Pb^{2+}-ISEs (having selectivity coefficient favoring lead(II) over cadmium(II)). It can be then expected that ISM in the structures of the paper substrates maintains the selectivity of the lead ionophore IV-based ISM.

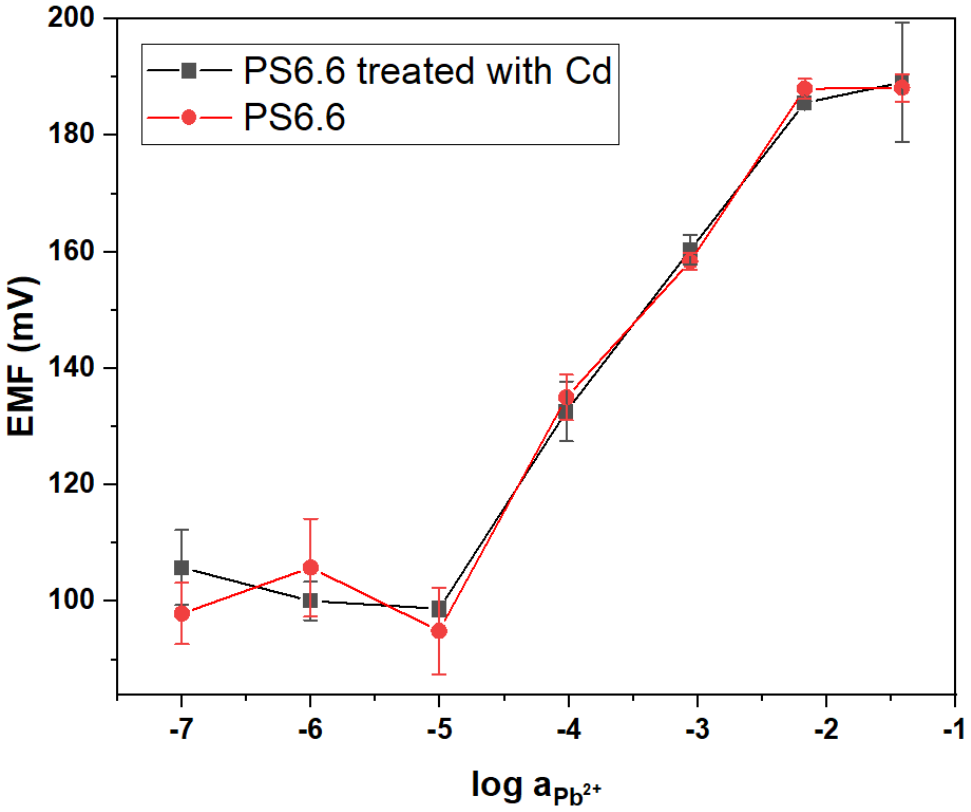

Figure 5. 7 Potentiometric response of Pb^{2+}-ISEs coupled with untreated PS6.0 and PS6.0 treated with 0.1 M Cd^{2+}

5.3.4. Characterization of ISM-modified paper substrates

The best performing ISM-modified paper substrates were characterized for their chemical and physical properties that may be influencing the potentiometric response when coupled with Pb^{2+}-ISEs. For example, liquid absorption capacity gradually decreased from PS6.3 to PS6.0. Similarly, the response time of the Pb^{2+}-ISEs increased from PS6.3 to PS6.0 (Table 5.2) This can be explained by the fact that membrane components occupy the available space in between and within the cellulose fibres that ultimately limits wicking ability of the paper. Both liquid absorption capacity and ISEs response times assure that all paper modifications are viable for analytical measurements within small liquid volumes and time of measurement not being longer

than typically assumed 60 s. Furthermore, as ISM is hydrophobic in nature with introduction of higher mass of membrane components to the paper substrate the imminent increase in hydrophobicity of the modified paper substrates was observed (Figure 5.8). Aside of ISM occupying the available space in between and within paper fibres, the increase in hydrophobicity of the paper substrates could also be a reason for the increase in Pb^{2+}-ISEs response time.

Table 5. 2 Liquid absorption capacity of the modified paper substrates and response time of the Pb^{2+}-ISEs when coupled with modified paper substrates.

PS	**Liquid absorption capacity (µL cm^{-2})**	**Potentiometric measurement response time of Pb^{2+}-ISEs (s)**
6.3	38.97 ± 5.31	16.7 ± 4.2
6.2	24.80 ± 4.84	18.7 ± 3.1
6.1	18.88 ± 3.98	20.0 ± 6.9
6.0	17.27± 3.27	24.0 ± 4.0

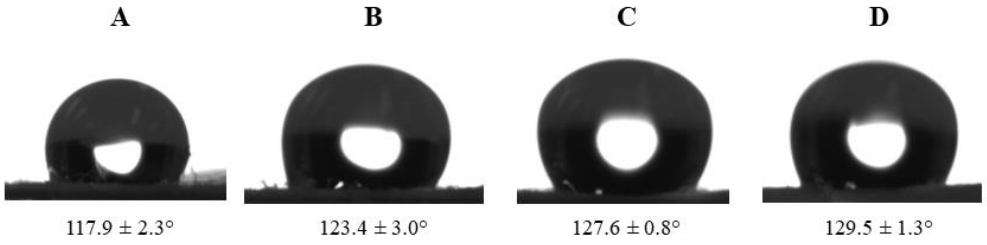

Figure 5. 8 Contact angle measurements: optical images taken in sessile drop mode for PS6.3 (A), PS6.2 (B), PS6.1 (C) and PS6.0 (D)

When considering the SEM images of the ISM-modified paper substrates (Figure 5.9), the images of modified paper substrates and unmodified paper substrate at different magnifications did not show much variation in terms of the distribution of the paper fibres and overall surface morphology. However, some granular structures could be observed at higher magnifications in modified paper substrates and the concentration of these structures increased with increasing membrane cocktail concentration (PS6.3 to PS6.0) suggesting that more and more ISM-components were distributed throughout the surface of the paper substrates. Figure 5.10 shows elemental mapping done with EDX where all ISM modified paper substrates indicate the presence of element chlorine apart from the usual carbon and oxygen present in unmodified paper substrates. The presence of chlorine was from PVC used for the modification of paper substrates (33.3 w/w% in ISM). Interestingly, in PS6.0 sulphur could also be observed in addition to chlorine, carbon and oxygen. Presence of sulphur most likely originates from lead ionophore IV used for modification (1% w/w in ISM). The absence of sulphur in EDX elemental mapping from PS6.1 to 6.3 could be due to the low concentration of ionophore within the paper substrates and relatively high detection limit of EDX. In order to investigate whether the extra elements from the paper modification distribute evenly, the individual maps of the elements were also obtained and shown in Figure 5.11 (left). All the elements were distributed throughout the surface of the paper, and the elements originating from the ISM seemed to be found along the edges of the paper fibres. The cross section of a modified paper substrate was also obtained and EDX was performed. Figure 5.11 (right) shows that ISM-components were distributed throughout the cross section of the paper substrate indicating full bulk of the paper substrate modification.

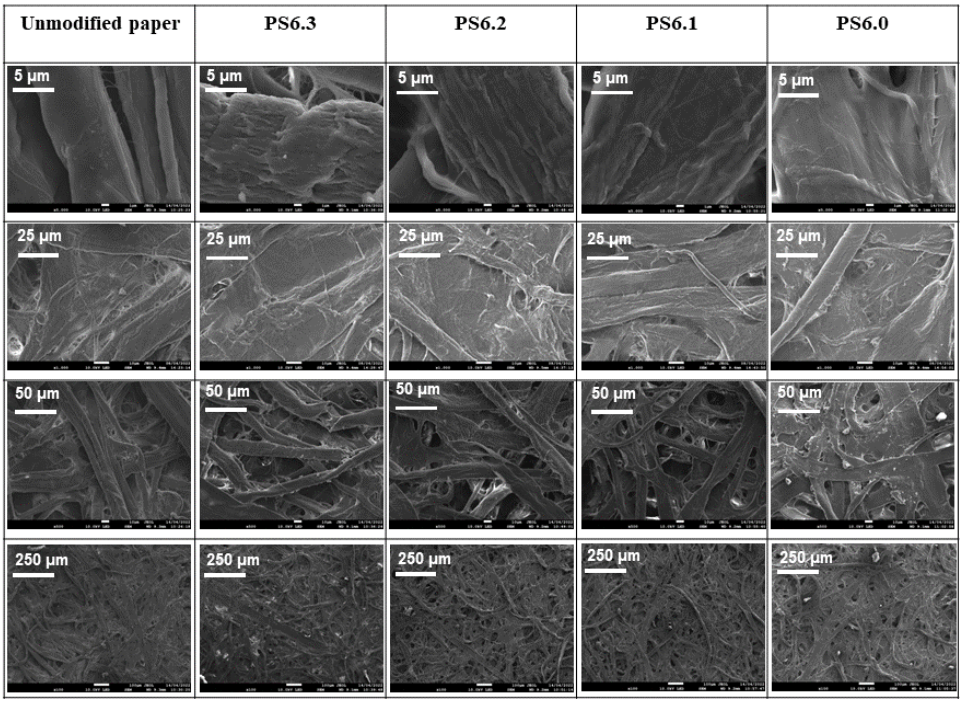

Figure 5. 9 SEM images for unmodified paper and ISM modified paper substrates at different magnifications

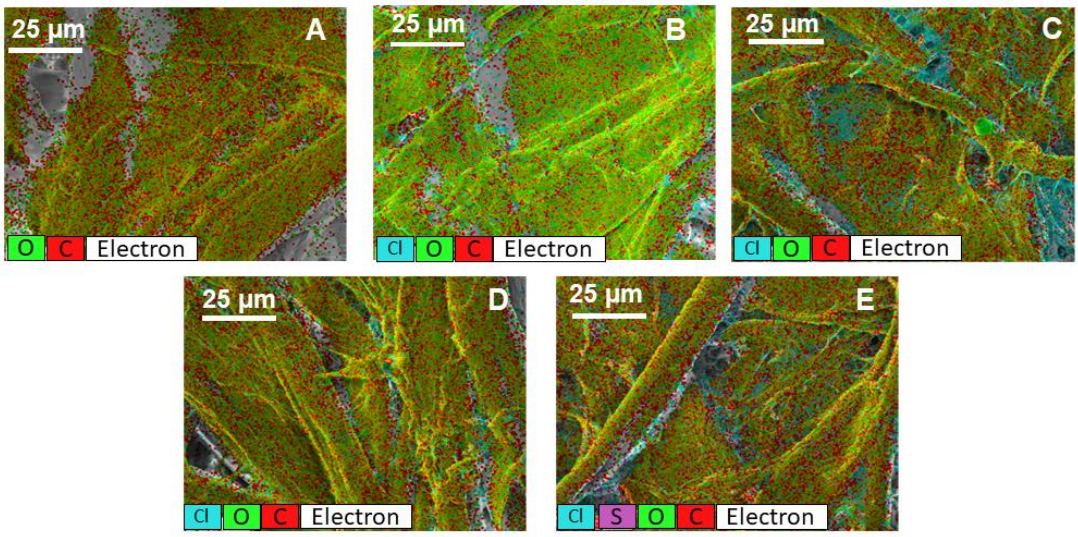

Figure 5. 10 Elemental analysis of surface of unmodified paper (A), PS6.3 (B), PS6.2 (C), PS6.1 (D), and PS6.0 (E)

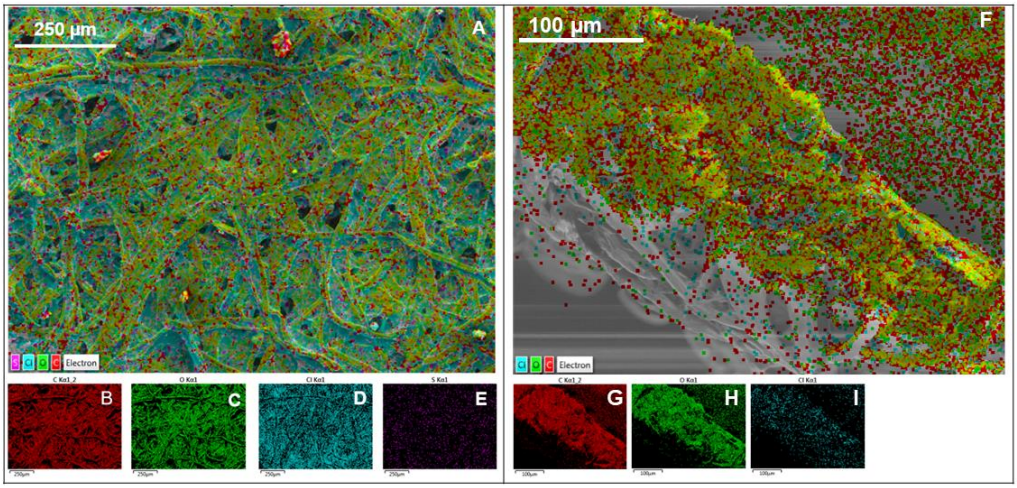

Figure 5. 11 Elemental mapping of surface (left) and cross section (right) of PS6.0 where A and F shows the overlapped elemental image and B, C, D, E, G, H, I show the individual element maps of carbon (red), oxygen (green), chlorine (light blue), and sulphur (purple)

FTIR study was performed to provide additional insight and supporting evidence into the chemical modification of paper substrates by ISM. As shown in Figure 5.12 and Table 5.3, the FTIR spectra indicated that the modification of PS6.0 paper substrate demonstrated multiple additional functional groups (as compared to the unmodified paper substrate) that are correlated to the ISM components applied [169–171].

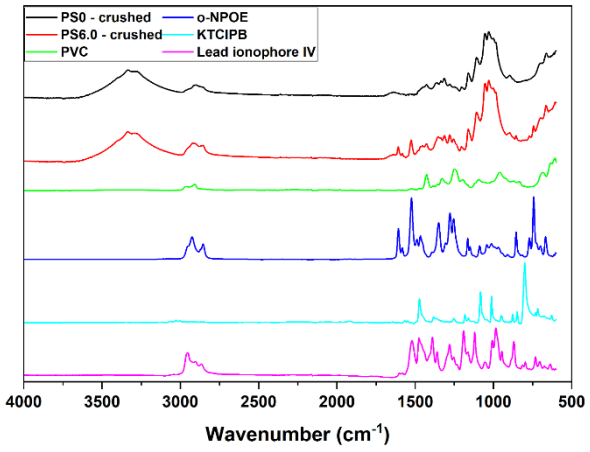

Figure 5. 12 FTIR of an unmodified paper substrate (PS0) as compared to PS6.0 and pure ISM-components.

Table 5. 3 Wavenumber regions and assigned functional groups

Origin	Group frequency, wavenumber (cm^{-1})	Assignment
O-H	3570–3200	Hydroxy group, H-bonded OH stretch
$-CH_2-$	2960-2850	methylene
C=C-C	1615–1580	Aromatic ring stretch
NO_2	1525	Nitro
CH_2-Cl	1426	Angular deformation
CH-Cl	1254	Out of plane angular deformation
	900–670 (several)	Aromatic C-H
C-H	770-730+710-690	Monosubstitution (phenyl)
	770-735	1,2-Disubstitution (ortho)

Peaks observed at 3344 cm^{-1} for both PS0 and PS6.0 indicates the presence of O-H functional groups in cellulose. A peak was observed at 2854 cm^{-1} in the PS6.0 spectrum but absent in the PS0 spectrum. The peak at 2858 cm^{-1} observed in the o-NPOE spectrum corresponds to $-CH_2-$ group and suggests presence of similar group in PS6.0 since the wavelength range for $-CH_2-$ group is 2960-2850 cm^{-1}. The peak at 2959 cm^{-1} for lead

ionophore IV could also be originating from the same group. Since o-NPOE contains an aromatic ring, the peak at 1605 cm^{-1} can be attributed to an aromatic ring stretch and could also be the reason for the peak at 1607 cm^{-1} for PS6.0. A peak appeared at 1526 cm^{-1} (corresponding to NO_2 group) in both PS6.0 and o-NPOE spectra but absent in PS0 spectrum. Peaks at 1427 cm^{-1} could be observed in both PS6.0 and PVC spectra, indicating presence of CH_2-Cl angular deformation. The peak observed at 1256 cm^{-1} in PS6.0 spectrum and at 1254 cm^{-1} in the PVC spectrum can be attributed to the CH-Cl out of plane angular deformation. Aromatic C-H group can be seen in a wide range of wavenumber and could be the reason for the peaks at 870 cm^{-1} for lead ionophore IV and 854 cm^{-1} for PS6.0. Peaks appearing in 700-770 cm^{-1} region for both PS0, PS6.0, o-NPOE and lead ionophore (IV) spectra could arise from C-H groups (Monosubstitution and 1,2-Disubstitution).

5.3.5. Determination of lead(II) in complex environmental samples using ISM-modified paper substrates coupled with Pb^{2+}-ISEs

Overall, the Pb^{2+} ion activities determined by the ISEs coupled with ISM-modified paper substrates (PS6.0) were found to be comparable to the total lead concentration determined by ICP-OES (Figure 5.13). The uncertainties of most measurements were within ± 20% between these two measurements with some slight deviation for wetland sample, cultivation soil sample and biowaste 1 sample. The higher variations of the results between potentiometric and ICP-OES measurements, for wetland and cultivation soil samples could be due to the possible interactions of Pb^{2+} with organic matter that is expected to be present in this type of samples. This would partially deplete the ionized lead(II) from the samples. For biowaste 1, the ionic strength of the leachate could possibly be high enough to shift the calibration and measurement apart inducing

measurement errors. Nonetheless, all measurements conducted bring a great promise to use ISM-component modified paper substrates coupled with Pb^{2+}-ISEs for measurement of ion activity in samples containing high solid-to-liquid ratios and complex environmental matrices.

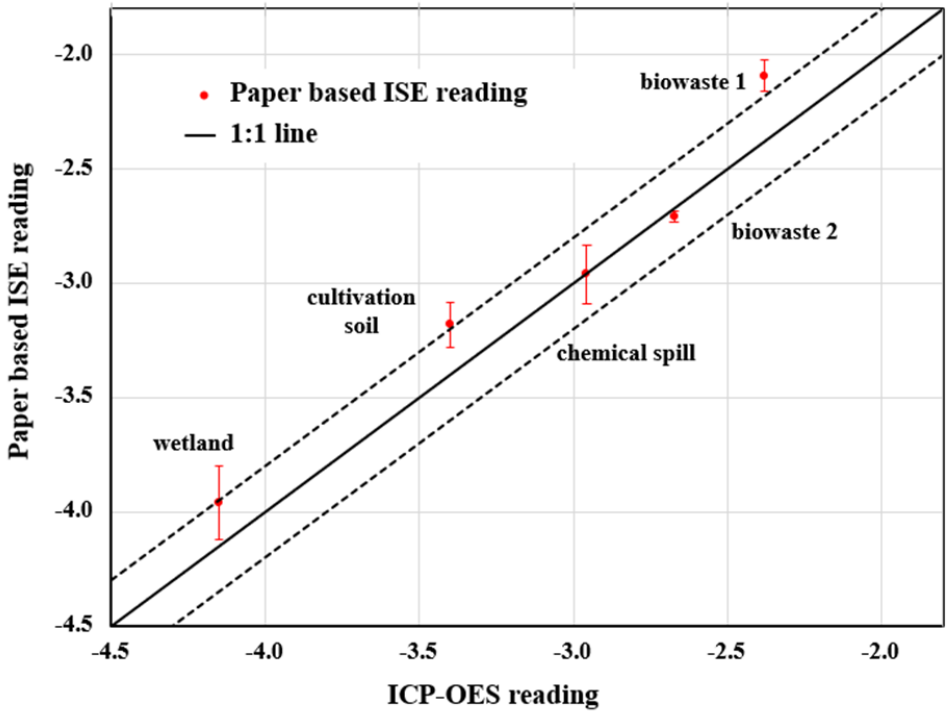

Figure 5. 13 Determination of lead (II) in samples with complex environmental matrices using ISM-component modified paper substrates coupled with Pb^{2+}-ISEs as compared to measurement done by ICP-OES.

5.4. Conclusions

ISM-component modified paper substrates were validated for their use as microfluidic sampling substrates when coupled with Pb^{2+}-ISEs. It was found that direct modification of paper substrates by traditional ISM cocktail used for preparation of Pb^{2+}-ISEs was the most optimal in: (i) eliminating super-Nernstian response of ISEs when unmodified paper substrates are used for solution sampling; (ii) improving the uncertainty of

measurements when unconditioned ISM-component modified paper substrates were used; and (iii) extending the linear working range of the sensor to be comparable to standard beaker-based measurements.

Moreover, the use the same chemicals to prepare ISM of ISE and modify the paper substrates simplify the procedure of preparation of the measuring set up and may have further direct economic benefits by limiting the preparation of the measuring setup to limited number of chemicals. Finally, having ISM on paper substrates simplifies the ISM | modified paper substrate interface by being more compatible with the one of ISM. It was found that ISM on paper substrates may influence the potentiometric response of the Pb^{2+}-ISEs used. For that reason, the unconditioned ISM-component modified paper substrates were found the best suited for successful determination of lead(II) in complex environmental samples.

CHAPTER 6 DETERMINATION OF SELECTIVITY OF Pb^{2+}-ISEs COUPLED WITH MODIFIED MICROFLUIDIC PAPER-BASED SOLUTION SAMPLING SUBSTRATES

6.1. Introduction

The quantification of heavy metals in environmental samples is vital for the maintenance of human health and environmental quality [21,22]. Among the analytical techniques available for quantification, potentiometry coupled with paper-based solution sampling offers many advantages such as reduction of cost, pretreatment procedures and sample volume needed for analysis [46,55]. Recently, several modifications were proven to be successful in overcoming challenges associated with physicochemical interactions between heavy metal samples and paper-based substrates used for solution sampling. These include modification with an inorganic salt [48] and acidification [49] of the paper substrate.

Generally, ion-selective electrodes (ISEs) can be characterized by their different parameters including working range, response slope, selectivity to the target ion, response time, stability, reproducibility from electrode-to-electrode or batch-to-batch [95]. The performance of Pb^{2+}-ISEs coupled with modified paper-based substrates mentioned above have been characterized based on many of these parameters. However, the determination of selectivity coefficients has not been thoroughly investigated since the modified paper substrates performed sufficiently well in complex environmental samples.

Selectivity coefficients of potentiometric ion sensors refer to the electrode's ability to distinguish the target analyte when other interfering ions are present. Quantification of potentiometric selectivity can be performed by experimental methods such as separate solutions method (SSM), fixed interference method (FIM), fixed primary ion method (FPM), two solution method (TSM), and matched potential method (MPM)[97]. Understanding the underlying chemical mechanisms governing ion-selective electrode responses can provide insights into the selectivity behavior. Factors such as ion-exchange processes[172], complexation reactions[173], diffusion processes[174], and membrane composition[175] contribute to selectivity.

The ionophore component of the ISM plays a critical role in the selectivity of the electrode [150]. In the case of experiments carried out for Pb^{2+}-ISEs with modified paper substrates, lead ionophore IV [176] has been used as the ionophore due its superior selectivity compared to other lead(II) ionophores available commercially [177]. Lead ionophore IV is a thioamide derivative of *p-tert*-butylcalix[4]arene and its superior behaviour is attributed to the affinity of lead (II) cations to the C=S bond and the similarity in dimensions between the cavity of the calix[4]arene and the lead (II) ion[177]. The selectivity values of this ionophore have been previously reported in solution based measurements (conventional setup) [168,178,179].

Since data on selectivity of electrodes utilizing paper-based sampling is almost non-existent, this study focuses on the determination of selectivity coefficients for Pb^{2+}-ISEs coupled with unmodified and modified paper-based substrates. The effect of specific paper-substrate modifications on selectivity coefficients will also be investigated as this

will aid in the further development of robust heavy metal sensors which can be used in environmental applications.

6.2. Experimental

6.2.1. Preparation of electrodes and paper substrates

Electrodes and paper substrates were prepared as mentioned in section 3.3. For the determination of selectivity, the best performing paper substrates from each type of modifications (metal and ISM based) were selected. To prepare metal modified paper substrates, grade 388 filter paper was coated with a layer of gold using a sputter coater. For each sputtering session, 40 mA current was applied at 3 Pa for 7.5 mins on each side of the paper to achieve a thickness of 38 nm gold. ISM modified paper substrates were prepared by soaking grade 388 filter paper in Pb^{2+}-ISM solution for 30 mins and then drying overnight at room temperature (23 ± 2 ˚C). Paper substrates were also prepared for the comparison with previously established paper modifications in literature, such as acid based modification. Acid modified paper substrates [49] were prepared by soaking grade 390 filter papers in 10^{-2} M HCl solution for 30 mins, and then drying in open air at room temperature (23 ± 2 ˚C) on a clean petri dish.

6.2.2. Selectivity measurements

Separate solutions method (SSM) was used to determine the selectivity coefficients of Pb^{2+}-ISEs for primary ion over nine different interfering ions. The ion sequence was estimated using literature available on selectivity of lead ionophore IV and validated through actual measurements [168,178,179].To do that, the beaker-based measurements were done prior to measurements with paper-based substrates to establish the ion sequence (from least to most interfering, finalized with measurement done with primary

ion). Calculation of selectivity coefficients were done only for unconditioned electrodes exhibiting close to Nernstian behaviour in activity range of $10^{-3.06}$ to $10^{-2.17}$ M Pb^{2+}. The uncertainty of selectivity coefficients was calculated by noting the EMF recorded with three electrodes (n=3). Nikolsky–Eisenmann equation was used for the calculation of selectivity coefficients [96].

6.3. Results and discussion

6.3.1. Selectivity of Pb^{2+}-ISEs in solution-based/traditional measuring setup

The solution-based selectivity coefficients of solid-contact Pb^{2+}-ISEs consisting of an ISM composed of 1% lead ionophore (IV), 0.5% KTClPB, 65.2% o-NPOE and 33.3% PVC dissolved in THF was determined with SSM. Figure 6.1 represents the selectivity of Pb^{2+}-ISEs in solution-based measurement setup. Mg^{2+} was observed to be the least interfering ion and Cd^{2+} was the most interfering ion. The Pb^{2+} slopes of E1, E2 and E3 for this trial were 25.0 ± 0.5, 26.8± 0.5 and 28.3± 0.2 mV dec^{-1}, respectively. The selectivity coefficient for E1, E2 and E3 range from -18.1± 0.1 to -6.2 ± 0.0, -17.3 ± 0.2 to -5.7 ± 0.1 and -16.5 ± 0.2 to -5.6 ± 0.1, respectively. The values have an uncertainty range from 0.3 to 0.8 (between the 3 electrodes). The final ion sequence was Mg^{2+}< Co^{2+}< Ca^{2+}< Ba^{2+}< Na^{+}< Zn^{2+}< K^{+}< Cu^{2+}< Cd^{2+}< Pb^{2+}. This was established as the default testing sequence for measurements with paper-based substrates. Malinowska et al. [168] reported selectivity coefficients for Pb^{2+}-ISEs consisting of a similar ISM composition but used electrode bodies with an internal filling solution (liquid contact electrodes). A mix of SSM and FIM were used for determination of selectivity. Gupta et al. [178] used sodium tetraphenyl borate (NaTPB) and dibutyl phthalate (DBP) in the

ISM, and used FIM and MPM for determination of selectivity. Ceresa and Pretsch [179] used liquid contact Pb^{2+}-ISEs using DOS in the ISM. The initial ion sequence after initial screening varied slighlty, namely between Cu^{2+} and Cd^{2+}, from the abovementioned literature.

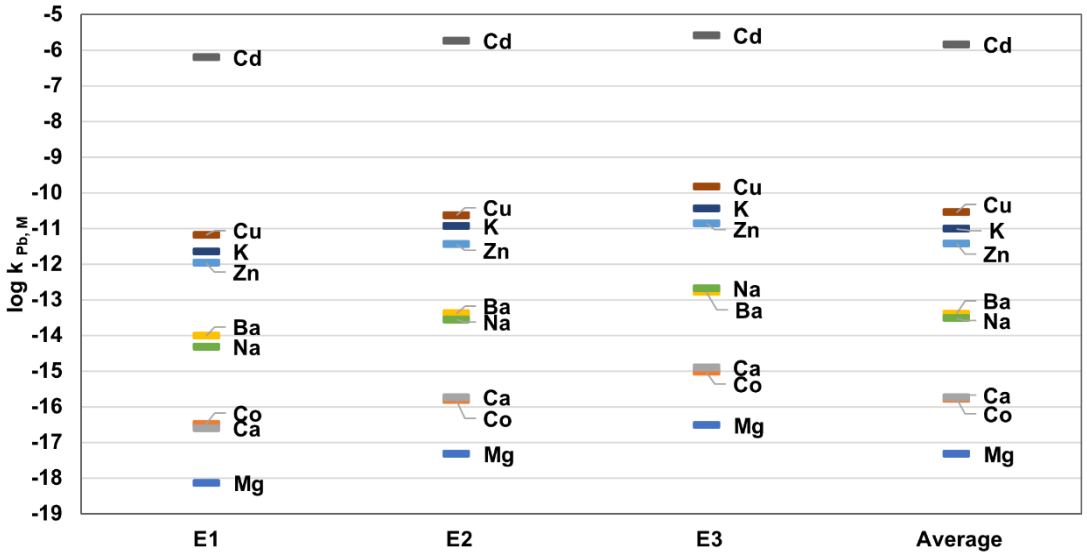

Figure 6. 1 Solution-based selectivity coefficients

6.3.2. Selectivity of Pb^{2+}-ISEs in unmodified paper-based measurement setup

Figure 6.2 shows the selectivity coefficients for Pb^{2+}-ISEs coupled with unmodified paper-based substrates. Similar to the solution-based trial, the least interfering ion was Mg^{2+} while the most interfering ion was Cd^{2+}. The Pb^{2+} slopes of E1, E2 and E3 for this trial were 26.9 ± 1.2, 27.3 ± 1.3 and 30.3 ± 3.9 mV dec^{-1}, respectively. The selectivity of Pb^{2+}-ISEs for unmodified paper substrates coupled with E1, E2 and E3 range from -14.4 ± 0.0 to -5.0 ± 0.0, -13.3 ± 0.0 to -4.5 ± 0.0 and -11.1 ± 0.2 to -3.6 ± 0.1, respectively. Although there was a larger average uncertainty from 0.7 to 2.3 between the electrodes

for selectivity, the metal ion had similar sequence, starting with Mg^{2+}< Co^{2+}< Ca^{2+}< Zn^{2+}< Ba^{2+}< Na^{+}< K^{+}< Cu^{2+}< Cd^{2+}< Pb^{2+}, respectively.

When comparing the values between solution-based and unmodified paper-based, there was only a slight shift in Zn^{2+} ion in the sequence. The log $k_{Pb, M}$ range of solution-based were -17.3 ± 0.8 to -5.8 ± 0.3 on average while the value for unmodified paper-based was -12.9 ± 1.6 to -4.4 ± 0.7. This means that solution-based results have a slightly higher variation than unmodified paper-based. Additionally, the standard deviation of average log $k_{Pb, M}$ for solution-based set-up ranged from 0.3 to 0.8 while for the unmodified paper-based set-up, standard deviation ranged from 0.7 to 2.3. Therefore, the result from unmodified paper-based was not as consistent as solution-based. This can be expected due to the physicochemical interactions between the metal ions and paper-based substrates. When used with solution-based measurements, the electrodes were submerged in the metal ion sample solution without any additional layer of a paper substrate which allows direct contact reducing other physical and chemical reactions that may affect actual results.

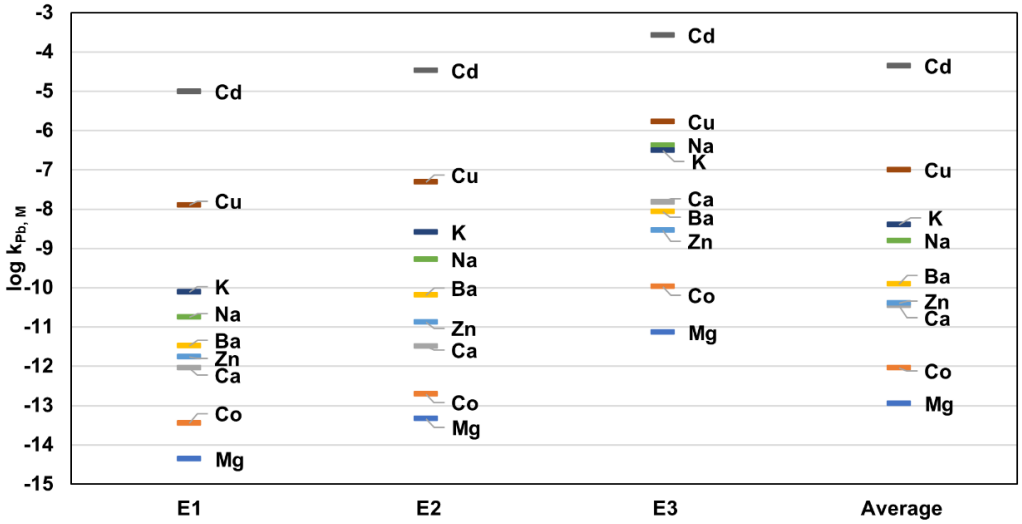

Figure 6. 2 Unmodified paper-based selectivity coefficients

6.3.3. Selectivity of Pb^{2+}-ISEs in gold modified paper-based measurement setup

Figure 6.3 illustrates the selectivity coefficients obtained for Pb^{2+}-ISEs coupled with gold modified paper substrates. The Pb^{2+} slopes of E1, E2 and E3 for this trial were 26.6 ± 3.0, 34.3 ± 2.4 and 28.1 ± 6.0 mV dec^{-1}, respectively. The log $k_{Pb, M}$ values for E1, E2 and E3 ranged from -15.7 ± 0.2 to -5.4 ± 0.1, -11.6 ± 0.1 to -4.1 ± 0.1 and -13.6 ± 0.2 to -4.5 ± 0.1, respectively. The uncertainty of average selectivity coefficients ranged from 0.7 to 2.1 (between 3 electrodes). The ion sequence was Mg^{2+}< Co^{2+}< Ca^{2+}< Ba^{2+}< Zn^{2+}< Na^{+}< K^{+}< Cu^{2+}< Cd^{2+}< Pb^{2+}, respectively. There was a slight shift in ion sequence in E1 as Co^{2+} and Ca^{2+}, Zn^{2+} and Na^{+} are in different positions when compared to E2 and E3 but it was considered insignificant. The selectivity values and order of interference obtained across electrodes remain relatively more consistent compared to unmodified paper-based measurements. The results also indicate that the ISE retains its selectivity despite being used with gold modified paper-based substrate.

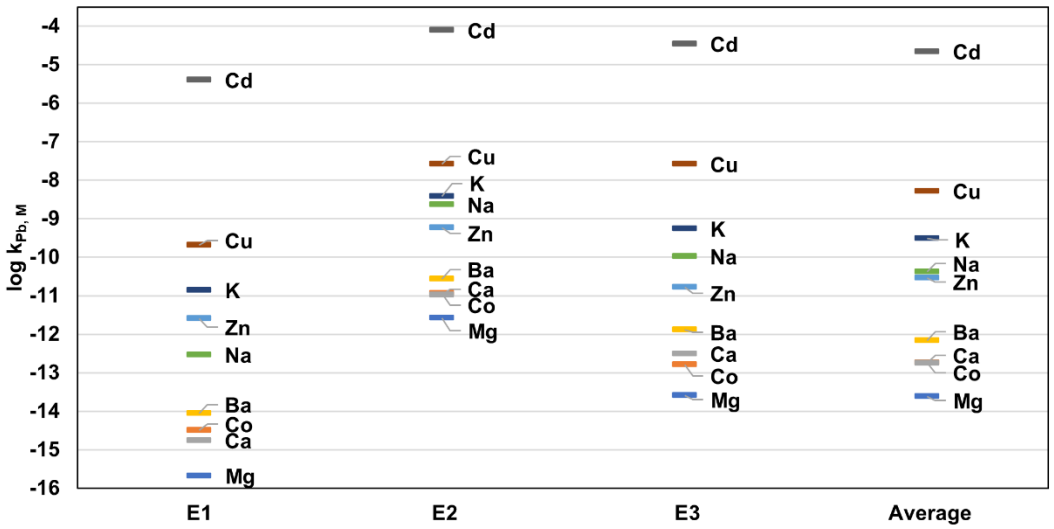

Figure 6. 3 Gold modified paper-based selectivity coefficients.

6.3.4. Selectivity of Pb^{2+}-ISEs in ISM modified paper-based measurement setup

Figure 6.4 represents the selectivity coefficients obtained with ISM modified paper-based measurement setup. The Pb^{2+}-ISEs slopes of E1, E2 and E3 for this trial were 26.5 ± 1.7, 31.1 ± 2.6 and 30.9 ± 4.6 mV dec^{-1}, respectively. The log $k_{Pb, M}$ for E1, E2 and E3 ranged from -14.0 ± 0.1 to -6.8 ± 0.1, -13.5 ± 0.1 to -5.7 ± 0.1 and -13.8 ± 0.0 to -6.0 ± 0.1, respectively. The uncertainty ranged from 0.1 to 0.6 (between 3 electrodes). The ion sequence was Mg^{2+} < Co^{2+}< Ca^{2+}< Ba^{2+}< Zn^{2+}< Na^{+}< K^{+}< Cu^{2+}< Cd^{2+}< Pb^{2+}, respectively.

When compared to solution-based sampling, the selectivity coefficients were comparable or slightly higher with those obtained when Pb^{2+}-ISEs used ISM modified paper as a sampling substrate. Naturally, the paper matrix may produce additional ionic content, making the selectivity coefficients biased and shifting the selectivity of the Pb^{2+}-ISEs to higher values when used with paper substrates. What is important to note is that the most interfering ions, namely Cu^{2+} and Cd^{2+} remain at low interference level validating the performance of the Pb^{2+}-ISM to be predominantly Pb^{2+} selective.

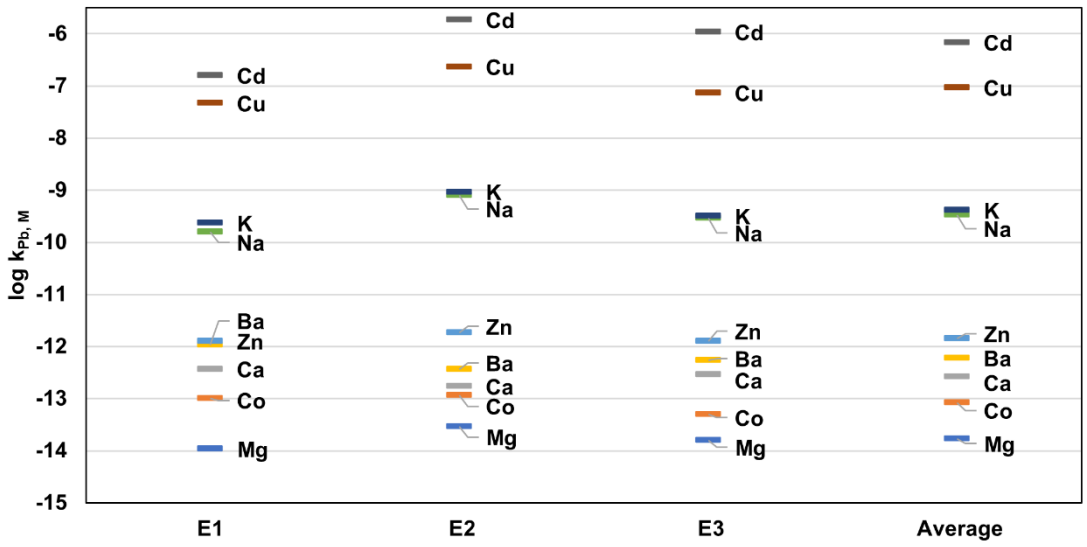

Figure 6. 4 ISM modified paper-based selectivity coefficients

6.3.5. Selectivity of Pb^{2+}-ISEs in acid modified paper-based measurement setup

Selectivity coefficients for acid modified paper-based measurement setup [49] was also determined so that it could be compared with modifications presented in this thesis. Results for acid modified paper-based substrates are shown in Figure 6.5. The Pb^{2+} slope of E1, E2 and E3 for this trial were 29.3 ± 1.0, 29.9 ± 1.3 and 31.3 ± 1.4 mV dec^{-1}, respectively. The log $k_{Pb, M}$ values for E1, E2 and E3 ranged from -14.9 ± 0.1 to -6.2 ± 0.0, -14.5 ± 0.0 to -6.1 ± 0.0 and -13.7 ± 0.0 to -5.9 ± 0.0, respectively. The uncertainty ranged from 0.2 to 0.6 (between 3 electrodes). The ion sequence was Mg^{2+} < Co^{2+}< Ca^{2+}< Ba^{2+}< Zn^{2+}< Na^{+}< K^{+}< Cu^{2+}< Cd^{2+}< Pb^{2+}, respectively.

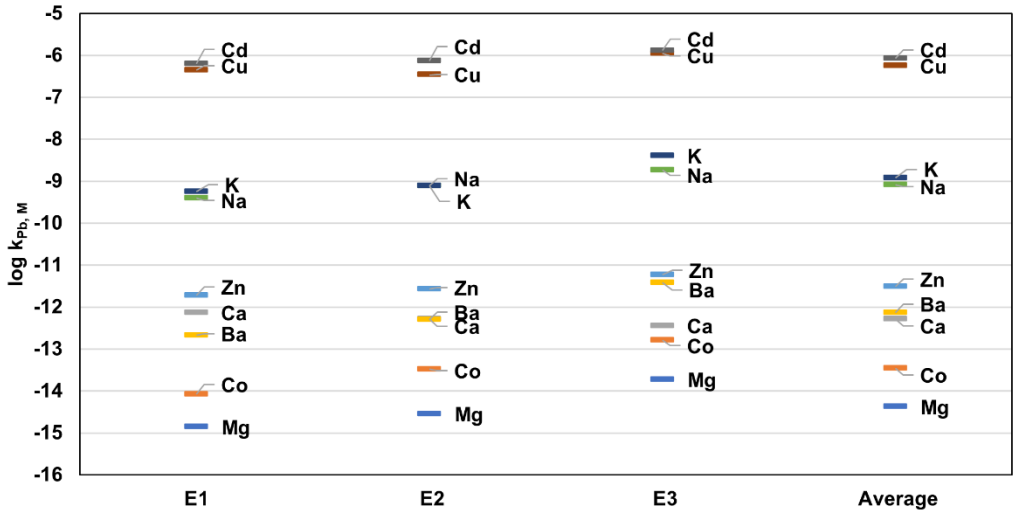

Figure 6. 5 Acid modified paper-based selectivity coefficients

6.3.6. Comparison of all modifications of paper substrates with solution-based sampling and unmodified paper-based substrate sampling

As shown in Figure 6.6 and Table 6.1, most of the modifications had ion sequence and selectivity values which were similar to each other. Cd^{2+} was the most interfering metal ion whereas Mg^{2+} was the least interfering metal ion across the different trials.

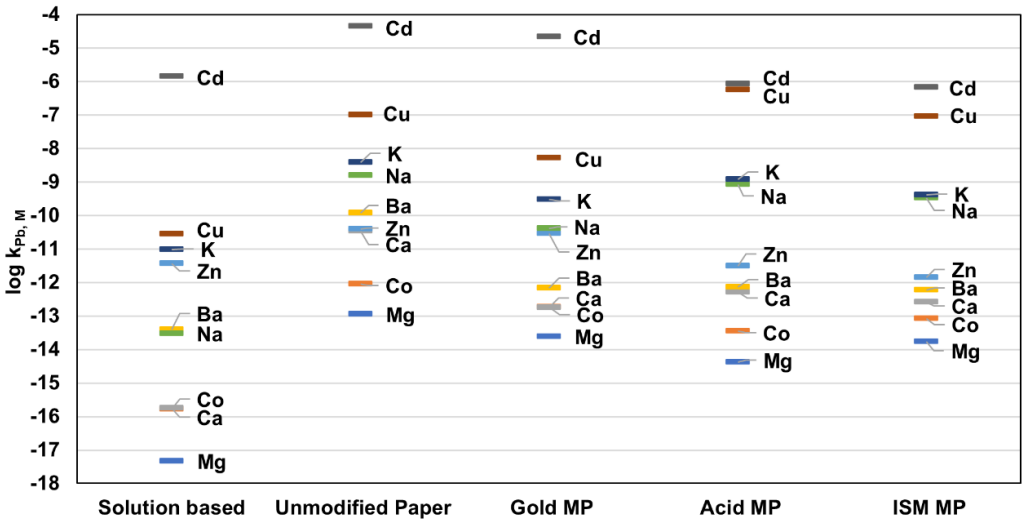

Figure 6. 6 Comparison of all selectivity coefficients from different modification of paper substrates, solution-based sampling, and unmodified paper substrates

Table 6. 1 Representative values of selectivity coefficients and slopes obtained by separate solution method for Pb^{2+}-ISEs in solution and incorporated with unmodified and modified paper; the slopes indicated are between $10^{-3.06}$ to $10^{-2.17}$ M of respective interfering ion.

j	$log\ K^{pot}_{Pb^{2+},j}$ in solution	Slope/mV dec^{-1} in solution	$log\ K^{pot}_{Pb^{2+},j}$ with unmodified paper	Slope/mV dec^{-1} with unmodified paper	$log\ K^{pot}_{Pb^{2+},j}$ with gold modified paper	Slope/mV dec^{-1} with gold modified paper	$log\ K^{pot}_{Pb^{2+},j}$ with ISM MP	Slope/mV dec^{-1} with ISM MP	$log\ K^{pot}_{Pb^{2+},j}$ with acid modified paper	Slope/mV dec^{-1} with acid modified paper
Mg^{2}	-17.3 ± 0.8	-15.4 ± 4.2	-12.9 ± 1.6	0.2 ± 8.7	-13.6 ± 2.1	-1.5 ± 3.5	-13.8 ± 0.2	12.1 ± 2.2	-14.4 ± 0.6	1.0 ± 2.0
Ca^{2}	-15.8 ± 0.8	20.1 ± 0.5	-10.5 ± 2.3	28.9 ± 0.2	-12.7 ± 1.9	24.2 ± 2.3	-12.6 ± 0.2	11.9 ± 1.2	-12.3 ± 0.2	13.4 ± 0.8
Co^{2}	-15.8 ± 0.7	16.8 ± 4.8	-12.0 ± 1.8	27.2 ± 2.3	-12.7 ± 1.8	22.7 ± 3.7	-13.1 ± 0.2	6.6 ± 6.4	-13.5 ± 0.6	21.1 ± 2.3
Na^{+}	-13.5 ± 0.8	13.1 ± 0.7	-8.8 ± 2.2	37.7 ± 0.9	-10.4 ± 2.0	18.8 ± 2.3	-9.5 ± 0.4	18.0 ± 2.1	-9.1 ± 0.3	25.0 ± 1.3
Ba^{2+}	-13.4 ± 0.6	26.3 ± 1.7	-9.9 ± 1.7	22.1 ± 0.1	-12.2 ± 1.8	28.8 ± 0.4	-12.2 ± 0.2	5.7 ± 4.2	-12.1 ± 0.2	15.4 ± 5.7
Zn^{2}	-11.4 ± 0.6	27.3 ± 0.4	-10.4 ± 1.7	18.0 ± 1.4	-10.5 ± 1.2	37.1 ± 3.8	-11.8 ± 0.1	12.6 ± 1.5	-11.5 ± 0.6	23.7 ± 1.7
K^{+}	-11.0 ± 0.6	51.8 ± 0.4	-8.4 ± 1.8	34.1 ± 0.4	-9.5 ± 1.2	25.9 ± 2.0	-9.4 ± 0.3	11.4 ± 2.3	-8.9 ± 0.3	32.2 ± 1.1
Cu^{2}	-10.6 ± 0.7	19.2 ± 0.9	-7.0 ± 1.1	38.7 ± 2.3	-8.3 ± 1.2	18.0 ± 1.2	-7.0 ± 0.4	50.6 ± 6.2	-6.3 ± 0.3	90.5 ± 3.0
Cd^{2}	-5.8 ± 0.3	30.8 ± 1.2	-4.4 ± 0.7	32.3 ± 1.0	-4.7 ± 0.7	37.6 ± 1.0	-6.2 ± 0.6	38.9 ± 2.2	-6.1 ± 0.2	35.5 ± 0.5
Pb^{2+}	0	28.3 ± 0.2	0	30.3 ± 3.9	0	28.1 ± 6.0	0	30.9 ± 4.6	0	31.3 ± 1.4

6.4. Conclusions

This study was done to determine of selectivity of Pb^{2+}-ISEs using separate solution method (SSM) when Pb^{2+}-ISEs were coupled with newly introduced paper-based microfluidic sampling substrates, and to compare the results with solution-based sampling and pairing with unmodified and a previously introduced modified paper substrate.

From the results, the paper modification for metal sputtering, acidified and ISM showed comparable results in terms of Cd^{2+} as the most interfering metal ion and Mg^{2+} as least interfering metal ion. The log $k_{Pb, M}$ values were also consistent throughout the different trials. The uncertainty between the values was small, which shows that the results are reliable. These modifications also had very similar ion sequence with only a few slight shifts in positions which are negligible.

CHAPTER 7 CONCLUSIONS AND FUTURE PROSPECTS

7.1. Conclusions

Paper-based potentiometry is a versatile technique that can be used to measure a wide range of ions. It is a relatively simple and inexpensive method that can be performed using readily available materials. This thesis explored the use of novel paper-based substrates for the simple, rapid, and convenient detection of heavy metals in environmental samples by potentiometry.

The first strategy involved modification of paper substrates with thin layers of metals that can act as spacers between the ISM and paper fiber surface. The potentiometric response of Pb^{2+}-ISEs coupled with paper substrates coated in gold, platinum and palladium was investigated. The magnitude of the super-Nernstian jump was found to be dependent on the thickness of the metal layer and whether the paper substrate modification was on one side or both sides of the paper substrate. Paper substrates coated on both sides with a 38 nm thick layer of gold was found to be most advantageous in controlling the super-Nernstian response and having a wider linear potential range. They were used for the sampling of simulated environmental samples and the results were comparable with those obtained by ICP-OES. A lifecycle analysis was performed to compare the use of ISEs with and without modified paper substrates and it further confirmed the benefits of using metal modified paper substrates for samples with high solid-to-liquid ratio.

The second study was on the use of ISM modified paper substrates for the potentiometric determination of heavy metals. Pb^{2+}-ISEs coupled with paper substrates incorporated with different combinations of ISM-components were studied. The best potentiometric

response was obtained by paper substrates incorporated with all the components available in the ISM. Variation of the membrane cocktail concentrations used to modify paper substrates indicated that the super-Nernstian response could be controlled by the use of 10 to 50 mg ml^{-1} ISM cocktail. The success of ISM modified paper substrates could be attributed to the improved compatibility with the ISM and the solution sampling substrate. The use of chemicals which are already used in the manufacturing of the Pb^{2+}-ISEs further enhances the economic aspect of the paper substrates.

The third and final study was on the determination of selectivity of the newly introduced paper-based substrates and comparison with traditional beaker-based sampling and other previously introduced strategy for the elimination/control of the super-Nernstian response. When using gold modified paper substrates and ISM modified paper substrates for solution sampling, the ion sequence of interfering ions was comparable to solution-based sampling, and it was confirmed that the ionophore retains its selectivity pattern. The selectivity of acidified paper substrates was also similar to the above.

7.2. Future prospects

Based on the literature review and the experimental work performed, the following recommendations are made for the extension of work presented in this thesis:

(i) **Determination of selectivity coefficients of Pb^{2+}-ISEs coupled with paper-based substrates:** Though chapter 6 provided a primary understanding about the variation of selectivity coefficients based on the paper substrate utilized, further work can be done to understand more about the influence of paper modification on selectivity. Mixed solution techniques can be used for selectivity determination. It is expected that SSM which assume determination of unbiased selectivity coefficients may not

be the most optimal methodology in systems where paper may contribute ions to the solution and ISE.

(ii) **Lowering the lower detection limit of ISEs coupled with paper-based sensing for heavy metals determination**: Though research has been conducted for the lowering of the lower detection limit of ISEs coupled with traditional beaker-based sampling [145,180], there is little research on the same done for paper-based sampling. Since the detection limit of all ISEs coupled with paper-based sampling is relatively modest, it would be required to investigate strategies to lower the detection limit and allow trace heavy metals analysis.

(iii) **Studies with other heavy metals**: The studies in this thesis were conducted with Pb^{2+} as a model heavy metal. Studies could be extended to other heavy metal ISEs Such work could also lead to multiplexed determination of heavy metal ions.

(iv) **Control of fouling effects**: Even though the use of paper-based sampling devices can greatly reduce the fouling effects on the sensor since it prevents direct contact of the sample and the sensor, fouling effects can still arise from physical, chemical, and biological (biofouling) interactions with the sample or the environment [181]. It can affect the reliability of the measurement and give rise to less accurate readings. The effect of biofouling and other degradation effects on sensors should be studied further.

(v) **Improving the affordability of modified paper-based sampling**: Although the unmodified cellulose-based paper substrates used for the study are relatively inexpensive and widely available, the production of modified paper-based substrates can still be expensive. More techniques can be explored for the modification of paper substrates such that the material and energy cost can be reduced. Additionally, the

feasibility of using mass production techniques such as inkjet printing could also be explored.

(vi) Enhancing repeatability of paper-based sensors: One of the challenges associated with the mass production of paper-based sensors is the tendency to have batch-to-batch variations in properties. Standardized manufacturing processes and quality control measures can be developed to enhance the repeatability within an acceptable error range.

(vii) Addressing issues related to practical usage of paper-based sensors: Some of the advantages of paper which helps in its usage for sensor materials can be viewed as a disadvantage in its practical usage. For example, because of its porosity to water, the functionality can be impacted if used in a high humidity environment. The mechanical strength and chemical stability can change over time depending on the environmental conditions. Such issues should be addressed to prolong the shelf life of paper-based sensors.

(viii) Disposal of waste sensors: Even though the cellulose component of paper-based sensors is generally biodegradable, the disposal of sensors containing hazardous materials must be performed in an environmentally safe manner and protocols must be developed accordingly.

REFERENCES

[1] W. Wu, S. Qu, W. Nel, J. Ji, The impact of natural weathering and mining on heavy metal accumulation in the karst areas of the Pearl River Basin, China, Sci. Total Environ. 734 (2020) 139480. https://doi.org/10.1016/j.scitotenv.2020.139480.

[2] C. Lors, C. Tiffreau, A. Laboudigue, Effects of bacterial activities on the release of heavy metals from contaminated dredged sediments, Chemosphere. 56 (2004) 619–630. https://doi.org/10.1016/j.chemosphere.2004.04.009.

[3] P. Wang, Z. Sun, Y. Hu, H. Cheng, Leaching of heavy metals from abandoned mine tailings brought by precipitation and the associated environmental impact, Sci. Total Environ. 695 (2019) 133893. https://doi.org/10.1016/j.scitotenv.2019.133893.

[4] E.L. Tucker, G.W. Chickering, C.J. Spreadbury, S.J. Laux, T.G. Townsend, A componential approach for evaluating the sources of trace metals in municipal solid waste, Chemosphere. 260 (2020) 127524. https://doi.org/10.1016/j.chemosphere.2020.127524.

[5] W.-L. Zhang, L.-Y. Zhao, Z.-J. Yuan, D.-Q. Li, L. Morrison, Assessment of the long-term leaching characteristics of cement-slag stabilized/solidified contaminated sediment, Chemosphere. 267 (2021) 128926. https://doi.org/10.1016/j.chemosphere.2020.128926.

[6] N. Muhammad, M. Nafees, L. Ge, M.H. Khan, M. Bilal, W.P. Chan, G. Lisak, Assessment of industrial wastewater for potentially toxic elements, human health (dermal) risks, and pollution sources: A case study of Gadoon Amazai industrial estate, Swabi, Pakistan, J. Hazard. Mater. 419 (2021) 126450. https://doi.org/10.1016/j.jhazmat.2021.126450.

[7] S. Heberlein, W.P. Chan, A. Veksha, A. Giannis, L. Hupa, G. Lisak, High temperature slagging gasification of municipal solid waste with biomass charcoal as a greener auxiliary fuel, J. Hazard. Mater. 423 (2022) 127057. https://doi.org/10.1016/j.jhazmat.2021.127057.

[8] Z.L. He, X.E. Yang, P.J. Stoffella, Trace elements in agroecosystems and impacts on the environment, J. Trace Elem. Med. Biol. 19 (2005) 125–140. https://doi.org/10.1016/j.jtemb.2005.02.010.

[9] M. Muchuweti, J.W. Birkett, E. Chinyanga, R. Zvauya, M.D. Scrimshaw, J.N. Lester, Heavy metal content of vegetables irrigated with mixtures of wastewater and sewage sludge in Zimbabwe: Implications for human health, Agric. Ecosyst. Environ. 112 (2006) 41–48. https://doi.org/10.1016/j.agee.2005.04.028.

[10] Z. Wang, J. Zhang, Q. Wu, X. Han, M. Zhang, W. Liu, X. Yao, J. Feng, S. Dong, J. Sun, Magnetic supramolecular polymer: Ultrahigh and highly selective Pb(II) capture from aqueous solution and battery wastewater, Chemosphere. 248 (2020) 126042. https://doi.org/10.1016/j.chemosphere.2020.126042.

[11] K. Zhao, L. Ge, T.I. Wong, X. Zhou, G. Lisak, Gold-silver nanoparticles modified electrochemical sensor array for simultaneous determination of chromium(III) and

chromium(VI) in wastewater samples, Chemosphere. 281 (2021) 130880. https://doi.org/10.1016/j.chemosphere.2021.130880.

[12] L.E. Monroy Sarmiento, K.A. Clavier, T.G. Townsend, Trace element release from combustion ash co-disposed with municipal solid waste, Chemosphere. 252 (2020) 126436. https://doi.org/10.1016/j.chemosphere.2020.126436.

[13] K. Yin, W.-P. Chan, X. Dou, G. Lisak, V.W.-C. Chang, Kinetics and modeling of trace metal leaching from bottom ashes dominated by diffusion or advection, Sci. Total Environ. 719 (2020) 137203. https://doi.org/10.1016/j.scitotenv.2020.137203.

[14] A. Molleda, A. López, M. Cuartas, A. Lobo, Release of pollutants in MBT landfills: Laboratory versus field, Chemosphere. 249 (2020) 126145. https://doi.org/10.1016/j.chemosphere.2020.126145.

[15] N. Slijepčević, D.T. Pilipović, Đ. Kerkez, D. Krčmar, M. Bečelić-Tomin, J. Beljin, B. Dalmacija, A cost effective method for immobilization of Cu and Ni polluted river sediment with nZVI synthesized from leaf extract, Chemosphere. 263 (2021) 127816. https://doi.org/10.1016/j.chemosphere.2020.127816.

[16] N. Muhammad, M. Nafees, M.H. Khan, L. Ge, G. Lisak, Effect of biochars on bioaccumulation and human health risks of potentially toxic elements in wheat (Triticum aestivum L.) cultivated on industrially contaminated soil, Environ. Pollut. 260 (2020) 113887. https://doi.org/10.1016/j.envpol.2019.113887.

[17] N. Muhammad, L. Ge, M.H. Khan, W.P. Chan, M. Bilal, G. Lisak, M. Nafees, Effects of different biochars on physicochemical properties and immobilization of potentially toxic elements in soil - A geostatistical approach, Chemosphere. 277 (2021) 130350. https://doi.org/10.1016/j.chemosphere.2021.130350.

[18] Q. Liao, L. He, G. Tu, Z. Yang, W. Yang, J. Tang, W. Cao, H. Wang, Simultaneous immobilization of Pb, Cd and As in soil by hybrid iron-, sulfate- and phosphate-based bio-nanocomposite: Effectiveness, long-term stability and bioavailablity/bioaccessibility evaluation, Chemosphere. 266 (2021) 128960. https://doi.org/10.1016/j.chemosphere.2020.128960.

[19] T. Zhou, M. Zhao, X. Zhao, Y. Guo, Y. Zhao, Simultaneous remediation and fertility improvement of heavy metals contaminated soil by a novel composite hydrogel synthesized from food waste, Chemosphere. 275 (2021) 129984. https://doi.org/10.1016/j.chemosphere.2021.129984.

[20] N.K. Joon, P. Ek, M. Zevenhoven, L. Hupa, M. Miró, J. Bobacka, G. Lisak, On-line microcolumn-based dynamic leaching method for investigation of lead bioaccessibility in shooting range soils, Chemosphere. 256 (2020) 127022. https://doi.org/10.1016/j.chemosphere.2020.127022.

[21] P.B. Tchounwou, C.G. Yedjou, A.K. Patlolla, D.J. Sutton, Heavy Metal Toxicity and the Environment, Mol. Clin. Environ. Toxicol. (2012) 133–164. https://doi.org/10.1007/978-3-7643-8340-4_6.

[22] J. Briffa, E. Sinagra, R. Blundell, Heavy metal pollution in the environment and their toxicological effects on humans, Heliyon. 6 (2020) e04691. https://doi.org/10.1016/j.heliyon.2020.e04691.

[23] K.N. Mikhelson, Ion-selective electrodes with sensitivity in strongly diluted solutions, J. Anal. Chem. 65 (2010) 112–116. https://doi.org/10.1134/S1061934810020024.

[24] E. Zdrachek, E. Bakker, Potentiometric Sensing, Anal. Chem. 93 (2021) 72–102. https://doi.org/10.1021/acs.analchem.0c04249.

[25] C.R. Rousseau, P. Bühlmann, Calibration-free potentiometric sensing with solid-contact ion-selective electrodes, TrAC Trends Anal. Chem. 140 (2021) 116277. https://doi.org/10.1016/j.trac.2021.116277.

[26] D. Cudjoe, P.M. Acquah, Environmental impact analysis of municipal solid waste incineration in African countries, Chemosphere. 265 (2021) 129186. https://doi.org/10.1016/j.chemosphere.2020.129186.

[27] A. Ahamed, L. Liang, M.Y. Lee, J. Bobacka, G. Lisak, Too small to matter? Physicochemical transformation and toxicity of engineered nTiO2, nSiO2, nZnO, carbon nanotubes, and nAg, J. Hazard. Mater. 404 (2021) 124107. https://doi.org/10.1016/j.jhazmat.2020.124107.

[28] S.Z.N. Ahmad, W.N. Wan Salleh, A.F. Ismail, N. Yusof, M.Z. Mohd Yusop, F. Aziz, Adsorptive removal of heavy metal ions using graphene-based nanomaterials: Toxicity, roles of functional groups and mechanisms, Chemosphere. 248 (2020) 126008. https://doi.org/10.1016/j.chemosphere.2020.126008.

[29] Chapter 2 Interactions of heavy metals, Interface Sci. Technol. 6 (2005) 28–164. https://doi.org/10.1016/S1573-4285(05)80021-3.

[30] R.K. Soodan, Y.B. Pakade, A. Nagpal, J.K. Katnoria, Analytical techniques for estimation of heavy metals in soil ecosystem: A tabulated review, Talanta. 125 (2014) 405–410. https://doi.org/10.1016/j.talanta.2014.02.033.

[31] K. Siraj, S.A. Kitte, Analysis of Copper, Zinc and Lead using Atomic Absorption Spectrophotometer in ground water of Jimma town of Southwestern Ethiopia, Int. J. Chem. Anal. Sci. 4 (2013) 201–204. https://doi.org/10.1016/j.ijcas.2013.07.006.

[32] APHA, Standard methods for the examination of water and wastewater, 21st ed., American Public Health Association, Washington, DC., 2005.

[33] F. Pan, Y. Yu, L. Yu, H. Lin, Y. Wang, L. Zhang, D. Pan, R. Zhu, Quantitative assessment on soil concentration of heavy metal–contaminated soil with various sample pretreatment techniques and detection methods, Environ. Monit. Assess. 192 (2020) 800. https://doi.org/10.1007/s10661-020-08775-4.

[34] E. Pretsch, The new wave of ion-selective electrodes, TrAC Trends Anal. Chem. 26 (2007) 46–51. https://doi.org/10.1016/j.trac.2006.10.006.

[35] Y.H. Cheong, L. Ge, G. Lisak, Highly reproducible solid contact ion selective electrodes: Emerging opportunities for potentiometry – A review, Anal. Chim. Acta. 1162 (2021) 338304. https://doi.org/10.1016/j.aca.2021.338304.

[36] Y.H. Cheong, L. Ge, N. Zhao, L.K. Teh, G. Lisak, Ion selective electrodes utilizing a ferrocyanide doped redox active screen-printed solid contact - impact of electrode response to conditioning, J. Electroanal. Chem. 870 (2020) 114262. https://doi.org/10.1016/j.jelechem.2020.114262.

[37] V. Krikstolaityte, R. Ding, T. Ruzgas, S. Björklund, G. Lisak, Characterization of nano-layered solid-contact ion selective electrodes by simultaneous potentiometry and quartz crystal microbalance with dissipation, Anal. Chim. Acta. 1128 (2020) 19–30. https://doi.org/10.1016/j.aca.2020.06.044.

[38] Y.H. Cheong, K. Sagar, G. Lisak, Evolution of electrochemical potentials mediated by lipophilic salts at the buried membrane interface of solid contact ion selective electrodes, Sens. Actuators B Chem. 349 (2021) 130766. https://doi.org/10.1016/j.snb.2021.130766.

[39] Y.H. Cheong, G. Lisak, Physically Tailoring Ion Fluxes by Introducing Foamlike Structures into Polymeric Membranes of Solid Contact Ion-Selective Electrodes, ACS Sens. 6 (2021) 3667–3676. https://doi.org/10.1021/acssensors.1c01413.

[40] G. Lisak, J. Cui, J. Bobacka, Paper-based microfluidic sampling for potentiometric determination of ions, Sens. Actuators B Chem. 207 (2015) 933–939. https://doi.org/10.1016/j.snb.2014.07.044.

[41] V. Krikstolaityte, R. Ding, E. Chua Hui Xia, G. Lisak, Paper as sampling substrates and all-integrating platforms in potentiometric ion determination, TrAC Trends Anal. Chem. 133 (2020) 116070. https://doi.org/10.1016/j.trac.2020.116070.

[42] N. Sharma, T. Barstis, B. Giri, Advances in paper-analytical methods for pharmaceutical analysis, Eur. J. Pharm. Sci. 111 (2018) 46–56. https://doi.org/10.1016/j.ejps.2017.09.031.

[43] S. Smith, J.G. Korvink, D. Mager, K. Land, The potential of paper-based diagnostics to meet the ASSURED criteria, RSC Adv. 8 (2018) 34012–34034. https://doi.org/10.1039/C8RA06132G.

[44] J. Cui, G. Lisak, S. Strzalkowska, J. Bobacka, Potentiometric sensing utilizing paper-based microfluidic sampling, Analyst. 139 (2014) 2133–2136. https://doi.org/10.1039/C3AN02157B.

[45] J.-H. Jin, J.H. Kim, S.K. Lee, S.J. Choi, C.W. Park, N.K. Min, A Fully Integrated Paper-Microfluidic Electrochemical Device for Simultaneous Analysis of Physiologic Blood Ions, Sensors. 18 (2018) 104. https://doi.org/10.3390/s18010104.

[46] R. Ding, Y.H. Cheong, A. Ahamed, G. Lisak, Heavy Metals Detection with Paper-Based Electrochemical Sensors, Anal. Chem. 93 (2021) 1880–1888. https://doi.org/10.1021/acs.analchem.0c04247.

[47] P. Su, K. Granholm, A. Pranovich, L. Harju, B. Holmbom, A. Ivaska, Sorption of metal ions to untreated, alkali-treated and peroxide-bleached TMP, Cellulose. 17 (2010) 1033–1044. https://doi.org/10.1007/s10570-010-9439-1.

[48] R. Ding, V. Krikstolaityte, G. Lisak, Inorganic salt modified paper substrates utilized in paper based microfluidic sampling for potentiometric determination of heavy metals, Sens. Actuators B Chem. 290 (2019) 347–356. https://doi.org/10.1016/j.snb.2019.03.079.

[49] R. Ding, Y.H. Cheong, K. Zhao, G. Lisak, Acidified paper substrates for microfluidic solution sampling integrated with potentiometric sensors for determination of heavy metals, Sens. Actuators B Chem. (2021) 130567. https://doi.org/10.1016/j.snb.2021.130567.

[50] R. Ding, G. Lisak, Sponge-based microfluidic sampling for potentiometric ion sensing, Anal. Chim. Acta. 1091 (2019) 103–111. https://doi.org/10.1016/j.aca.2019.09.024.

[51] G. Lisak, T. Arnebrant, T. Ruzgas, J. Bobacka, Textile-based sampling for potentiometric determination of ions, Anal. Chim. Acta. 877 (2015) 71–79. https://doi.org/10.1016/j.aca.2015.03.045.

[52] S. Li, C. Zhang, S. Wang, Q. Liu, H. Feng, X. Ma, J. Guo, Electrochemical microfluidics techniques for heavy metal ion detection, Analyst. 143 (2018) 4230–4246. https://doi.org/10.1039/C8AN01067F.

[53] B. Bansod, T. Kumar, R. Thakur, S. Rana, I. Singh, A review on various electrochemical techniques for heavy metal ions detection with different sensing platforms, Biosens. Bioelectron. 94 (2017) 443–455. https://doi.org/10.1016/j.bios.2017.03.031.

[54] R. Ding, M. Fiedoruk-Pogrebniak, M. Pokrzywnicka, R. Koncki, J. Bobacka, G. Lisak, Solid reference electrode integrated with paper-based microfluidics for potentiometric ion sensing, Sens. Actuators B Chem. 323 (2020) 128680. https://doi.org/10.1016/j.snb.2020.128680.

[55] G. Lisak, Reliable environmental trace heavy metal analysis with potentiometric ion sensors - reality or a distant dream, Environ. Pollut. 289 (2021) 117882. https://doi.org/10.1016/j.envpol.2021.117882.

[56] M.S. Engin, A. Uyanik, S. Cay, H. Icbudak, Effect of the Adsorptive Character of Filter Papers on the Concentrations Determined in Studies Involving Heavy Metal Ions, Adsorpt. Sci. Technol. 28 (2010) 837–846. https://doi.org/10.1260/0263-6174.28.10.837.

[57] J.E. Fergusson, The Heavy Elements: Chemistry, Environmental Impact and Health Effects, Elsevier Science Limited, 1990.

[58] J.H. Duffus, "Heavy metals" a meaningless term? (IUPAC Technical Report), Pure Appl. Chem. 74 (2002) 793–807. https://doi.org/10.1351/pac200274050793.

[59] V. Kumar, R.D. Parihar, A. Sharma, P. Bakshi, G.P. Singh Sidhu, A.S. Bali, I. Karaouzas, R. Bhardwaj, A.K. Thukral, Y. Gyasi-Agyei, J. Rodrigo-Comino, Global evaluation of heavy metal content in surface water bodies: A meta-analysis

using heavy metal pollution indices and multivariate statistical analyses, Chemosphere. 236 (2019) 124364. https://doi.org/10.1016/j.chemosphere.2019.124364.

[60] Heavy Metals in the Environment: Origin, Interaction and Remediation, Volume 6 - 1st Edition, (n.d.). https://www.elsevier.com/books/heavy-metals-in-the-environment-origin-interaction-and-remediation/bradl/978-0-12-088381-3 (accessed October 30, 2022).

[61] A. Nayak, M.S. Jena, N.R. Mandre, Beneficiation of Lead-Zinc Ores – A Review, Miner. Process. Extr. Metall. Rev. 43 (2022) 564–583. https://doi.org/10.1080/08827508.2021.1903459.

[62] Lead - Element information, properties and uses | Periodic Table, (n.d.). https://www.rsc.org/periodic-table/element/82/lead (accessed October 30, 2022).

[63] R.L. Canfield, M.H. Gendle, D.A. Cory-Slechta, Impaired Neuropsychological Functioning in Lead-Exposed Children, Dev. Neuropsychol. 26 (2004) 513–540. https://doi.org/10.1207/s15326942dn2601_8.

[64] J.L. Pirkle, R.B. Kaufmann, D.J. Brody, T. Hickman, E.W. Gunter, D.C. Paschal, Exposure of the U.S. population to lead, 1991-1994, Environ. Health Perspect. 106 (1998) 745–750. https://doi.org/10.1289/ehp.98106745.

[65] R.Z. Sokol, N. Berman, The effect of age of exposure on lead-induced testicular toxicity, Toxicology. 69 (1991) 269–278. https://doi.org/10.1016/0300-483X(91)90186-5.

[66] A.L. Wani, A. Ara, J.A. Usmani, Lead toxicity: a review, Interdiscip. Toxicol. 8 (2015) 55–64. https://doi.org/10.1515/intox-2015-0009.

[67] CDC - Immediately Dangerous to Life or Health Concentrations (IDLH): Lead compounds (as Pb) - NIOSH Publications and Products, (2018). https://www.cdc.gov/niosh/idlh/7439921.html (accessed November 1, 2022).

[68] S. Greenfield, I.Ll.W. Jones, C.T. Berry, L.G. Bunch, New light sources in spectroscopy: The high-frequency torch: Some facts, figures and thoughts, Proc. Soc. Anal. Chem. 2 (1965) 111–113. https://doi.org/10.1039/SA9650200105.

[69] R.H. Scott, V.A. Fassel, R.N. Kniseley, D.E. Nixon, Inductively coupled plasma-optical emission analytical spectrometry, Anal. Chem. 46 (1974) 75–80. https://doi.org/10.1021/ac60337a031.

[70] M. Bettinelli, G.M. Beone, S. Spezia, C. Baffi, Determination of heavy metals in soils and sediments by microwave-assisted digestion and inductively coupled plasma optical emission spectrometry analysis, Anal. Chim. Acta. 424 (2000) 289–296. https://doi.org/10.1016/S0003-2670(00)01123-5.

[71] D. Sollitto, M. Romic, A. Castrignanò, D. Romic, H. Bakic, Assessing heavy metal contamination in soils of the Zagreb region (Northwest Croatia) using multivariate geostatistics, Catena. 80 (2010) 182–194. https://doi.org/10.1016/j.catena.2009.11.005.

[72] J. Olesik, ICP-OES Capabilities, Developments, Limitations, and Any Potential Challengers?, Spectroscopy. 35 (2020) 18–21.

[73] ICP-OES principle, ICP-OES Analysis, ICP-OES FAQ's | Agilent, (n.d.). https://www.agilent.com/en/support/atomic-spectroscopy/inductively-coupled-plasma-optical-emission-spectroscopy-icp-oes/icp-oes-faq (accessed November 21, 2022).

[74] ICP-OES Sample Preparation - SG, (n.d.). https://www.thermofisher.com/sg/en/home/industrial/spectroscopy-elemental-isotope-analysis/spectroscopy-elemental-isotope-analysis-learning-center/trace-elemental-analysis-tea-information/icp-oes-information/icp-oes-sample-preparation.html (accessed November 1, 2022).

[75] A.L. Rosen, G.M. Hieftje, Inductively coupled plasma mass spectrometry and electrospray mass spectrometry for speciation analysis: Applications and instrumentation, Spectrochim. Acta - Part B At. Spectrosc. 59 (2004) 135–146. https://doi.org/10.1016/j.sab.2003.09.004.

[76] T. Meisel, J. Moser, N. Fellner, W. Wegscheider, R. Schoenberg, Simplified method for the determination of Ru, Pd, Re, Os, Ir and Pt in chromitites and other geological materials by isotope dilution ICP-MS and acid digestion, Analyst. 126 (2001) 322–328. https://doi.org/10.1039/b007575m.

[77] K. Tiede, A.B.A. Boxall, D. Tiede, S.P. Tear, H. David, J. Lewis, A robust size-characterisation methodology for studying nanoparticle behaviour in 'real' environmental samples, using hydrodynamic chromatography coupled to ICP-MS, J. Anal. At. Spectrom. 24 (2009) 964–972. https://doi.org/10.1039/B822409A.

[78] A. Taylor, S. Branch, D. Halls, M. Patriarca, M. White, Atomic spectrometry update. Clinical and biological materials, foods and beverages, J. Anal. At. Spectrom. 18 (2003) 385–427. https://doi.org/10.1039/b301135f.

[79] I. Rodushkin, E. Engström, D.C. Baxter, Isotopic analyses by ICP-MS in clinical samples, Anal. Bioanal. Chem. 405 (2013) 2785–2797. https://doi.org/10.1007/s00216-012-6457-x.

[80] M. Weiss, C. Riedl, J. Frank, J. Fleig, A. Limbeck, Quantitative analysis of the platinum surface decoration on lanthanum strontium iron oxide thin films via online-LASIL-ICP-MS, Microchem. J. 166 (2021) 106236. https://doi.org/10.1016/j.microc.2021.106236.

[81] Comparison of ICP-OES and ICP-MS for Trace Element Analysis - SG, (n.d.). https://www.thermofisher.com/sg/en/home/industrial/environmental/environmental-learning-center/contaminant-analysis-information/metal-analysis/comparison-icp-oes-icp-ms-trace-element-analysis.html (accessed November 1, 2022).

[82] A Beginner's Guide to ICP-MS, Mass Spectrometry basics | Agilent, (n.d.). https://www.agilent.com/en/product/atomic-spectroscopy/inductively-coupled-plasma-mass-spectrometry-icp-ms/what-is-icp-ms-icp-ms-faqs (accessed December 1, 2022).

[83] ICP-MS Sample Preparation - SG, (n.d.). https://www.thermofisher.com/sg/en/home/industrial/spectroscopy-elemental-isotope-analysis/spectroscopy-elemental-isotope-analysis-learning-center/trace-elemental-analysis-tea-information/inductively-coupled-plasma-mass-spectrometry-icp-ms-information/icp-ms-sample-preparation.html (accessed November 1, 2022).

[84] K. Fuwa, Memories of Sir Alan Walsh: atomic absorption spectroscopy in the field of trace elements in biology, Spectrochim. Acta Part B At. Spectrosc. 54 (1999) 2005–2009. https://doi.org/10.1016/S0584-8547(99)00115-9.

[85] AAS Data Analysis - SG, (n.d.). https://www.thermofisher.com/sg/en/home/industrial/spectroscopy-elemental-isotope-analysis/spectroscopy-elemental-isotope-analysis-learning-center/trace-elemental-analysis-tea-information/atomic-absorption-aa-information/aa-data-analysis.html (accessed December 1, 2022).

[86] AAS Sample Preparation - SG, (n.d.). https://www.thermofisher.com/sg/en/home/industrial/spectroscopy-elemental-isotope-analysis/spectroscopy-elemental-isotope-analysis-learning-center/trace-elemental-analysis-tea-information/atomic-absorption-aa-information/aa-sample-preparation.html (accessed November 2, 2022).

[87] M. Sperling, Flame and Graphite Furnace Atomic Absorption Spectrometry in Environmental Analysis, in: Encycl. Anal. Chem., John Wiley & Sons, Ltd, 2006. https://doi.org/10.1002/9780470027318.a0805.

[88] Atomic Fluorescence Spectroscopy (AFS): An Overview, News-Medicalnet. (2022). https://www.azolifesciences.com/article/Atomic-Fluorescence-Spectroscopy-(AFS)-An-Overview.aspx (accessed December 1, 2022).

[89] S.J. Hill, A.S. Fisher, Atomic Fluorescence, Methods and Instrumentation*, in: J.C. Lindon (Ed.), Encycl. Spectrosc. Spectrom. Second Ed., Academic Press, Oxford, 1999: pp. 78–83. https://doi.org/10.1016/B978-0-12-374413-5.00371-7.

[90] J.L. Gómez-Ariza, F. Lorenzo, T. García-Barrera, Guidelines for routine mercury speciation analysis in seafood by gas chromatography coupled to a home-modified AFS detector. Application to the Andalusian coast (south Spain), Chemosphere. 61 (2005) 1401–1409. https://doi.org/10.1016/j.chemosphere.2005.04.083.

[91] Q. Ding, C. Li, H. Wang, C. Xu, H. Kuang, Electrochemical detection of heavy metal ions in water, Chem. Commun. 57 (2021) 7215–7231. https://doi.org/10.1039/D1CC00983D.

[92] K.-H. Lubert, K. Kalcher, History of Electroanalytical Methods, Electroanalysis. 22 (2010) 1937–1946. https://doi.org/10.1002/elan.201000087.

[93] E. Bakker, P. Bühlmann, E. Pretsch, Carrier-Based Ion-Selective Electrodes and Bulk Optodes. 1. General Characteristics, Chem. Rev. 97 (1997) 3083–3132. https://doi.org/10.1021/cr940394a.

[94] P.C. Meier, Two-parameter debye-hückel approximation for the evaluation of mean activity coefficients of 109 electrolytes, Anal. Chim. Acta. 136 (1982) 363–368. https://doi.org/10.1016/S0003-2670(01)95397-8.

[95] K.N. Mikhelson, Ion-Selective Electrode Characteristics, in: K.N. Mikhelson (Ed.), Ion-Sel. Electrodes, Springer, Berlin, Heidelberg, 2013: pp. 33–49. https://doi.org/10.1007/978-3-642-36886-8_3.

[96] W.E. Morf, The Principles of Ion-selective Electrodes and of Membrane Transport, New York, 1981.

[97] Y. Umezawa, P. Buhlmann, K. Umezawa, K. Tohda, S. Amemiya, Potentiometric Selectivity Coefficients of IonSelective Electrodes. Part I. Inorganic Cations (Technical Report), Pure Appl. Chem. - PURE APPL CHEM. 72 (2000) 1851–2082. https://doi.org/10.1351/pac200072101851.

[98] G.G. Guilbault, Recommendations for Publishing Manuscripts on Ion-Selective Electrodes* *Reprinted from IUPAC Information Bulletin, No. 1, pp. 69–74 (1978), with permission from the International Union of Pure and Applied Chemistry., in: J.D.R. Thomas (Ed.), Ion-Sel. Electrode Rev., Elsevier, 1980: pp. 139–143. https://doi.org/10.1016/B978-0-08-026044-0.50008-1.

[99] R.P. Buck, Ion selective electrodes, potentiometry, and potentiometric titrations, ACS Publ. (2002). https://doi.org/10.1021/ac60341a020.

[100] Bernard. Fleet, T.H. Ryan, M.J.D. Brand, Factors affecting the response time of a calcium selective liquid membrane electrode, Anal. Chem. 46 (1974) 12–15. https://doi.org/10.1021/ac60337a036.

[101] M. Farré, L. Kantiani, D. Barceló, Chapter 7 - Microfluidic Devices: Biosensors, in: Y. Picó (Ed.), Chem. Anal. Food Tech. Appl., Academic Press, Boston, 2012: pp. 177–217. https://doi.org/10.1016/B978-0-12-384862-8.00007-8.

[102] A.W. Martinez, S.T. Phillips, B.J. Wiley, M. Gupta, G.M. Whitesides, FLASH: A rapid method for prototyping paper-based microfluidic devices, Lab. Chip. 8 (2008) 2146–2150. https://doi.org/10.1039/B811135A.

[103] A.W. Martinez, S.T. Phillips, G.M. Whitesides, E. Carrilho, Diagnostics for the Developing World: Microfluidic Paper-Based Analytical Devices, Anal. Chem. 82 (2010) 3–10. https://doi.org/10.1021/ac9013989.

[104] Z.W. Zhong, Z.P. Wang, G.X.D. Huang, Investigation of wax and paper materials for the fabrication of paper-based microfluidic devices, Microsyst. Technol. 18 (2012) 649–659. https://doi.org/10.1007/s00542-012-1469-1.

[105] A. Sinha, M. Basu, P. Chandna, Chapter Five - Paper based microfluidics: A forecast toward the most affordable and rapid point-of-care devices, in: A. Pandya, V. Singh (Eds.), Prog. Mol. Biol. Transl. Sci., Academic Press, 2022: pp. 109–158. https://doi.org/10.1016/bs.pmbts.2021.07.010.

[106] Y. Lin, D. Gritsenko, S. Feng, Y.C. Teh, X. Lu, J. Xu, Detection of heavy metal by paper-based microfluidics, Biosens. Bioelectron. 83 (2016) 256–266. https://doi.org/10.1016/j.bios.2016.04.061.

[107] J. Adkins, K. Boehle, C. Henry, Electrochemical paper-based microfluidic devices, ELECTROPHORESIS. 36 (2015) 1811–1824. https://doi.org/10.1002/elps.201500084.

[108] A.T.K. Perera, D.-T. Phan, S. Pudasaini, Y. Liu, C. Yang, Enhanced sample pre-concentration by ion concentration polarization on a paraffin coated converging microfluidic paper based analytical platform, Biomicrofluidics. 14 (2020) 014103. https://doi.org/10.1063/1.5133946.

[109] A.T.K. Perera, S. Pudasaini, Y. Liu, J.W. Chew, C. Yang, Detecting Micromolar Antibiotics: Preconcentration by Ion Concentration Polarization (ICP) at a Paper-Nafion Junction, (2023). https://doi.org/10.2139/ssrn.4463124.

[110] P.B. Deroco, D. Wachholz Junior, L.T. Kubota, Paper-based Wearable Electrochemical Sensors: A New Generation of Analytical Devices, Electroanalysis. 35 (2023) e202200177. https://doi.org/10.1002/elan.202200177.

[111] S. Nishat, A.T. Jafry, A.W. Martinez, F.R. Awan, Paper-based microfluidics: Simplified fabrication and assay methods, Sens. Actuators B Chem. 336 (2021) 129681. https://doi.org/10.1016/j.snb.2021.129681.

[112] J. Szűcs, R.E. Gyurcsányi, Towards Protein Assays on Paper Platforms with Potentiometric Detection, Electroanalysis. 24 (2012) 146–152. https://doi.org/10.1002/elan.201100522.

[113] R. Ding, N.K. Joon, A. Ahamed, A. Shafaat, M. Guzinski, M. Wagner, T. Ruzgas, J. Bobacka, G. Lisak, Gold-modified paper as microfluidic substrates with reduced biofouling in potentiometric ion sensing, Sens. Actuators B Chem. 344 (2021) 130200. https://doi.org/10.1016/j.snb.2021.130200.

[114] B. Lou, C. Chen, Z. Zhou, L. Zhang, E. Wang, S. Dong, A novel electrochemical sensing platform for anions based on conducting polymer film modified electrodes integrated on paper-based chips, Talanta. 105 (2013) 40–45. https://doi.org/10.1016/j.talanta.2012.11.062.

[115] M. Novell, M. Parrilla, G.A. Crespo, F.X. Rius, F.J. Andrade, Paper-Based Ion-Selective Potentiometric Sensors, Anal. Chem. 84 (2012) 4695–4702. https://doi.org/10.1021/ac202979j.

[116] S.T. Mensah, Y. Gonzalez, P. Calvo-Marzal, K.Y. Chumbimuni-Torres, Nanomolar Detection Limits of Cd2+, Ag+, and K+ Using Paper-Strip Ion-Selective Electrodes, Anal. Chem. 86 (2014) 7269–7273. https://doi.org/10.1021/ac501470p.

[117] E.T.S.G. da Silva, S. Miserere, L.T. Kubota, A. Merkoçi, Simple On-Plastic/Paper Inkjet-Printed Solid-State Ag/AgCl Pseudoreference Electrode, Anal. Chem. 86 (2014) 10531–10534. https://doi.org/10.1021/ac503029q.

[118] P. Sjöberg, A. Määttänen, U. Vanamo, M. Novell, P. Ihalainen, F.J. Andrade, J. Bobacka, J. Peltonen, Paper-based potentiometric ion sensors constructed on ink-jet printed gold electrodes, Sens. Actuators B Chem. 224 (2016) 325–332. https://doi.org/10.1016/j.snb.2015.10.051.

[119] J. Hu, W. Zhao, P. Bühlmann, A. Stein, Paper-Based All-Solid-State Ion-Sensing Platform with a Solid Contact Comprising Colloid-Imprinted Mesoporous Carbon and a Redox Buffer, ACS Appl. Nano Mater. 1 (2018) 293–301. https://doi.org/10.1021/acsanm.7b00151.

[120] M. Borchardt, C. Dumschat, karl Cammann, M. Knoll, Disposable ion-selective electrodes, Sens. Actuators B Chem. 25 (1995) 721–723. https://doi.org/10.1016/0925-4005(95)85159-3.

[121] I. Shitanda, M. Komoda, Y. Hoshi, M. Itagaki, An instantly usable paper-based screen-printed solid-state KCl/Ag/AgCl reference electrode with long-term stability, Analyst. 140 (2015) 6481–6484. https://doi.org/10.1039/C5AN00617A.

[122] S.M. Armas, A.J. Manhan, O. Younce, P. Calvo-Marzal, K.Y. Chumbimuni-Torres, Ready-to-use single-strip paper based sensor for multiplex ion detection, Sens. Actuators B Chem. 255 (2018) 1781–1787. https://doi.org/10.1016/j.snb.2017.08.194.

[123] W.-J. Lan, X.U. Zou, M.M. Hamedi, J. Hu, C. Parolo, E.J. Maxwell, P. Bühlmann, G.M. Whitesides, Paper-Based Potentiometric Ion Sensing, Anal. Chem. 86 (2014) 9548–9553. https://doi.org/10.1021/ac5018088.

[124] J. Hu, K.T. Ho, X.U. Zou, W.H. Smyrl, A. Stein, P. Bühlmann, All-Solid-State Reference Electrodes Based on Colloid-Imprinted Mesoporous Carbon and Their Application in Disposable Paper-based Potentiometric Sensing Devices, Anal. Chem. 87 (2015) 2981–2987. https://doi.org/10.1021/ac504556s.

[125] R. Kawahara, P. Sahatiya, S. Badhulika, S. Uno, Paper-based potentiometric pH sensor using carbon electrode drawn by pencil, Jpn. J. Appl. Phys. 57 (2018) 04FM08. https://doi.org/10.7567/JJAP.57.04FM08.

[126] E.W. Nery, L.T. Kubota, Integrated, paper-based potentiometric electronic tongue for the analysis of beer and wine, Anal. Chim. Acta. 918 (2016) 60–68. https://doi.org/10.1016/j.aca.2016.03.004.

[127] T. Sakata, M. Hagio, A. Saito, Y. Mori, M. Nakao, K. Nishi, Biocompatible and flexible paper-based metal electrode for potentiometric wearable wireless biosensing, Sci. Technol. Adv. Mater. 21 (2020) 379–387. https://doi.org/10.1080/14686996.2020.1777463.

[128] B. Liang, Q. Cao, X. Mao, W. Pan, T. Tu, L. Fang, X. Ye, An Integrated Paper-Based Microfluidic Device for Real-Time Sweat Potassium Monitoring, IEEE Sens. J. 21 (2021) 9642–9648. https://doi.org/10.1109/JSEN.2020.3009327.

[129] A.M. Yehia, M.A. Farag, M.A. Tantawy, A novel trimodal system on a paper-based microfluidic device for on-site detection of the date rape drug “ketamine,” Anal. Chim. Acta. 1104 (2020) 95–104. https://doi.org/10.1016/j.aca.2020.01.002.

[130] H.T. Sahin, M.B. Arslan, A Study on Physical and Chemical Properties of Cellulose Paper Immersed in Various Solvent Mixtures, Int. J. Mol. Sci. 9 (2008) 78–88.

[131] Fillers for papermaking: A review of their properties, usage practices, and their mechanistic role :: BioResources, (n.d.). https://bioresources.cnr.ncsu.edu/ (accessed November 3, 2022).

[132] X. Huang, X. Qian, J. Li, S. Lou, J. Shen, Starch/rosin complexes for improving the interaction of mineral filler particles with cellulosic fibers, Carbohydr. Polym. 117 (2015) 78–82. https://doi.org/10.1016/j.carbpol.2014.09.047.

[133] J. Ding, N. He, G. Lisak, W. Qin, J. Bobacka, Paper-based microfluidic sampling and separation of analytes for potentiometric ion sensing, Sens. Actuators B Chem. 243 (2017) 346–352. https://doi.org/10.1016/j.snb.2016.11.128.

[134] A.H. Kamel, X. Jiang, P. Li, R. Liang, A paper-based potentiometric sensing platform based on molecularly imprinted nanobeads for determination of bisphenol A, Anal. Methods. 10 (2018) 3890–3895. https://doi.org/10.1039/C8AY01229F.

[135] J. Ding, B. Li, L. Chen, W. Qin, A Three-Dimensional Origami Paper-Based Device for Potentiometric Biosensing, Angew. Chem. Int. Ed. 55 (2016) 13033–13037. https://doi.org/10.1002/anie.201606268.

[136] L.-M. Fu, Y.-N. Wang, Detection methods and applications of microfluidic paper-based analytical devices, TrAC Trends Anal. Chem. 107 (2018) 196–211. https://doi.org/10.1016/j.trac.2018.08.018.

[137] F. Kong, Y.F. Hu, Biomolecule immobilization techniques for bioactive paper fabrication, Anal. Bioanal. Chem. 403 (2012) 7–13. https://doi.org/10.1007/s00216-012-5821-1.

[138] Z. Li, L. Shao, Z. Ruan, W. Hu, L. Lu, Y. Chen, Converting untreated waste office paper and chitosan into aerogel adsorbent for the removal of heavy metal ions, Carbohydr. Polym. 193 (2018) 221–227. https://doi.org/10.1016/j.carbpol.2018.04.003.

[139] T. Bhattacharjee, M. Islam, D. Chowdhury, G. Majumdar, In-situ generated carbon dot modified filter paper for heavy metals removal in water, Environ. Nanotechnol. Monit. Manag. 16 (2021) 100582. https://doi.org/10.1016/j.enmm.2021.100582.

[140] H. Farrah, W.F. Pickering, The effect of pH and ligands on the sorption of heavy metal ions by cellulose, Aust. J. Chem. 31 (1978) 1501–1509. https://doi.org/10.1071/ch9781501.

[141] J. Bobacka, Potential Stability of All-Solid-State Ion-Selective Electrodes Using Conducting Polymers as Ion-to-Electron Transducers, Anal. Chem. 71 (1999) 4932–4937. https://doi.org/10.1021/ac990497z.

[142] FTIR Spectroscopy Basics - SG, (n.d.). https://www.thermofisher.com/sg/en/home/industrial/spectroscopy-elemental-isotope-analysis/spectroscopy-elemental-isotope-analysis-learning-center/molecular-spectroscopy-information/ftir-information/ftir-basics.html (accessed December 7, 2022).

[143] ISO, International Standard 14040 and 14044. Environmental Management - Life Cycle Assessment - Principles and Framework, Requirements and Guidelines., (2006).

[144] K.N. Mikhelson, ISE Constructions, in: K.N. Mikhelson (Ed.), Ion-Sel. Electrodes, Springer, Berlin, Heidelberg, 2013: pp. 135–148. https://doi.org/10.1007/978-3-642-36886-8_8.

[145] G. Lisak, J. Bobacka, A. Lewenstam, Recovery of nanomolar detection limit of solid-contact lead (II)-selective electrodes by electrode conditioning, J. Solid State Electrochem. 16 (2012) 2983–2991. https://doi.org/10.1007/s10008-012-1725-4.

[146] S. Mathison, E. Bakker, Effect of Transmembrane Electrolyte Diffusion on the Detection Limit of Carrier-Based Potentiometric Ion Sensors, Anal. Chem. 70 (1998) 303–309. https://doi.org/10.1021/ac970690y.

[147] JEOL USA | Smart Coater - Fully Automated Sputter Coater, (n.d.). https://www.jeolusa.com/PRODUCTS/Sample-Preparation-Tools/Smart-Coater (accessed August 17, 2021).

[148] G. Lisak, A. Ivaska, A. Lewenstam, J. Bobacka, Multicalibrational procedure for more reliable analyses of ions at low analyte concentrations, Electrochimica Acta. 140 (2014) 27–32. https://doi.org/10.1016/j.electacta.2014.02.091.

[149] A. Ahamed, L. Ge, K. Zhao, A. Veksha, J. Bobacka, G. Lisak, Environmental footprint of voltammetric sensors based on screen-printed electrodes: An assessment towards “green” sensor manufacturing, Chemosphere. 278 (2021) 130462. https://doi.org/10.1016/j.chemosphere.2021.130462.

[150] R.D. Johnson, L.G. Bachas, Ionophore-based ion-selective potentiometric and optical sensors, Anal. Bioanal. Chem. 376 (2003) 328–341. https://doi.org/10.1007/s00216-003-1931-0.

[151] A. Ceresa, E. Bakker, B. Hattendorf, D. Günther, E. Pretsch, Potentiometric Polymeric Membrane Electrodes for Measurement of Environmental Samples at Trace Levels: New Requirements for Selectivities and Measuring Protocols, and Comparison with ICPMS, Anal. Chem. 73 (2001) 343–351. https://doi.org/10.1021/ac001034s.

[152] F. Faridbod, P. Norouzi, R. Dinarvand, M.R. Ganjali, Developments in the Field of Conducting and Non-conducting Polymer Based Potentiometric Membrane Sensors for Ions Over the Past Decade, Sensors. 8 (2008) 2331–2412. https://doi.org/10.3390/s8042331.

[153] C. Bahro, S. Goswami, S. Gernhart, D. Koley, Calibration-free Solid-State Ion-Selective Electrode Based on a Polarized PEDOT/PEDOT-S-Doped Copolymer as Back Contact, Anal. Chem. 94 (2022) 8302–8308. https://doi.org/10.1021/acs.analchem.2c00748.

[154] R. De Marco, G. Clarke, B. Pejcic, Ion-Selective Electrode Potentiometry in Environmental Analysis, Electroanalysis. 19 (2007) 1987–2001. https://doi.org/10.1002/elan.200703916.

[155] T. Forrest, E. Zdrachek, E. Bakker, Thin Layer Membrane Systems as Rapid Development Tool for Potentiometric Solid Contact Ion-selective Electrodes, Electroanalysis. 32 (2020) 799–804. https://doi.org/10.1002/elan.201900674.

[156] R. Wang, X. Du, X. Ma, J. Zhai, X. Xie, Ionophore-based pH independent detection of ions utilizing aggregation-induced effects, Analyst. 145 (2020) 3846–3850. https://doi.org/10.1039/D0AN00486C.

[157] H. Shibata, T.G. Henares, K. Yamada, K. Suzuki, D. Citterio, Implementation of a plasticized PVC-based cation-selective optode system into a paper-based analytical device for colorimetric sodium detection, Analyst. 143 (2018) 678–686. https://doi.org/10.1039/C7AN01952A.

[158] E. Hupa, U. Vanamo, J. Bobacka, Novel Ion-to-Electron Transduction Principle for Solid-Contact ISEs, Electroanalysis. 27 (2015) 591–594. https://doi.org/10.1002/elan.201400596.

[159] Z. Jarolímová, T. Han, U. Mattinen, J. Bobacka, E. Bakker, Capacitive Model for Coulometric Readout of Ion-Selective Electrodes, Anal. Chem. 90 (2018) 8700–8707. https://doi.org/10.1021/acs.analchem.8b02145.

[160] J. Zhai, D. Yuan, X. Xie, Ionophore-based ion-selective electrodes: signal transduction and amplification from potentiometry, Sens. Diagn. 1 (2022) 213–221. https://doi.org/10.1039/D1SD00055A.

[161] U. Schaller, E. Bakker, U.E. Spichiger, E. Pretsch, Ionic additives for ion-selective electrodes based on electrically charged carriers, ACS Publ. (2002). https://doi.org/10.1021/ac00075a013.

[162] E.M. Zahran, A. New, V. Gavalas, L.G. Bachas, Polymeric plasticizer extends the lifetime of PVC-membrane ion-selective electrodes, Analyst. 139 (2014) 757–763. https://doi.org/10.1039/C3AN01963B.

[163] J.D.R. Thomas, Solvent polymeric membrane ion-selective electrodes, Anal. Chim. Acta. 180 (1986) 289–297. https://doi.org/10.1016/0003-2670(86)80011-3.

[164] K.N. Mikhelson, Ionophore-Based ISEs, in: K.N. Mikhelson (Ed.), Ion-Sel. Electrodes, Springer, Berlin, Heidelberg, 2013: pp. 51–95. https://doi.org/10.1007/978-3-642-36886-8_4.

[165] K.N. Mikhelson, The Basics of the ISEs, in: K.N. Mikhelson (Ed.), Ion-Sel. Electrodes, Springer, Berlin, Heidelberg, 2013: pp. 11–32. https://doi.org/10.1007/978-3-642-36886-8_2.

[166] N. Ruecha, O. Chailapakul, K. Suzuki, D. Citterio, Fully Inkjet-Printed Paper-Based Potentiometric Ion-Sensing Devices, Anal. Chem. 89 (2017) 10608–10616. https://doi.org/10.1021/acs.analchem.7b03177.

[167] J. Hu, A. Stein, P. Bühlmann, A Disposable Planar Paper-Based Potentiometric Ion-Sensing Platform, Angew. Chem. Int. Ed. 55 (2016) 7544–7547. https://doi.org/10.1002/anie.201603017.

[168] E. Malinowska, Z. Brzózka, K. Kasiura, R.J.M. Egberink, D.N. Reinhoudt, Lead selective electrodes based on thioamide functionalized calix[4]arenes as

ionophores, Anal. Chim. Acta. 298 (1994) 253–258. https://doi.org/10.1016/0003-2670(94)00266-5.

[169] J. Coates, Interpretation of Infrared Spectra, A Practical Approach, in: Encycl. Anal. Chem., John Wiley & Sons, Ltd, 2006. https://doi.org/10.1002/9780470027318.a5606.

[170] J. Chen, X.A. Nie, J.C. Jiang, Y.H. Zhou, Thermal degradation and plasticizing mechanism of poly(vinyl chloride) plasticized with a novel cardanol derived plasticizer, IOP Conf. Ser. Mater. Sci. Eng. 292 (2018) 012008. https://doi.org/10.1088/1757-899X/292/1/012008.

[171] A. Mancilla-Rico, J. de Gyves, E. Rodríguez de San Miguel, Structural Characterization of the Plasticizers' Role in Polymer Inclusion Membranes Used for Indium (III) Transport Containing IONQUEST® 801 as Carrier, Membranes. 11 (2021) 401. https://doi.org/10.3390/membranes11060401.

[172] E. Grygolowicz-Pawlak, G.A. Crespo, M. Ghahraman Afshar, G. Mistlberger, E. Bakker, Potentiometric Sensors with Ion-Exchange Donnan Exclusion Membranes, Anal. Chem. 85 (2013) 6208–6212. https://doi.org/10.1021/ac400470n.

[173] V.V. Egorov, N.D. Borisenko, E.M. Rakhman'ko, Ya.F. Lushchik, S.S. Kacharsky, The effect of the ion exchanger site-counterion complex formation on the selectivities of ISEs, Talanta. 44 (1997) 1735–1747. https://doi.org/10.1016/S0039-9140(97)00042-8.

[174] V.V. Egorov, A.D. Novakovskii, E.A. Zdrachek, Modeling of the effect of diffusion processes on the response of ion-selective electrodes by the finite difference technique: Comparison of theory with experiment and critical evaluation, J. Anal. Chem. 72 (2017) 793–802. https://doi.org/10.1134/S1061934817070048.

[175] K. Maksymiuk, E. Stelmach, A. Michalska, Unintended Changes of Ion-Selective Membranes Composition—Origin and Effect on Analytical Performance, Membranes. 10 (2020) 266. https://doi.org/10.3390/membranes10100266.

[176] Lead ionophore IV Selectophore® 145237-46-3, (n.d.). http://www.sigmaaldrich.com/ (accessed March 3, 2022).

[177] M. Guziński, G. Lisak, J. Kupis, A. Jasiński, M. Bocheńska, Lead(II)-selective ionophores for ion-selective electrodes: A review, Anal. Chim. Acta. 791 (2013) 1–12. https://doi.org/10.1016/j.aca.2013.04.044.

[178] V.K. Gupta, R. Mangla, S. Agarwal, Pb(II) Selective Potentiometric Sensor Based on 4-tert-Butylcalix[4]arene in PVC Matrix, Electroanalysis. 14 (2002) 1127–1132. https://doi.org/10.1002/1521-4109(200208)14:15/16<1127::AID-ELAN1127>3.0.CO;2-7.

[179] A. Ceresa, E. Pretsch, Determination of formal complex formation constants of various Pb2+ ionophores in the sensor membrane phase, Anal. Chim. Acta. 395 (1999) 41–52. https://doi.org/10.1016/S0003-2670(99)00311-6.

[180] G. Lisak, T. Sokalski, J. Bobacka, L. Harju, K. Mikhelson, A. Lewenstam, Tuned galvanostatic polarization of solid-state lead-selective electrodes for lowering of the detection limit, Anal. Chim. Acta. 707 (2011) 1–6. https://doi.org/10.1016/j.aca.2011.09.026.

[181] A.N. Raditya, D. O'Hare, Review—Electrochemical Sensor Biofouling in Environmental Sensor Networks: Characterisation, Remediation and Lessons from Biomedical Devices, J. Electrochem. Soc. 167 (2020) 127503. https://doi.org/10.1149/1945-7111/aba931.